1952

Residual stress and the yield strength of steel beams, Welding Journal, Vol. 131, p. 205-s, 1952, Reprint No. 78 (52-3)

C. H. Yang

L. S. Beedle

B. G. Johnston

Welded Continuous Frames And Their Components

RESIDUAL STRESS AND THE YIELD STRENGTH OF STEEL BEAMS

BY
Ching Huan Yang
Lynn S. Beedle
and
Bruce G. Johnston

LEHIGH UNIVERSITY

Welded Continuous Frames and Their Components

Progress Report No. 6

RESIDUAL STRESS AND THE YIELD STRENGTH OF STEEL BEAMS

by

Ching Huan Yang, Lynn S. Beedle, and Bruce G. Johnston

This work has been carried out as a part of an investigation sponsored jointly by the Welding Research Council and the Department of the Navy with funds furnished by the following:

American Institute of Steel Construction
American Iron and Steel Institute
Column Research Council (Advisory)
Institute of Research, Lehigh University
Office of Naval Research (Contract No. 39303)
Bureau of Ships
Bureau of Yards and Docks

Fritz Engineering Laboratory
Department of Civil Engineering and Mechanics
Lehigh University
Bethlehem, Pennsylvania

September 10, 1951

Fritz Laboratory Report No. 205B.8

TABLE OF CONTENTS

RESIDUAL STRESS AND THE YIELD STRENGTH OF STEEL BEAMS

(I) S Y N O P S I S

This paper contains an analytical and experimental study of the behavior of welded continuous steel beams tested in the elastic and plastic ranges. Emphasis has been given to factors that affect the yield strength of steel members, including stress concentrations and residual stresses. The influence of the latter on the buckling strength is also discussed. Some basic assumptions of the simple plastic theory are examined and compared with the test results.

(II) I N T R O D U C T I O N

Under certain conditions continuous or "rigid" frames require less material than statically determinate structures designed for the same loads. In conventional elastic design methods, structures are designed with respect to the load at which the calculated maximum stress reaches the yield point, henceforth called the "initial yield load" of the structure. In the case of statically indeterminate structures (and to a lesser degree in determinate structures), a further increase in load may be realized even though yielding has occurred at some cross-sections.

Use of the so-called "simple plastic theory" has been suggested by a number of authors, who have

recommended design on the basis of ultimate strength. (19) (8) (16) It has been suggested that increased economy can be achieved if the design can be based on a load greater than that at initial yield.

Questions are occassionally raised with regard to the possible application of the simple plastic theory. One reason for such inquiries is that too little is known regarding the basic plastic behavior of steel structures. A study of the literature reveals, for example, that most of the previous experimental work involved specimens made of rectangular shaped sections and test models were usually normalized or annealed before test. Test models were restricted in size.

This report is one of a series in which the elastic and plastic behavior of full-size steel members and frames are being studied. (1) (2) (3) (4) In addition, the limitations and possibilities of plastic design and plastic analysis are being explored in this project being carried out at Lehigh University in the Fritz Engineering Laboratory under the direction of the Lehigh Project Subcommittee of Welding Research Council.*

---

* Members of this Subcommittee of the Structural Steel Committee are: (T. R. Higgins, Chairman, A. Amirikian, Lynn S. Beedle, H. C. Boardman, J. M. Crowley, S. Epstein, F. H. Frankland, LaMotte Grover, L. E. Grinter, H. D. Hussey, B. G. Johnston, J. Jones, C. Kreidler, H. W. Lawson, Bureau of Ships (Code 350, J. Vasta and E. M. MacCutcheon), N. M. Newmark, A. E. Poole, C. E. Webb, and W. H. Weiskopf.

In order to investigate the behavior of welded continuous frame structures, a series of tests on simulated frames and continuous beams were carried out to furnish additional information regarding elastic and initial plastic deformations and to correlate these results with existing analysis and design procedures. Single span beams with overhang were used to simulate continuous beams and frames with constant moment of inertia. Rolled steel wide flange sections were chosen in this program. All the beams had an overall length of twenty-eight feet and were tested in the as-delivered condition since the purpose of this program was to simulate the behavior of real structures as closely as possible.

It has been established that welding may introduce in structural members residual stresses of the same magnitude as the yield stress of the base material. Connection details introduce local concentrations of stress. Also, structural steel members in the as-delivered condition contain residual stresses due to cooling after rolling. The effects of these factors on the initial yield load have been observed and analyzed in this paper. The buckling strength of columns or beams under certain conditions will be reduced by the presence of residual stress and a brief examination is made of this influence.

Reserved for later reports are studies of the ultimate strength and deflections of continuous beams, inelastic local and lateral buckling of steel members, and shear failure in webs of WF sections.

(III) TEST PROGRAM

(1) TEST SET-UP

The set-up for the continuous beam program is shown schematically in Fig. 1. A beam, shown under test in Fig. 2, rests on two rollers that are in turn, supported by two columns. A 14WF136 section is used as the base beam.

Loading equipment, dynamometers, and instruments are similar to those described in Progress Report No. 2 (2)

A bracing frame was used to prevent lateral deflection, Fig. 3. The surfaces of the vertical guides were lubricated prior to the test, and the specimen was allowed to deflect vertically with only slight friction. A "friction" test was conducted prior to each main test to assure this condition. Such a bracing frame as shown in Fig. 3 will not prevent all motion in the lateral direction. More recently an improvement has been made in the design. Support is of the flex-bar type, a larger percentage of the lateral motion being prevented.

Apparatus for testing the control beam was identical to that used in the previous beam test program. (1) Over a 14-ft. span, third-point loading was applied through rollers on special loading brackets.

(2) TEST PROGRAM AND PREPARATION OF SPECIMEN

One simply-supported control beam and five continuous beams were tested, as listed in Table I.

Except for B3, all the continuous beams were tested to simulate a "fixed-ended" beam of 14-foot span, thereby also simulating the interior span of a continuous beam of many spans. This was accomplished by applying load at the ends of the overhanging portions sufficient to return the member to a level position at the supports after the application of each load increment. In Test B3 less than full restraint was provided at support points, the cantilever ends being maintained at the same deflection as at the supports; thus a single bay portal frame was simulated. Loading carriers welded to the specimen at each load point brought the applied load directly to the web of the beam, Table I.

Table I also shows the different details used on identical tests (2, 4 and 5) in order to give a range in the magnitude of possible welding effects including residual stress and stress concentration. In any one beam the same detail was used at each support. Case (a)

TABLE I - TESTS CONDUCTED ON SIMULATED CONTINUOUS BEAMS AND FRAMES AND ON CONTROL BEAM (B1)

Test Number	Size of Member	Loading	Support Detail
B_1	8WF40 (I)	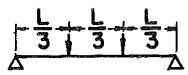	
B_2	"	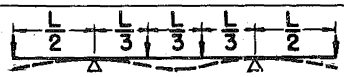	a
B_3	"		a
B_4	"		b
B_5	"	"	c
B_7	14WF30 (I)	"	b

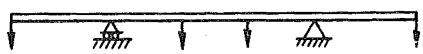

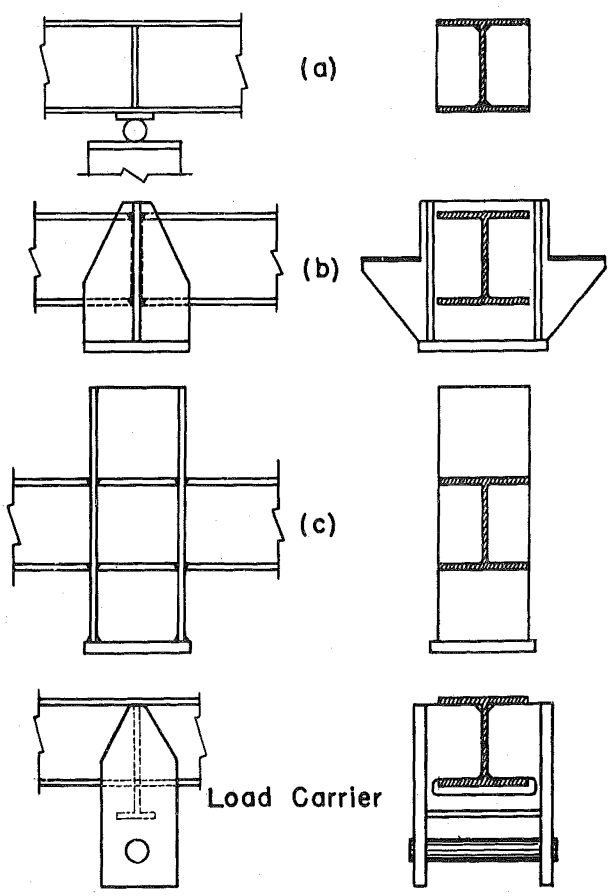

Connection Details

is the simplest form. The splice plate of case (b) involves more welding and is a common structural detail. Case (c) which involves the greatest amount of welding is typical of an interior connection.

In addition to the variables of stress concentration, type of connection, and of end restraint, a third variable studied in preliminary fashion was that of shape of section. B7 is identical with B4 except that a 14WF30 section was used rather than the 8WF40 shape. The former has the proportions of a beam section while the latter is a "column" section.

All specimens were tested in the as-delivered condition and had section properties as shown in Table i. Tension and compression coupons were tested from representative positions in the members.

TABLE i

Beam Section		Area	Depth	Flange Width	Flange Thickness	Web Thickness	I_x	Z_x
		in^2	in.	in.	in.	in.	$in.^4$	$in.^3$
8WF40	Hand Book	11.76	8.25	8.077	.558	.365	146.3	
	Measured	11.66	8.32	8.06	.552	.370	147.0	39.65
	%Variation	-0.85	+0.84	-0.87	-1.07	+1.37	+0.05	
14WF30	Hand Book	8.81	13.86	6.733	.383	.270	289.6	
	Measured	9.11	13.78	6.82	.382	.281	295.3	48.35
	%Variation	+3.33	-0.06	+1.50	-0.34	+1.1	+2.05	

(3) STRAIN GAGES, DEFLECTION GAGES AND LEVEL BARS

About sixty SR-4 strain gages were used on each test. Those near the support points of the beam were used to obtain the strain distribution in the elastic and plastic ranges to make possible a study of the combined effects of stress concentration, residual stress, and the change of mechanical properties of the material due to welding. AX-5 type strain gages were mounted on the web of the beam in the region of maximum shear stress. Uniaxial strain gages were also mounted along the pure bending section of the beam to secure data for experimental M-Ø curves. A typical strain gage layout on a test specimen is shown in Fig. 4.

On each continuous beam test deflectionswere measured at thirteen points along the beam using Ames dial gages. Measurements were referred to the neutral axis of the beam at the support points by means of the deflection gage supporting rig. The detail at the beam support point is shown in Fig. 5. Dial gages fitted with sharpened points were mounted on B4 and B5 between the upper and lower flanges near the supports to measure the local buckling of the compression flange.

Rotations at each load point were measured with level bars. In the test of beam B3 rotations were measured at the support points as well, Fig. 5. In the remainder of the program zero angle change was maintained at the supports.

On all tests except B2, two level bars were mounted perpendicular to the longitudinal axis of the beam to measure lateral buckling rotation of the central span. Level bar supports may be seen in Fig. 14.

Whitewash (hydrated lime) was applied to indicate the yielding pattern and the progression of yield zones.

(4) TEST PROCEDURE

The sequence of load increments, measurements, etc., was outlined before each test. Readings were set on the dynamometer strain indicators and loads were applied slowly, evenly, and in small increments to hold the reading and maintain constant the test condition of the specimen. Readings of dial gages, level bars and SR-4 gages were then taken.

When yielding occurs under constant load in the plastic range, a specified period of time must elapse to permit the penetration of yield zones into the specimen. An arbitrary criterion was adopted for taking readings under such circumstances as follows: When the increase of deflection in the central dial gage of the beam was less than 0.002" within 15 minutes, a complete set of readings was taken. The test then proceeded with another increment of load. Even this procedure meant that a single test required a considerable amount of time, usually approaching a week of continuous testing, on a 24-hour-per-day basis.

All tests except one were carried through the plastic range continuously, to avoid the discontinuous increase of strength of the beam introduced by the effect of strain aging. (Such an effect was observed in a previous investigation [1].) In the control beam test B1 loads were returned to zero after each increment to measure the permanent set.

Loads were kept constant while readings were taken. Curves of some deflection and strain data were plotted against load during each test as a check on the proper functioning of apparatus.

(IV) BENDING STRENGTH OF WF-SECTIONS UNDER PURE MOMENT

(1) M-Ø RELATION OF BENDING MEMBERS

In elastic and simple plastic beam theory the strain due to bending is assumed to very linearly over a cross-section normal to the axis of the beam. The stress and strain relation for each fibre of the bent member is assumed to be the same as that determined in a simple tension test. Tension and compression properties are assumed identical. The results of coupon tests are given in Appendix A.

In accordance with the assumptions of beam theory and assuming that the material does not exhibit an upper yield point, the M-Ø relation for a WF section has been computed and is plotted in Fig. 6.* It is based on an idealized stress-strain diagram that consists of two straight lines. At point 1 the elastic limit has been reached and $\emptyset_y = M_y/EI$. At point 2 the member is partially plastic. The bending moment in the beam section will approach a limit, point 3, as Ø becomes very large. The limiting moment is called the "plastic hinge moment", M_p.

---

* Calculation of M-Ø curves has been made in Progress Report No. 1 [1]. Ø, the curvature, is the unit angle change and is measured in radians per in.

$$M_p = \sigma_y Z,$$

where Z = plastic modulus; the static moment of the entire cross-section about its neutral axis.

σ_y = lower yield point stress.

In the simple plastic theory (typified by Fig. 6) the strain hardening effect of mild steel is neglected. (19) (8) Considering the strain-hardening effect measured on a number of test coupons a theoretical M-ϕ curve is shown in Fig. 7. Strain hardening commences when the unit rotation reaches ϕ_s (ten to twenty times the yield-point curvature) and at point 4 strain hardening is evident in the stress-distribution. The web material has a higher yield point than the flange and this has been taken into account as shown in the stress-distribution at point 3. Equations for calculating important points on this curve have been published (4).

The theoretical curves in both Figs. 6 and 7 are based upon the further assumptions that no local buckling occurs and that residual stresses are absent.

Experimental M-ϕ curves of continuous beams B2, B3, B4, and B5 plotted from deflection and strain gages are shown in Figs. 8 and 9. Similar data for control beam B1 are given in Figs. 10 and 11. These curves which extend only into the early plastic range show that the observed

plastic strength is as much as ten percent lower than the predicted value. On the other hand it has been observed in tests of annealed 4" I-beams at the Fritz Laboratory that higher strengths than the calculated values were indicated by the M-Ø curves.

These discrepancies between experiment and theory result from the rather crude assumption in the theory that plastic strain in uniformly proportional to the distance from the neutral axis of the beam. When yielding begins in the flanges of a WF-section, the plastic strain is assumed to be uniformly distributed as shown in Fig. 12 (1c). Actually local plastic zones are formed due to stress concentration and they penetrate the beam much deeper than assumed in the theory as in Fig. 12 (1d). At the same time some regions in the outer fiber of the flange are still in the elastic range. Figs. 14 and 16, (tests B3 and B7) show such localized yield zones as revealed by whitewash. The different stages of yielding are evident, with lines which penetrate to different depths. Yielded zones in highly polished rectangular specimens have been photographed by Roderick and Phillips. (16) Kohlbounner (13) tested a series of I-beams and observed that the specimens yielded in a layer by layer action. Thence, he concluded that such beams can not be considered as quasi-isotropic in the plastic range.

Thus the stress and strain relation as described in connection with Figs. 6 and 7 cannot hold true either at the plastic zones or in the elastic zones of a section under the same moment. For a beam under a certain constant moment, the average value of ϕ of the member will depend on the number of local plastic zones initiated. Since the initiation of local plastic zones is affected by stress concentrations, residual stresses and non-uniform mechanical properties of the material, the ϕ-value at a cross-section of a bending member is therefore not a function of the moment alone. Different ϕ-values may be obtained at a section under the same moment due to the presence of the above factors. Since the geometric shape and heat treatment of the bending member will affect stress concentration and residual stresses, the early part of the M-ϕ relation of the member is consequently also affected by them.

Thus, depending directly on the mode of yielding of structural steel and indirectly on stress-concentration and residual stress, a larger or smaller ϕ-value is obtained at a particular moment. This means that the simple plastic theory will not predict structural behavior as closely as elastic theory since the assumptions are but rough approximations to what actually happens in the structural member.

Although no positive proof is given, the fact that as-delivered specimens consistently show a lower strength than that predicted by the simple plastic theory (based on the measured material properties) may thus be explained partly on the basis of stress-concentration and residual stress in the member. There are an increased number of local plastic yield zones, and the formation of these local plastic zones in the beam section will result in a higher ϕ-value even though the moment is kept unchanged since portions of the beam yield which are assumed to be elastic in the theory.

Referring to Fig. 15, this photograph of beam B7 was taken at a moment of 1580 in-kips well below the predicted yield moment of 1640 in-kips. The yield zones are just beginning to penetrate into the web and the measured ϕ-value is about .00026 rad/in as determined from an average of strain measurements. (Fig. 24). In Fig. 16 the moment on the section under pure bending is 1611 in-kips, still below the theoretical initial yield moment, but the ϕ-value has increased to about .00035 radians per inch as the yield zones extended further toward the neutral axis.

Similar evidence is available from the tests in which an 8WF40 section was used. Referring to Fig. 17 (M = 1150 in-kips, ϕ = .00032 rad/in), yield zones have formed in the compression flange.* Fig. 8 shows

---

* The formation of these lines will be discussed later.

that this yielding was accompanied by a sudden increase in ϕ due to the formation of yield zones at this load. In Fig. 18, yield zones are shown in the compression flange of the central portion of B3 at a moment of 1250 in-kips (the calculated yield moment is 1325 in-kips). The measured curvature of .00036 rad/in (Fig. 8,9) is greater than predicted by the theory.

As the rotation of the member increases, the plastic zones spread toward the neutral axis and the strain distribution of the actual case (Fig. 12 (2d)) then approaches the one assumed in the theory as in Fig. 12 (2c). At the larger rotations the moment should approach that predicted by the simple plastic theory.

This hypothesis has been confirmed by test results as indicated in the M-ϕ curves plotted in Fig. 13. These M-ϕ curves for 3 different beams were plotted from strain gages located near the support as shown in the same figure. A discrepancy between the experimental and theoretical values is shown in the early part of the curves, but the experimental curve approaches the theoretical value as the plastic zone extends closer to the neutral axis of the beam.

It is emphasized that the measurements of Fig. 13 are near a support in a region of moment gradient. Thus large local unit angle changes are restricted to a relatively short length of beam. In the center, however,

where the moment is uniform, a very large over all rotation is required before the local rotations become large. This is evident from Fig. 19 where, in spite of the large rotations, the ϕ-values are still less than those coincident with strain-hardening.

Fig. 13 shows that the later increase in moment with increase in ϕ occurs prior to the onset of strain-hardening, the slope of the experimental curves being greater than any measured in a region of strain-hardening. The theoretical curve of Fig. 13 is based on the measured material properties and takes strain-hardening into account.

Suppose now, that the member is well-annealed, removing the cooling and welding residual stresses. Better agreement with theory in the early part of the M-ϕ curve is observed. In the 4" annealed I-beam tests mentioned earlier, the observed strength was higher than the predicted value. Fig. 20 shows such a beam. Yield zones evident from the white wash, are not distributed along the beam in the section under uniform moment as was the case for as-delivered specimens but are concentrated near the load points. Yielding was initiated at the load points due to stress concentration and as the load was increased, the yielded zones gradually progressed toward the center of the beam span from each support. However, the measurement of ϕ was made

at the center. The central portion, though under the same moment, was still in the elastic range while the section near the loading points went very far into the plastic range. No plastic zone started at the central portion possibly because the beam was annealed and its mechanical properties quite uniform. On the other hand, the beginning of plastic zones in the continuous beam tests was quite different. In the central span which was under constant moment, yield lines were initiated at several places when the load reached a certain value, as shown in Fig. 17 and 18. Residual stresses introduced due to cooling after rolling in the continuous beam probably are the reason for the initiation of more plastic zones in as-delivered beams because the mechanical properties are not uniform.

The behavior observed in the annealed 4" I-beam tests is in confirmation of the phenomenon that a lower stress is required to begin a slip band adjacent to one already formed than to initiate an original band. (22) The stress-relief anneal for the member was probably effective in making uniform the mechanical properties, raising the upper yield point (this effect was actually observed in some of the beam tests), facilitating the formation of slip bands adjacent to ones already formed rather than along the beam.

The M-Ø curve for beam B7 (14WF30 section) is plotted in Fig. 21. Owing to its geometric shape, severe local and lateral plastic buckling was observed in this specimen. Thus this M-Ø curve failed to reach the calculated value even after the yielding deeply penetrated into the web, see Fig. 22. The problem of plastic buckling will be discussed in a later report.

In engineering design, due to the fact that the deflection of a structure must usually be held within a certain limit, the early part of the M-Ø curves will be a region of importance (3). Thus, the reduction (due, indirectly, to residual stress) imposes a possible limitation on the use of plastic design methods. The supports of a completely restrained beam must rotate about 8 times the elastic limit value before the last plastic hinge is formed (4). This is beyond the value at which the moment is less than predicted for the example shown in Fig. 13 so that no over all reduction would be experienced. However, if the last "plastic hinge" were in a uniform moment section then a reduction in strength is to be expected if one is to ignore the counteracting influence of strain-hardening.

Not to be overlooked is the importance of annealing. Investigators using rectangular sections consistently report good agreement between test and the simple plastic theory, and as previously pointed out, good agreement

was observed with annealed WF [redacted] specimens previously tested as simple beams at the Fritz Engineering Laboratory.

(2) STRAIN DISTRIBUTION IN PLASTIC BENDING

In the previous section it was pointed out that in the early part of the plastic range, local plastic zones are initiated in the constant moment portions of the continuous beams. It is obvious then that the assumption of linear strain distribution does not hold true in the plastic range. When the beam is also under shear force due to a transverse load, this assumption is even further from the actual case. Figs. 23 (1) (B7) and 23 (2) (B2) show the strain distribution in beam sections under pure bending. Fig. 23 (3) shows the strain distribution of a beam section under bending and small shear force. Fig. 23 (4) shows a section under bending and high shear force. These diagrams indicate that the assumption holds very well in the elastic range, but not in the plastic range.

The discrepancy between the assumed and the actual strain distribution at one section may be very high, but the integrated angle change and deflection over a certain length of the beam by using the assumption may still give close agreement with the test results.

Actually the deformation curve of a member under bending in the plastic range is determined by the portion which remains elastic. It is not necessary that the

strain in the plastic region be proportional to the distance from the neutral axis. The magnitude of it can be any value larger than ϵ_y, the maximum elastic strain, if strain hardening is not considered.

M-Ø curves plotted from measurements of strain on the webs of tested beams show that the M-Ø relation of a section is not much affected by the localized plastic strains in the outer fibers which were seen in Fig. 23. Fig. 24 and Fig. 25 show the M-Ø curves of two different sections of Beam B7; one under pure moment and the other under bending moment and small shear force. Considering each location separately the three sets of gages are in reasonable agreement with one another.

(V) YIELD STRENGTH OF CONTINUOUS STEEL BEAMS

(1) FACTORS AFFECTING THE YIELD STRENGTH OF STEEL MEMBERS

In structural design, calculation of the initial yield load by conventional elastic theory usually excludes such factors as residual stress and stress concentration. The nature of these factors is discussed in the following paragraphs and some typical residual stress distributions are shown.

a. Residual Stress due to Non-uniform cooling after rolling

As-delivered rolled sections contain residual stresses caused by uneven cooling after rolling. Since the finishing rolling temperature of steel sections is above the recrystalization temperature, it is not likely that rolling, as such, introduces residual stress.

As an example of the formation of residual stress due to uneven cooling in a WF beam, assume that the temperature after rolling is uniform and that there are no residual stresses in the section. The cooling rate at the central part of the flange is lower than at the edges. The greater contractions of the two edges due to the proportionately higher cooling rates would cause compression stresses at the central part of the flange and tensile stresses at the two edges. If no plastic

flow occurred during cooling, this thermal stress would disappear when the temperature again became uniform. It is known however, that the tensile or compressive strength of steel is low at high temperature. Compressive thermal strains introduced at the center may exceed the corresponding compressive strength during cooling. Plastic flow will then take place at the central part of the flange. Subsequently, when the member is cooled to room temperature, the central portion of the flange will be left with tensile residual stress and the edges with compressive residual stress.

The residual strain measured in the flanges of WF-sections in Progress Report 1 [1] are reproduced in Fig. 26. As expected the edges are in compression and the center in tension.

The initiation of yielding and progression of yield lines in the continuous beam tests may be deduced from the known residual stress pattern. Measurements show that the compression residual stress at the edge of the flange is higher than the tensile stress at the center. This has also been observed by other investigators [20]. Thus, in bending, the edge of the compression flange should reach the yield stress first, and yield lines should be initiated there. On the other hand, the tension flange of the same section of the beam should reach the yield stress at a higher load and its yield zones should be

initiated at the center of the flange. The yield zones will be initiated in both the tension and the compression flanges at loads that are theoretically less than the calculated initial yield load neglecting residual stress.

Fig. 28 shows the first appearance of yield lines in the central span of B4 on the compression flange at the edge (load W = 46 kips). Fig. 29 shows the initial yield lines in the tension flange which started at the center of the span well after the development of lines in the compression flange (W = 54 kips). When strain gages are mounted on the tension and compression flanges, the compression flange consistently reaches the yield stress first. The compression and tension yield points have the same average. (See Appendix A).

In a recent inspection it has been observed that no yield lines are formed due to cooling and prior to cold straightening of the member. A rough appearance of the mill scale at the junction of the web and flange is the only visible evidence of the plastic deformation which occurred there during the cooling cycle.

b. Residual Stress due to Cold Bending or Cambering

Rolled sections are usually slightly bowed after rolling due to differential cooling rates. Cold bending is nearly always necessary to straighten the sections in

the mill before delivery. Due to such bending beyond the yield strength, a pattern of residual stress is usually left in some parts of the rolled section which differs from the cooling residual stress pattern. A typical distribution of residual stress due to cold bending is shown in Fig. a.*

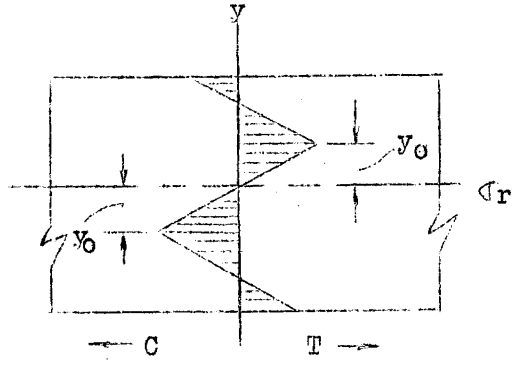

Fig. a:- Residual stress due to cold bending.

The magnitude of residual stress along the section will be:**

$$\sigma_{r1} = \sigma_y \left[\frac{y}{I} \left(\frac{I_p}{y_o} - Z_p \right) - \left(\frac{y - y_o}{y_o} \right) \right] \text{-------(1)}$$

$$\sigma_{r2} = \frac{\sigma_y\, y}{I} \left[\frac{I_p}{y_o} - Z_p \right] \text{----------(2)}$$

---

* In a discussion of residual stresses due to cold bending, Timoshenko [17] shows the distribution for a rectangular cross-section deformed initially to its ultimate strength and then unloaded.

** The derivation is in Appendix B, Eqs. 18, 19.

Subscripts 1 and 2 refer to the stress when y is greater than or less than y_o respectively.

σ_y = yield point stress

y = distance to fibre from the neutral axis

I_p = moment of inertia of the plastic part

Z_p = plastic modulus of the plastic part

y_o = distance to point of maximum penetration of yielding

I = moment of inertia

The maximum possible residual stress occurs when y_o approaches zero ($M_o = M_p$) and

$$(\sigma_r)_{max} = \sigma_y. \text{ ----------(3)}$$

The existence of the pattern of residual stress shown in Fig. a will either raise or lower the initial yield strength of the section depending upon the direction of M_o and the subsequently applied moment. The above expressions apply no matter about which axis the member is bent. Fig. 30 and 31 show Lueder's lines on the mill scale of a rolled section prior to test. Fig. 30 with its diagonal lines shows a member which was probably cold bent ("gagged") in such a way that the flange shown was under tension. Thus yield lines, inclined at about 45° to the beam axis and caused by tensile stress, are in evidence near the center of the flange where the tensile

residual stress due to cooling is located. Such is not the case in Fig. 31, the lines formed probably being due to cold bending about the weak axis. The similarity of these patterns of yield lines with those seen during the conduct of beam tests is confirmation that the yielding is due to cold bending.

The residual stress pattern measured across another WF-section, (1) is reproduced here in Fig. 27. The pattern is one which would be expected from cold bending.

The practice of cambering steel members undoubtedly leaves a similar stress pattern to that shown in Fig. a. The initial yield strength of the member would be reduced by the residual stresses if load is applied in a direction opposite to that of the camber. Unfortunately, the load applied to a cambered section of a bridge or craine girder is usually in this "weaker" direction, so that a lowering of yield strength would be expected. This problem is now examined.

According to the A.I.S.C. handbook, the maximum camber of a 21 WF 112 beam with a span of 25' is 1". The maximum moment applied at every section of the beam during cambering is assumed to be a constant (beam under pure bending). Thus the curvature after cambering is also a constant, or, from Eq. 15 of Appendix B,

$$\frac{d^2v}{dx^2} = -\frac{\sigma_y}{EI}\left[\frac{I_p}{y_o} - Z_p\right] = C_1 \qquad \text{----------(4)}$$

$$\frac{dv}{dx} = C_1 x + C_2$$

$$v = \frac{C_1 x^2}{2} + C_2 x + C_3 \text{ ----------(5)}$$

At

$$x = 0,\ v = 0$$

$$x = L,\ v = 0$$

Thus, $C_3 = 0$

and $C_2 = -\frac{C_1 L}{2}$

From Eq. (5),

$$v = \frac{C_1}{2} x^2 - Lx$$

Now, at $x = L/2$, $v = 1"$, the maximum camber; therefore

$$C_1 = -\frac{8}{L^2}$$

Substituting into Eq. (4),

$$\frac{I_p}{y_o} - Z_p = + \frac{8\ EI}{L^2 \sigma_y}$$

For the assumed problem,

$$L = 12 \times 25 \text{ in.}$$

$$I = 2621 \text{ in.}^4$$

and assuming

$$E = 30 \times 10^3 \text{ ksi}$$

$$\sigma_y = 33 \text{ ksi}$$

then,

$$\frac{I_p}{y_o} - Z_p = 204 \text{ in.}^3$$

Solving the above equation,

$$y_o = 5.5''$$

At the extreme fibre (eq. (21) of Appendix B)

$$\sigma_{r1} = \sigma_y \left[\frac{h}{2I} \left(\frac{I_p}{y_o} - Z_p \right) - \left(\frac{h-2\,y_o}{2\,y_o} \right) \right]$$

and by substituting the known quantities,

$$\sigma_{r1} = -0.096\,\sigma_y$$

The negative sign signifies that the stress at the extreme fibre of the member is reversed after the load is removed. The flange loaded in tension during cambering would thus contain compression residual stresses at the extreme fibre. But this flange is normally the compression flange when used in a structure such as a bridge. Thus there is a reduction of yield strength of the member due to cambering of approximately ten percent.

However, cambering will remove other residual stresses in the flanges (welding, cooling and cold straightening) which in themselves tend to reduce the initial yield load. Thus the exact magnitude of the reduction in yield strength due to cambering is expected to be quite variable. Theoretically, the ultimate strength would not be affected by the cambering process -- only the initial yield load.

c. Residual Stresses due to Welding

Residual stresses are developed in welded structures when dimension changes in heating and cooling cannot take place freely. (5) These are similar to those developed due to uneven cooling as discussed previously. The pattern of welding residual stress is usually very complicated because a large number of factors are involved such as the type of welds, the material, the welding procedure and the shape of the structure to be welded.

In the members tested in this program the welding involved was all in the vicinity of connections and load carriers. Thus the welding residual stresses would be localized and the pattern complex. The surface yield lines produced by welding load carrying stiffeners were shown in Fig. 27 of Progress Report No. 1 (1).

In the event structural beams were built up by welding web plates to flange plates, a pattern of stresses should be obtained similar to that found due to cooling residual stresses described earlier. The mechanism for formation of these welding residual stresses is similar (6); tensile stresses would be found at the junction of web and flange and compressive stresses at the flange edges. Thus the superposition of bending stresses on the member is expected to have a similar effect to that described earlier. This has been

confirmed in the test of built-up connections described in Progress Report 4, Part I. (4) See for example Fig. 48 of that paper.

d. Stress Concentration

The ordinary beam theory generally used in structural design will not predict precisely the stress distribution at the ends or support points of a structural member. Discontinuities introduced by welds, supports, and changes of section occurring in a structural member cause local stress concentrations. Therefore, local yielding usually takes place in the structure well below the calculated initial yield load. As a result, early non-linear behavior may be expected.

The three different support details shown in Table I were adopted in part to vary the magnitude of stress concentration. Although detail (a) involves the least amount of welding, the disturbance to the assumed shear distribution will probably be the greatest since the flange rests directly on the support. Cases (b) and (c), together with the load carriers, would provide more nearly the theoretically assumed shear distribution, but some deviation is still to be expected.

(2) TEST RESULTS AND DISCUSSION

The combined effects of welding residual stress and stress concentration cause local yielding at low loads at the supports. At portions of the member removed from the connections the cooling or cold-straightening residual stresses will cause a reduction in the load at which yielding first occurs and this yielding may extend over a greater length of beam than that due to welding residual stress. The seriousness of residual stress in a member under flexure will depend in part on the resultant influence on the load-deformation relationship.

Local yielding at supports and load points generally changes the linear load-deflection relation into a non-linear one, but the change is usually very small. On the other hand, when the load carrying stresses exceed the yield stress level, the change in the load-deflection relation is usually more drastic. Hardy Cross (9) has differentiated between "load-carrying stresses" and "participation stresses" and has emphasized the importance of evaluating the relative importance of the latter. Residual stresses due to welding at supports and the accompanying stress-concentrations constitute a "participation stress" that is not serious. On the other hand the participation stress due to cooling residual stress will be of greater importance since it is distri-

buted all along the member. Thus in Fig. 16 where the beam is under pure bending, the addition of load-carrying and participation stresses would produce yielding all along the member at a lower load than predicted, resulting in a greater increase in deflection.

In most structures excessive deflections are objectionable. The justification for the present design methods that largely ignore residual and local stress concentration is the fact that the deflections of structures so designed are automatically limited. The criterion of strength of structures in reality always has been one of deflection rather than stress, so long as the stress level did not violate some other design condition. Consequently, the over-all influence of residual stress and stress concentration on the strength of a structure may be evaluated by considering the influence of these combined factors upon the deformations.

In the following paragraphs the data has been arranged under a number of headings which classify the means by which stress concentration and residual stress has been evaluated: i.e., (a) Local Plastic Flow, (b) Strain Measurements, (c) M-ϕ Measurements, and (d) Deflection Measurements. Two additional sections have been included. In (e) dealing with welding residuals at supports, moment-load relations are studied; section (f) is a summary.

a. Local Plastic Flow

Table ii indicates loads at which yield lines first appeared at supports and at loading points as a result of stress concentration and welding residual stresses combined with load carrying stresses. The location of yield lines is at the supports and load carriers, the lines usually forming in the web in a manner which indicates that yielding occurred due to combined bending moment and shear force. Fig. 32 shows the location of the first observed yield lines in test B7 and is typical of the first yield zones. Fig. 33 and 34 show lines at supports and load points where welding residual stress is probably an important factor. In this particular test (B4) these lines were formed at the load increment which followed that in which lines similar to those in Fig. 32 were formed.

TABLE ii - OBSERVED FIRST YIELD LINES

Beam No.	Load At Which Yield Lines First Appeared kips	Calculated Initial Yield Load kips	100x Col 2/ Col 3 %
B2	9	35.5	25.4
B3	10.5	47.5	22.2
B4	15	35.5	42.3
B5	18	35.5	50.6
B7	18	43.8	41.6

Table ii shows that local yielding occurred at loads as low as about 25% of the calculated initial yield load. B2 and B3 yield at the lowest loads, and one possible reason is that the reaction at the supports is transmitted directly through the flange to the stiffener (see Table I). The stress concentration factor is undoubtedly greater than in the case of B4, B5, and B7. Also, since B2 and B3 were not spliced at the support, a greater amount of welding residual stress was probably present.

The tests show that local yielding occurs at proportionately lower loads when the member is continuous over the support (B2 and B3) than when the support load is transmitted to the member by a splice plate (B4, B7) or a column stub (B5). In the latter cases local yielding occurred at about 45% of the calculated initial yield load.

b. Strain Measurements

The arrangement of SR-4 gages mounted on the flange of B3 in the vicinity of the support is shown in Fig. 4. These gages were installed to observe variations in strain due to stress-concentration and residual stress. The data from the strain gages on the top flange over the support is plotted in Fig. 35. As determined by a deviation from a straight-line relationship, local yield

was observed at a load of about W = 24 kips while the calculated initial yield load for the beam is W = 47.5 kips. The earliest deviation is observed at gage No. 9 directly over the support point. The influence of the connection disappears very rapidly. (Compare gages 8 and 7 with No. 9). The relative increase in strain at loads below 30 kips for gages 10 and 11 is possibly due to the fact that the gages are located in a region of high shear and since the web does not carry its proportionate share of the moment the flanges carry increased strain.

The data from strain gages mounted on B5 also indicate a non-linear behavior at low loads close to the support. Figs. 36, 37 and 38 show that the outer fiber of the beam section 2 inches from the juncture with the columns started to yield at a much lower moment than the sections which were 6 inches from each column. At 16 inches distance from the column flange (Fig. 38) the discrepancy between test and theory is still less although local deviations still exist.

Rosette gages mounted on the web of B4 make possible the comparison of experimental with the theoretically predicted maximum strain distribution on the web of the beam near a support and a load point. These relationships are shown in Fig. 39. The early portion of the average experimental curves are very close to the theoretical ones. However, local yielding caused deviation

between experimental and theoretical curves as the loads were increased. The theoretical moment shear strain curves in Fig. 39 were computed on the basis of shear and flexure beam formulas.

c. M-Ø Measurements at Beam Center

The strain data just presented were all collected from gages located at the supports or load points and are thus sensitive to stress-concentrations and welding residual stresses. Since these two factors are not present in the center of the beam span, the influence of the cooling residual stresses may be observed from M-Ø curves previously presented , Figs. 8, 9, 10, 11 and 24. Comparing the experimental moment carried at the predicted initial yield rotation, $\emptyset_y$, with the theoretical value, the % reduction in moment due to cooling residual stress is shown in Table iii.

TABLE iii - THE REDUCTION IN YIELD STRENGTH DUE TO COOLING RESIDUAL STRESSES

Beam	Calculated Initial Yield Moment	Observed Moment at Calculated $\emptyset_y$	% Reduction of Moment
B2	1325	1180	10.9
B3	1325	124C	6.4
B4	1325	1190	10.2
B5	1325	1200	9.5
B7	1636	1510	7.5

The reduction ranges from about 6% to 11%. Examination of Figs. 8, 9, 10, 11 and 24 show that the % increase in ϕ at the calculated initial yield moment is greater than the above percentage reductions in moment.

d. Deflection Measurements

Non-linear behavior due to local yielding at loads lower than predicted is reflected in the load deflection curves.

The values of the initial yield load and corresponding deflections of the beams have been theoretically calculated and are tabulated with results of tests as shown in Table iv. It indicates the overall influence of residual stress and stress-concentration upon yield strength. Two methods of comparison have been used to specify the "Yield Strength". Measured and theoretical deflections are compared at the calculated initial yield load (column 5) and measured and theoretical loads are compared at the calculated initial yield deflection (column 7). Fig. b demonstrates the method by which the data in Table iv was obtained, the increment of deflection at P_y and the reduction of strength at δ_y being indicated.

TABLE iv - YIELD STRENGTH OF CONTINUOUS BEAMS

Comparison of ℄ Deflections at Calculated Initial Yield Load				
Beam No.	Calculated Initial Yield Load kips	Cal. ℄ Defl. at Initial Load (in.)	Obs. Defl. at Cal. Initial Load (in.)	% Increment of Defl.
Column 1	Column 2	Column 3	Column 4	Column 5
B2	35.5	.30	.42	40.0%
B3	47.5	.79	1.47	88.0%
B4	35.5	.30	.41	36.6%
B5	35.5	.30	.34	13.3%
B7	43.8	.178	.24	35.8%

Comparison of Load at Calculated Initial Yield ℄ Deflection		
Beam No.	Observed Load at Calculated Deflections kips	% Red. of Load
	Column 6	Column 7
B2	27	23.9
B3	40.5	14.7
B4	28	21.1
B5	32	9.9
B7	33	24.1

B2, B4, B5, B7 B3

LOAD DETAILS

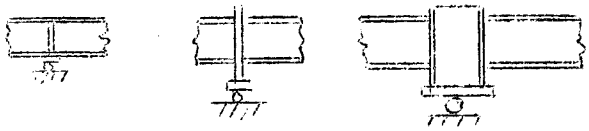

B2,B3 B4, B7 B5

SUPPORT DETAILS

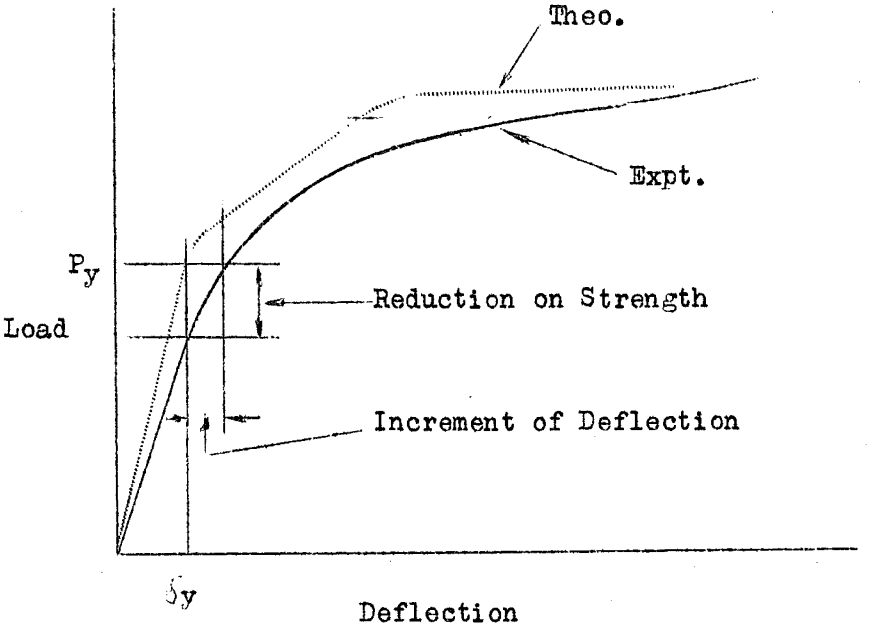

Fig. b:- Hypothetical load deflection curve showing method for determining the yield strength.

The experimental load-deflection curves are shown in Figs. 43, 44, and 45.

The tests show that the beams reached the calculated deflections at lower loads than predicted (ranging from 10% to 25%) and that at the calculated initial yield load the deflections were greater than predicted (ranging from 13 to 88 percent).

The effects of local yielding on the deflection of structures also depends on the type of loading (or restraint) on them. Beam B3 was tested to simulate a single-span frame. The ends of the two over-hanging beams were maintained at the

same elevations as the two supports. The loading and simulated frame are shown in Fig. c. In the elastic range the moment diagram of the beam will then be such that the moments at the supports and the center are equal (Fig. c).

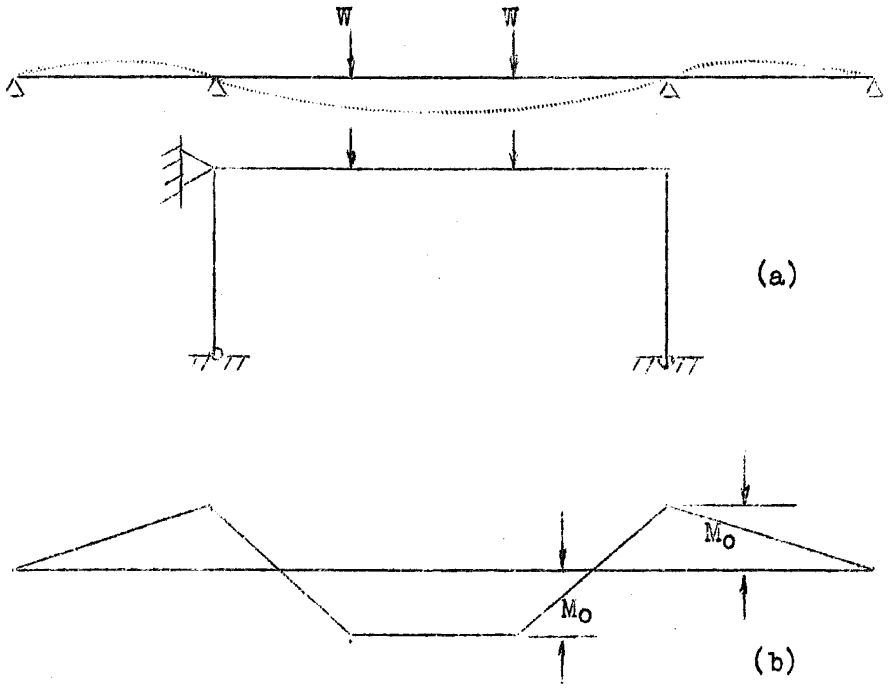

Fig. c:- Test B3. Loading arrangement and distribution of moment.

The calculated initial yield load is W = 47.5 kips at which both moments should be the same and equal to 1325 inch-kips. The corresponding calculated maximum deflection will be 0.79 inches. At the same load the deflection observed in the test was 88% greater. (Table iv).

The percentage increment of deflection at the calculated initial yield load for the rest of beams in Table iv is smaller. In tests 2, 4, 5, and 7 "fixed-ended" conditions were simulated at the supports. Fig. d shows the corresponding moment diagram.

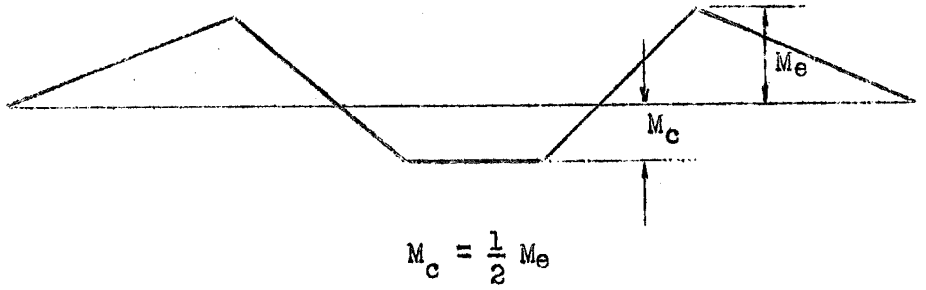

Fig. d:- Distribution of moment in Tests 2, 4, 5, 7.

In this case, the two ends of the central section of the beam will start to yield before the theoretical initial yield load of the beam is reached. But the theoretical magnitude of the moment in the central section is only one half that of the support moment when the beam is perfectly elastic. Therefore, the central section should not start to yield at all until the load on the beam has increased by a certain amount. During this period the end sections will continue to deform, and before the central section yields the support moments will approach the plastic hinge moments. Thus, the effects of residual stress and stress concentration at the

ends will largely be eliminated. The deflection of the beam at the initial yield load will still be higher than the calculated value, but the ratio of increasing deflection will not be as great as in the case of B3.

Comparing B2, B4, and B5 (Table iv), the only variable is the connection detail. The sequence of decreasing increment of deflection is accounted for, in part, by the increased restraint against shear deformation provided by the increased stiffness of the connections.

Table iv also shows that B4 and B7 -- identical except for shape of cross-section -- behaved in similar fashion in the region of their respective initial yield loads. Thus, from these tests there is no significant influence of shape of section on the yield strength. It is expected that this may not be true in the plastic range.

In some structures deflection is critical. In others, large deformations may be tolerated. The above discussion and the comparisons made in Table iv concern the region of the initial yield load. This was done because the statistical nature of the factor of safety does not eliminate the possibility of loads exceeding the working load. However, when deflections are examined in routine procedures, the limitation is usually based on the deflection at working loads. Table v presents a comparison similar to that contained in Table iv except at the working load.

TABLE v

Beams Limited by Load				
Beam No.	Working[1] Load	Cal. Defl. at Working Load	Obs. Defl. at Working Load	% Increment of Deflection
B2	21.5	0.18	0.21	16.7
B3	28.8	0.48	0.52	8.3
B4	21.5	0.18	0.18	0
B5	21.5	0.18	0.21	16.7
B7	26.5	0.11	0.13	18.2

Beams Limited by Deflection				
Beam No.	Limit[2] Deflection	Load at Limit Deflection		% Reduction in Load
		Theoret.	Exper.	
B2	0.47	-	-	-
B3	0.47	28.1	25.9	7.8
B4	0.47	-	-	-
B5	0.47	-	-	-
B7	0.47	-	-	-

---

1 Elastic limit load ÷ 1.65

2 AISC Specification - 1/360 x span length in inches

Deflections are larger than predicted ranging from zero to about 18%. If the deflection were to be limited by the AISC specification it would be necessary to reduce the theoretical working load for B3 from 28.8 kips to 28.1 kips. Due to residual stress and stress concentration, Table v indicates a further reduction of about 8%.

c. Welding Residual Stress at Supports

The effect of welding residual stress at supports has been considered by Amirikian [7]. The example is reproduced in Fig. 40 for illustration. The "decrease" shown in (c) is a decrease in moment at the support over that which would be theoretically computed and does not represent an actual reduction in moment under increasing loads. For example, a variation in the experimental moment-curvature relationship such as that shown by the solid line in Fig. c indicates, for a given end rotation ϕ_1, that the connection will carry only a moment M_1 instead of the predicted moment M_y.

Quoting from Reference 7, "Under dead loading as well as under initial applied loading, the changes of stress in members of a frame due to plastic yielding at the joints may be of such magnitude as to require a revision of our present methods of analysis of continuous structures".

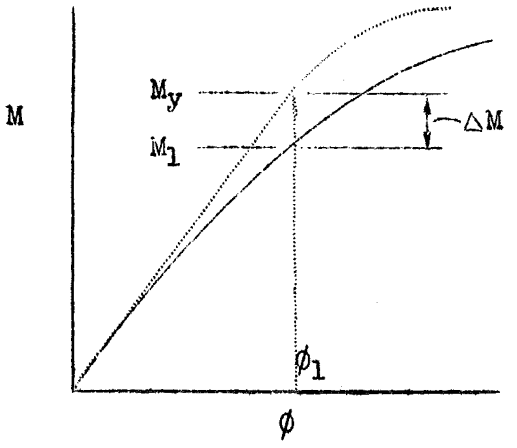

Fig. e:- Hypothetical decrease in moment capacity at a joint for a given unit rotation.

For simplicity, assume that the ends of the beam are built-in. In Fig. f the moments at the central section and at the two ends of the beam are plotted against the load. The dotted

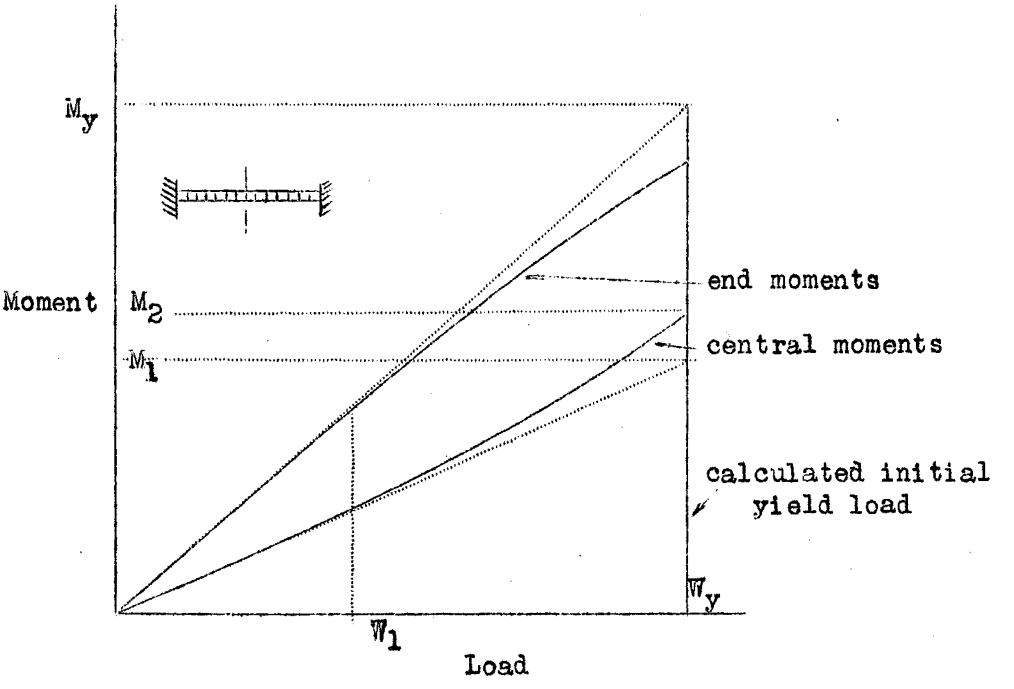

Fig. f:- Hypothetical moment load characteristics of beam with welding effects at joints.

lines represent the elastic case where end moments have a value equal to 50% of the central moment. Assuming typical inelastic behavior shown in Fig. 40 at a load W_1, the center section is called upon to carry a greater moment than predicted (M_2 instead of $M_1 = 1/2\ M_y$).

When the results of the continuous beam tests are presented in this manner (Fig. 41) they do not show the redistribution of moment expected according to the previous discussion. (The dotted lines represent theoretical curves which have been determined by a numerical integration process).* But this does not mean that there was no local plastic yielding at the supports below the calculated yield load. In fact it has already been demonstrated that this did occur. The redistribution of moments shown in Fig. f is under the assumption that the central part of the beam does not yield locally. In the tested beams local yielding occurred both at the supports and in the central section near the loading point. Examples were given in Fig. 32, 33 and 34. Therefore, the curves in Fig. 41 do not show significant redistribution of end and central moments at loads below their calculated initial yield strength because the effects of local yielding at supports are offset by local yielding at load points.

---

* Similar theoretical curves have been used by Horne (12) in a paper which describes (on a theoretical basis) the influence of strain-hardening on the ultimate strength.

A more critical case, theoretically, is that of the fixed-ended beam with central concentrated load. In Fig. g,

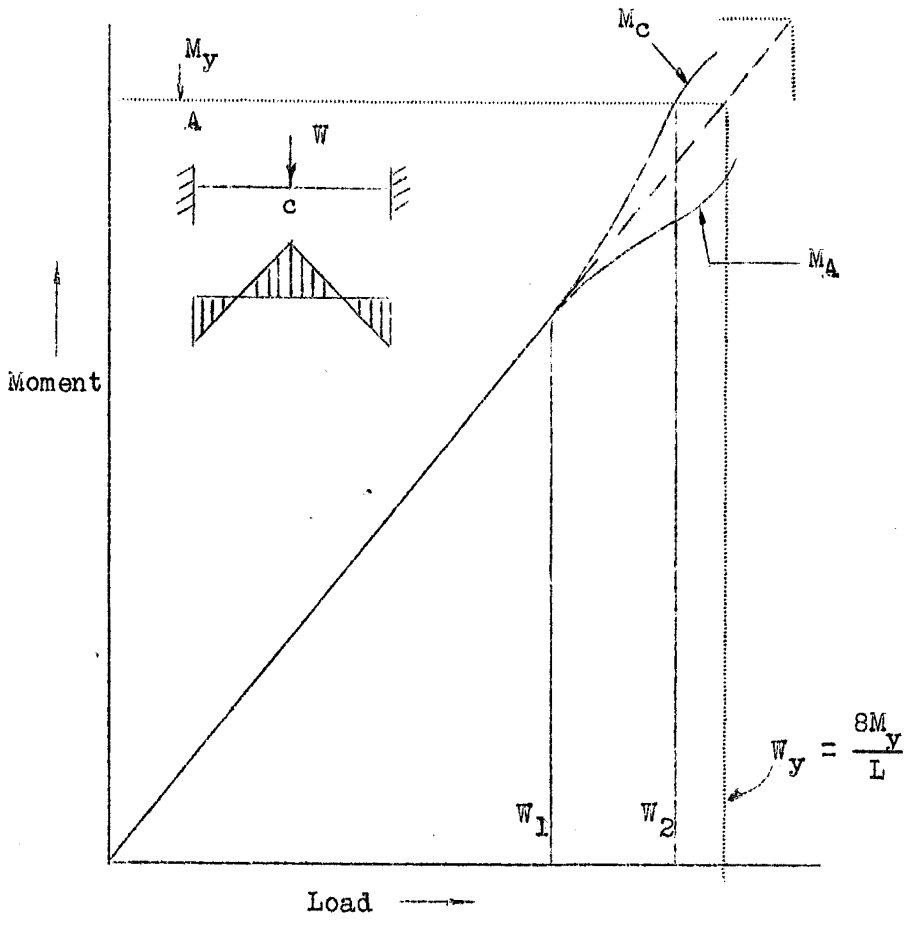

Fig. g:- Hypothetical redistribution of moment due to yielding at supports only.

if at load W_1 the connection yields, then the center is called upon to carry greater moment than predicted. Thus when load W_2 is reached the central section will yield at a load which is less than W_y. On the other hand if local yielding only occurs at the central section of the beam

and the connections remain perfectly elastic, the moment will be increased at the supports. B3, although of different loading and end restraint, also has equal moments at the center and the support and its behavior shown in Fig. 41 indicates that the distribution of moment was not affected substantially.

These tests show that the welding of a stiffener between flanges causes local yielding at lower bending moments and is thus of more significance than yielding in butt welds to splice plates and columns. In B4, for example, flange yielding occurred over the support (Fig. 33) and the load point (Fig. 34) at the same time and at a load of about 18 kips. However the moment at the support is twice as great as that at the center, indicating a more serious condition created by the load-carrier and intermediate stiffener. In Fig. 41 no deviation in the moment-load relation from theoretical values is seen at a load of 18 kips. (In Fig. 43 B4 does indicate an increase in deflection). Thus the effects of yielding at supports and load points offset one another. This is also true of B5 and B7 where the details are similar. The slight discrepancy in B2 and B3 (Fig. 41) is observed because the support detail is an intermediate stiffener and is similar in its welding effects to the load-carrier (Table I). As predicted by Amirikian, a change in moment-distribution occurs, but the deviation is of small magnitude and does not exceed about 8% at the theoretical initial yield load.

Local yielding did increase the deflections of the beams by larger increments, percentagewise, as was shown in Table iv. The load-deflection curves of the beams tested are shown in Figs. 43, 44, and 45. The theoretical curves are indicated by the dashed lines in each case. A portion of the improved behavior of B4 over B2 and B5 over B4 is due to the increased stiffness of connections which has been mentioned earlier. Yielding of the web due to shear force occurred on the two sections that extend between the supports and third point loads.

Amirikian [7] has emphasized the importance of welding residual stresses at beam connections. Actually, as observed from the experiments, the presence of cooling residual stress is also an important factor and in some cases will have a greater effect. In Fig. 42 the early part of the load deflection curve of beam No. B3 is plotted to a larger scale. Yield lines just appeared in the web of the beam in regions close to the supports and loading points at a load of W = 10.5 kips. It is evident that the deflection measurement was scarcely sensitive to the change at this load. As the load increased the local yield lines increased in number, but they were confined to these very small areas near the supports and loading points.

At a load W = 40.5 kips, yield lines suddenly developed in the compression flange along the whole central portion

of the beam between the loading points (Fig. 17). At the same time the yield lines in the compression flange near the supports had spread to a much larger area than the local yield lines previously developed.

Apparently local yielding due to welding residual stresses and stress concentration commenced at a load which was about 20% of the calculated initial yield load. The bending stresses in the compression flange near the supports and in the central portion of the beam superimposed with the compression residual stresses due to cooling reached the yield point at a load between 37.5 kips and 40.5 kips. Fig. 42 shows that the deflection increment due to local yielding below a load of 37.5 kips to be very small. But deflections started to increase drastically above the load at which the cooling residual stresses came into effect. Therefore, it seems that the cooling residual stresses are of more importance in causing an increase in deflections than are welding residual stresses and stress concentration at the connections.

f. Summary

To summarize the above discussions the yield strength of structures is affected by factors such as stress concentration and residual stress. The presence of these factors will increase the deflection of the structure. Welding residual stresses and stress concentration at the

joints of continuous beams have rather small effects on the deflections when compared with cooling residual stresses. However, it is expected that the effects of welding residual stresses will be more pronounced if the welds are applied all along the structural member. This is the case when an I section is made up of plate material or in large built-up connections. The cooling residual stresses are present no matter whether riveted, bolted or welded construction is used.

The magnitude of redistribution of moment, and hence stress, due to local yielding is of small magnitude and does not compare to the percentage increase in deflection due to the same factors.

If it is considered that the increase in deflections (for permanent set under load) due to stress concentration and residual stress is critical then it appears that the present design theory of a permissable working stress based on the initial yield point would require modification. Such a modification could be an increase in the factor of safety to cover the effects of cooling residual stress.

Since safe structures are designed according to presently accepted specifications, it is probable that the factor of safety already covers the possible reduction of strength of steel structures due to residual stress. However, it appears that the percentage reduction due to this factor has not generally been realized since the term "Presence of Residual Stress and Stress Concentration" is not usually found in lists of possible unavoidable errors in design [3].

(VI) ULTIMATE STRENGTH OF CONTINUOUS BEAMS

In the structure tested which had the ability to deform plastically, there is no particular significance in the initial yield load. Yielding due to residual stresses and stress concentrations combined with load carrying stresses actually occurred at loads well below those predicted according to conventional theory. The accelerated increase in deflections commenced either at loads lower than or greater than the initial yield load. For such structures, then, although designs based upon it have been successful, the initial yield load is not a particularly rational basis for design. Deflection seems to be the more logical criterion and this concept has been examined elsewhere. (3)

The effects of residual stresses or stress concentration at a beam section are theoretically eliminated after the section has been subjected to a certain amount of plastic straining. From test results it has been observed that the plastic hinge moment of the beam sections agree with the calculated values after yielding has completely penetrated into the web of the section. Since the plastic hinge moment is not reduced by residual stress and stress concentration, the ultimate strength of a structure is not likely affected unless inelastic local buckling is introduced.

This subject will be discussed in detail in a separate report. In this paper attention is restricted to the yield strength of the beams tested.

(VII) THE INFLUENCE OF RESIDUAL STRESS ON THE BUCKLING STRENGTH OF STRUCTURAL MEMBERS

Residual stress reduces the yield strength of a beam or frame; it also affects the buckling strength of structural steel members. Consider the example of a steel plate which has cooling residual stresses uniformly distributed along the member with the symmetrical pattern at each cross-section as shown in Fig. h. Under the compression load shown, the edges of the plate will start to yield as soon as the average stress σ reaches the value

$$\sigma = \sigma_y - \sigma_{rc}$$

where σ is the applied stress, σ_y, the lower yield point stress, and σ_{rc} the compression residual stress at the edges.

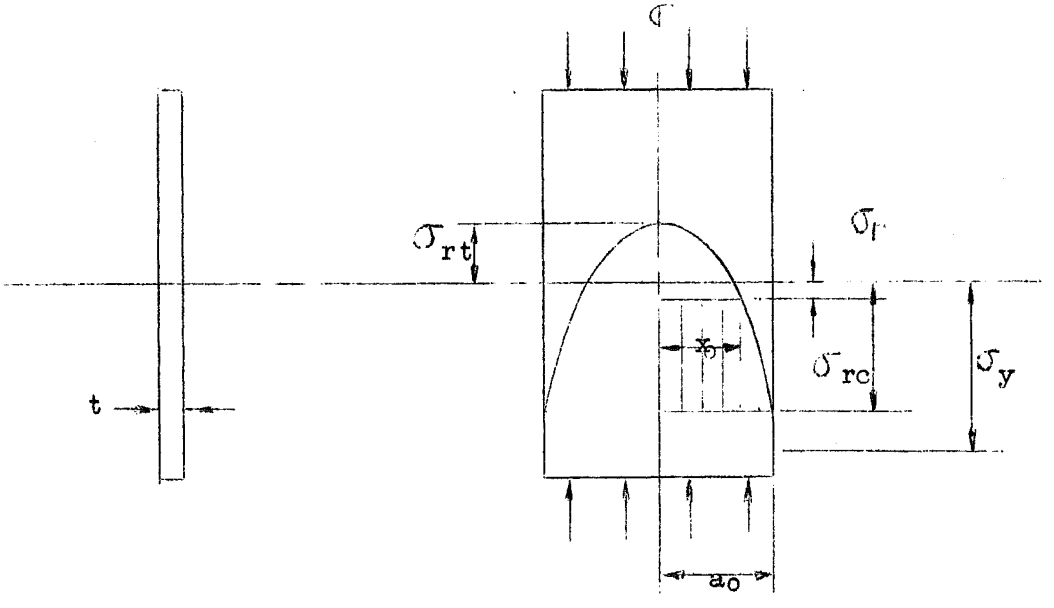

Fig. h:- Plate containing residual stress and subjected to a uniform compressive stress at the ends.

If the yielded parts of the plate are considered to be perfectly plastic,* the bending stiffness of those portions will reduce to zero. When the tangent modulus concept for buckling is used, the buckling strength of the compression member will be equivalent to that of a compression member considering only the elastic part.

If the residual stress pattern is known, the buckling strength of the plate of Fig. h about its weak axis can be found in terms of the tangent modulus of its average stress-strain diagram considering the residual stresses in it. Consider for example that uniform compression is applied to the ends of the specimen. In Fig. j is shown the resultant combination of residual and load-carrying stress. The material is assumed to have a linear stress-strain diagram. Also the load-carrying strain is assumed constant over the whole cross-section.

Let A = one-half of the total cross sectional area of the plate

$A = a_{ct}$

A_e = one half of the elastic area

$A_e = tx_o$

x_o = one-half the width of the elastic portion

σ_r = residual stress function

σ = average stress on the cross section of the plate

---

* The stress-strain diagram is idealized to consist of two straight lines with slopes E and zero.

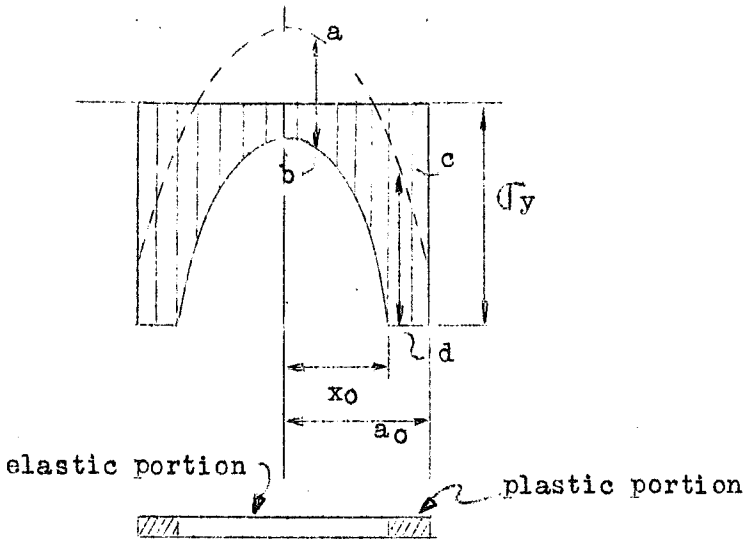

Fig. j:- Resultant stress - distribution upon application of external force sufficient to cause a certain amount of yielding.

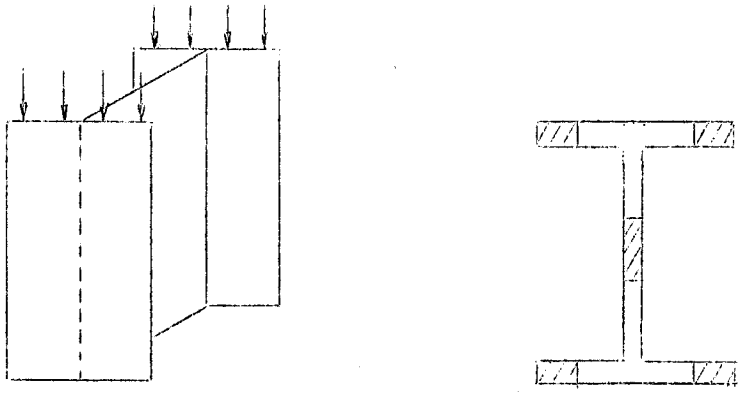

Fig. k:- Short compression specimen of WF shape at a load sufficient to cause yielding due to residual stress.

When $\sigma_{rc} + \sigma$ exceeds σ_y, part will be elastic and part plastic. The total force at the cross-section must balance the applied force, σ x A. Prior to loading, however, the net force was zero since the residual stresses were in equilibrium. Thus the net force after loading is made up of an increment of force in the plastic part (x between x_o and a_o, stress magnitude c-d) and an increment of force in the elastic part (x between zero and x_o, stress magnitude a-b). Since

$$c\text{-}d = \sigma_y - \sigma_r$$

and

$$a\text{-}b = \sigma_y - \left|\sigma_r\right|_{x_o}$$

then

$$\sigma_A = \int_{x_o}^{a_o} (\sigma_y - \sigma_r)\, dx + t\, x_o \left(\sigma_y - \sigma_{r|_{x_o}}\right) \quad \ldots(6)$$

$$(o < x_o < a_o)$$

σ_r in the above equation can be determined by measuring or in some cases it can be solved as an analytic function.

x_o can be found by solving equation (6). Then

$$E_t = \frac{d\sigma}{d\epsilon} = E\,\frac{Ae}{A} = E\,\left(\frac{xo}{ao}\right)$$

This value of E_t may be used to predict the buckling strength of the compression member according to the concept of tangent modulus theory from the equation,

$$P_t = \pi^2\,\frac{E_t\, I}{L^2} \qquad \text{----------(7)}$$

For purposes of illustration of the possible effect of residual stress upon the buckling strength of structural members, a typical distribution for the flanges of wide flange shapes is selected in which the pattern is parabolic in shape with the compression residual stress equal to 20 ksi and the maximum tensile value in the flange center equal to 10 ksi. The residual stress function, σ_r, for a 10-inch-wide-flange is then given by,

$$\sigma_r = 10 - 1.2\, x^2,$$

positive when in tension, the distance x being measured from the centerline of the flange. The material is assumed to have a yield point stress of 40 ksi. Substituting this expression into Eq. (6) an expression for x_o is obtained, enabling a direct calculation of E_t for various assumed values of σ. The column curve may then be drawn and this is shown in Fig. 46.

The average stress-strain diagram could be obtained by determining strain-values to correspond with the above assumed stress-values from the relation

$$\epsilon = \frac{\sigma_y - |\sigma_r|}{E} x_o \qquad \text{----------(8)}$$

The resulting average stress-strain curve as modified by the assumed residual stress pattern is shown in Fig. 47. Of course, a curve determined experimentally from a member containing residual stress would be similar to Fig. 47 and

could be used to determine the column curve of Fig. 46.

For sections of different cross-sectional shapes the buckling strength can be found in a similar way. Assume a residual stress pattern as in Fig. 26 in a WF shape. When the average applied stress reaches a certain magnitude, portions of the cross-section will yield as shown in Fig. k. The buckling strength of it can be calculated by considering only the elastic part. Thus the buckling load should be computed according to the expression

$$P_{cr} = \frac{\pi^2 E I_e}{L^2} \qquad (9)$$

where I_e is the moment of inertia of the portion which remains elastic.

In the case of the rectangular section bent about the weak axis

$$E_t I = E I_e$$

This is also very nearly true for the WF section bent about its strong axis since the web contributes only a small portion to the moment of inertia. However for the rectangular section bent about its strong axis and for the I-section bent about its weak axis the term EI_e will be considerably less than E_tI. Thus the buckling strength will be reduced over that value predicted by the tangent modulus concept alone. While it was recognized by the authors some time ago that the buckling strength of a WF

shaped member would be that of the part remaining elastic, these ideas were not generally circulated nor were they extended. The problem has been discussed in a dissertation (21) by one of the authors. According to pre-publication abstract, Osgood * has recently obtained a "general expression for the buckling load of a column containing residual stresses assumed to be the same at every cross-section and so distributed over the cross-section that the Engesser-Shanley theory may be applied".

When residual stressses are not the same at all sections of the compressed member, the problem becomes one of the buckling strength of a member of varying cross-sectional areas. At local sections which are cold-bent or which contain welding residual stresses, it can be considered that the dimension is reduced at those sections due to yielding caused by local residual stresses. The effect will be generally smaller than that of the cooling residual stresses which are distributed all along the member.

Fig. 46 shows the large reduction in column strength that may be expected from the rather common pattern of residual stress shown in Fig. h. This implies, of course, that the material behaves as assumed in the theory. Actually as was discussed earlier, yielding is not uniformly distributed along the member, but yield zones penetrate into the member at intervals along it. Thus the effective stress-strain diagram will be something different from that shown

---

* W. R. Osgood, "Residual Stresses in Columns", presented at the First U. S. National Congress of Applied Mechanics, Chicago, Illinois, 1951.

in Fig. 47, thus modifying the column curve of 46. Further experimental work is needed here and a part of this is being carried on in current investigations.

An important question to be answered is the following: Can a satisfactory column-strength curve for heavy steel columns be based on small samples removed from flange and web if the cutting out of the small samples relieves the residual stresses in the columns? The evidence from the above discussion indicates that a satisfactory column curve for steel cannot be obtained from tests of small coupons and this trend has been confirmed experimentally by pilot tests on complete cross-sections of WF steel specimens.

The influence of residual stress on the buckling strength of a compression member is seen to be significant Since residual stress causes a reduction in yield strength, it may also be a factor in local buckling. Since flange elements eventually buckle locally in the plastic range, yielding at lower loads than predicted may also reduce the local buckling strength of a bending member. This factor has not been examined in these tests and would probably require tests of annealed and unannealed specimens.

It is probable that the factor of safety for columns has included the reduction in carrying capacity due to residual stress, although the percentage reduction due to this factor has not generally been appreciated. This indicates once more that experience and prior satisfactory performance is now, as it has always been, an important factor in design.

(VIII) C O N C L U S I O N S

1. While this report emphasizes the influence of residual stresses and stress concentration upon the yield strength of steel beams, it is not to be assumed that the plastic range and ultimate strength are of any lesser importance. Since there is not space here to treat the whole problem, and since most engineers are concerned with design based upon the initial yield load, it was considered that the influence of the various factors on the yield strength should be presented first.

2. According to experimental data, the assumption of a uniform distribution of plastic strain in a bending member is far from the actual picture. Making use of this assumption, the M-ϕ relation of a bending section gives better agreement with test results for annealed specimens than for as-delivered specimens. (The annealed tests were carried out in a previous program).

3. There is a difference in the behavior of as-delivered and of annealed specimens over and above a difference in material properties. The process of initiation and propagation of plastic zones in a bending member is affected by residual stress and stress concentration which indirectly affect the M-ϕ relation. As-delivered specimens consistently show a reduction of about 10% in moment capacity in the early part of the plastic range. However, when yielding

later penetrated to the neutral axis the moment capacity approaches the value predicted on the basis of coupon tests.

4. Due to residual stress and stress concentration local yielding may occur in a structure at a load very much lower than usually predicted by theory. In these tests such yielding occurred at loads as low as about 20% of the predicted initial yield load.

5. The initial yield strength of a structure is reduced by the presence of residual stress and stress concentration no matter whether load or deflection is used as the criterion. In these tests the reduction of load was as much as 24% and the increase in deflection at the initial yield load ranged from 13% to 88%.

6. Concerning the increase of deflection in a structure, cooling residual stress is a more important factor than welding residual stress or stress concentration.

7. There was no significant influence of shape of cross section on the yield strength.

8. The initial yield strength of a cold-straightened beam may be raised or lowered depending on the direction of cold-straightening and of load application. Cambered beams would have their yield strengths reduced due to the necessary cold bending process. Expressions for determining the residual stress distribution are presented.

9. The stress concentration and residual stress involved in the welding of stiffeners between flanges of a member causes local yielding at lower bending moments and is thus of more significance than yielding in butt welds to splice plates and columns.

10. The buckling strength of a structural member is reduced by residual stresses. Cooling residual stresses, distributed along the member, are expected to be more severe in this respect than residual stresses formed due to cold bending.

11. The evidence indicates that a satisfactory column curve for steel cannot be obtained from tests of small coupons.

12. For use in predicting the strength of a column of rectangular cross-section containing residual stress, a method for determining the tangent modulus is suggested. A general expression is presented which integrates the effective stress distribution across the member.

13. For members of different cross-sectional shapes than rectangular and which contain residual stress, the buckling strength is theoretically reduced over that predicted by the tangent modulus concept alone. The buckling strength under these conditions would be that of the part remaining elastic. Additional studies, including experimental are needed to see if these reductions actually occur.

14. The specimens tested in this program were all rolled shapes. While it is expected that the residual stress patterns will be similar in members which are built up by welding web plates to flange plates, there will probably be considerable variation from member to member and along the same member. Also the influence of residual stress due to longitudinal welds may be different. An investigation along these lines would be worthwhile.

15. It is probable that the factor of safety for steel members has always included the reduction in carrying capacity due to residual stress and stress concentration. However, the percentage reduction due to this factor has not generally been appreciated. If the increase of deflection is considered critical then a change in design procedure that would allow greater working loads must be approached with extreme caution. However, in structures in which deflection is not a critical item from a statistical point of view, then there is nothing in the results of these tests which would prevent the further consideration of so-called "plastic design" procedures. Although at least one structure has been designed according to this procedure, general application of plastic theory should await the study of some further limitations, local instability of flange elements being one of the most critical.

(IX) ACKNOWLEDGEMENTS

The authors wish to express their appreciation to the sponsors who have made this investigation possible. Acknowledgement is also expressed for the help and support received from members of the Lehigh Project Subcommittee (Welding Research Council) and that of its chairman, Mr. T. R. Higgins. Mr. William Spraragen, Director of Welding Research Council and Mr. LaMotte Grover, Chairman of the Structural Steel Committee, have generously contributed their suggestions and criticism of the project.

This work has been carried out in the Fritz Engineering Laboratory of which Professor William J. Eney is Director. Acknowledgement is due Mr. Jan Ruzek, Mr. EdmundKaminsky and Mr. Helmut Bauer for their assistance with the illustrations. Thanks is expressed to Mr. Kenneth R. Harpel, foreman, and the staff of machinists and technicians in the Fritz Laboratory.

The authors express appreciation to Mr. A. Amirikian for his cooperation in making available an illustration for the report.

The Column Research Council, through its Research Committee D, has also supported the overall investigation, "Welded Continuous Frames and their Components", in an advisory capacity.

(X) REFERENCES

Reports in Lehigh Series

1. Luxion, W. W., and Johnston, B. G., "Plastic Behavior of Wide Flange Beams", The Welding Journal Supplement A.W.S., vol. 27, No. 11, November 1948.

2. Beedle, L. S., Ready, J. A., and Johnston, B. G., "Tests of Columns Under Combined Thrusts and Moments", Proceedings of the Society for Experimental Stress Analysis, vol. 3, No. 1, 1950. WRC Bulletin No. 8.

~~Ready, J. A., and Johnston, B. G., "Progress Report No. 2."~~

3. Yang, C. H., Beedle, L. S., and Johnston, B. G., "Plastic Design and the Deformation of Structures", Progress Report No. 3, Welding Research Supplement, vol. 16, No. 7, July 1951, p.348-s.

4. Topractsoglou, A. A., Beedle, L. S., and Johnston, B. G., "Connections for Welded Continuous Portal Frames", Part I: Welding Research Supplement, vol. 16, No. 7, July 1951, p. 359-s; Part II: Welding Research Supplement, vol. 16, No. 8, August 1951, p. 397-s; Part III to be published.

References

5. Adams, C. A. and others, "The Weld Stress Problem" Supplement to the Journal of the American Welding Society, June 1945, p. 313.

6. American Welding Society, "Welding Handbook", Third Edition, 1950.

7. Amirikian, A., "Future Development in Welded Steel Buildings", The Welding Journal A.W.S., vol. 27, No. 8, August 1948, p. 593.

8. Baker, J. F., "A Review of Recent Investigation in Behavior of Steel Frames in the Plastic Range", Journal of the Institute of Civil Engineering, January 1949.

9. Cross, H., "The Relation of Analysis to Structural Design", Transactions ASCE, vol. 101, 1936, p. 1363.

10. Donnell, L. H., "Plastic Flow as an Unstable Process", Journal of Applied Mechanics, vol. 9, June 1942.

11. Greenberg, H. J., and Prager, W., "On Limit Design of Beams and Frames", Technical Report No. 5, Brown University, October 1949.

12. Horne, M. R., "The Effect of Strain-Hardening on the Equilization of Moments in the Simple Plastic Theory", Welding Research (Br.) V5 N1, February 1951, p. 147.

13. Kohlbrunner, C. F., Zurich, "Stability in the Elastic and Plastic Range of Plates Subjected to Compression (Report of Tests), International Assoc. for Bridge and Structural Engineering, vol. iv, 1935.

14. Nadai, A., "Plasticity", McGraw Hill Co., New York, 1941.

15. Osgood, W. R., "Notes on Compression Testing of Metals and the Column-Strength Curve", Subcommittee A. Mechanical Properties of Metals, Committee on Research, Column Research Council, 1950.

16. Roderick, J. W., and Philip, I. H., "Carrying Capacity of Simply Supported Mild Steel Beams", Academic Press Inc., New York, 1950.

17. Timoshenko, S., "Strength of Materials", vol. II, Second Edition, D. Van Nostrand Co., Inc., New York, 1941.

18. Van den Broek, "Elastic Energy Theory", Wiley and Sons, New York, 1946.

19. Van den Broek, J. F., "Theory of Limit Design", John Wiley and Sons, Inc., New York, 1948.

20. Wilson, W. M. and Hai, C. C., "Residual Stresses in Welded Structures", University of Illinois Bulletin, vol. 43, No. 40, February 1946.

21. Yang, C. H., "The Plastic Behavior of Continuous Beams", Ph.D Dissertation, Lehigh University, 1950.

22. Zehner, C. and Hollomon, J. H., "Deformation of Metals", Journal of Applied Physics, vol. 17, No. 2, February, 1946.

(XI) NOMENCLATURE

E	Modulus of elasticity.
E_t	Tangent modulus.
f	Shape factor.
h	Depth of section.
I	Moment of inertia.
I_e	Moment of inertia of the elastic part of a section.
I_p	Moment of inertia of the plastic part of a section.
L	Total length of a column or a beam.
M	Moment.
M_p	Full plastic moment, often termed "plastic hinge" moment.
M_y	Moment at which flexural yield point is reached.
S	Section modulus ~~point is reached.~~
P	Load on a column.
P_t	Tangent modulus load.
t	Thickness of the web of an I-section or a plate.
y	Distance to the neutral axis.
Z	Plastic modulus.
Z_p	Plastic modulus of the plastic part of a section.
V	Deflection of a beam.
ε	Strain
σ	Normal stress.
σ_r	Residual stress function.
σ_{rt}	Tensile residual stress.
σ_{rc}	Compressive residual stress.

σ_y Lower yield point stress.

ϕ Rotation per unit length, Curvature.

W Concentrated load.

P_{cr} Critical load.

(XII) A P P E N D I C E S

Appendix A

Coupon Test Results

The mechanical properties of the material of the beams were determined by simple tension and compression tests to secure necessary data for theoretical computations. A constant strain rate of about 1 micro in. per second was adopted for all tests. Most tensile tests were carried into the strain hardening range. Due to the difficulty of measuring the strain, compression tests were stopped before reaching the strain-hardening range. In all calculations the material is assumed to have identical stress strain properties in tension and compression. Two typical stress-strain curves plotted from test data are shown in Fig. 48. Idealized diagrams consisting of 3 straight lines in the elastic, plastic and strain-hardening regions were used in theoretical computations and were based upon average test data. The average results are given in Table vi.

Table vi

Summary of Coupon Test Results

Section and Location of Coupons	Type of Test	Upper Yield Point σ_{uy} (ksi)	Lower Yield Point σ_{ly} (ksi)	Elastic Strain ϵ_y (in/in)	Plastic Strain ϵ_s (in/in)	Strain Harden. Modulus C (ksi)	Ultimate Strength (ksi)
8WF40 flange (10 tests)	Ten-	37.75	37.55	-	-	-	-
8WF40 web (5 tests)	sion	39.76	39.52	-	-	-	-
8WF40 flange (6 tests)	Com-	37.63	37.35	-	-	-	-
8WF40 web (5 tests)	pression	38.08	37.92	-	-	-	-
8WF40 flange (8 tests)	Ten-	-	37.6	.00124	.0139	636	64.8
8WF40 web (3 tests)	sion	-	38.5	.00129	.0141	644	66.2
14WF30 flange(8 tests)	Ten-	-	38.2	.00126	.0161	599	62.2
14WF30 web (4 tests)	sion	-	40.7	.00137	.0185	615	67.7

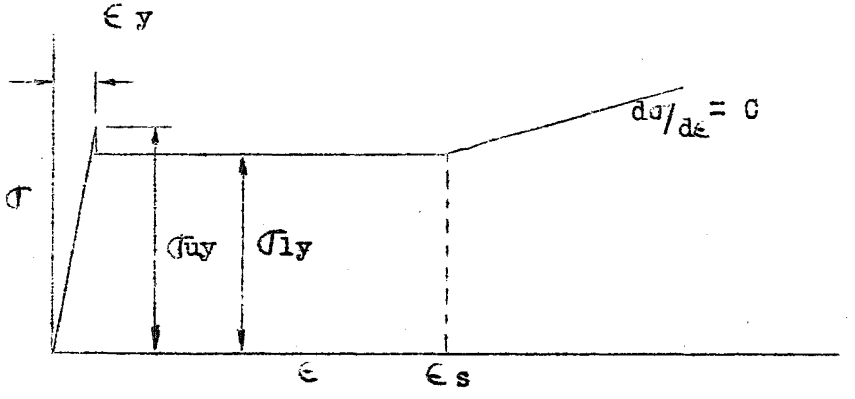

Explanation of terms

Appendix B

Residual Stress in a Plastically Bent Beam

A short length of a beam is under a bending moment M_o, Fig. 1. In Fig. 1b the yielded portion of the section is represented by the shaded area, and the stress distribution is as shown in the solid lines in Fig. 1c

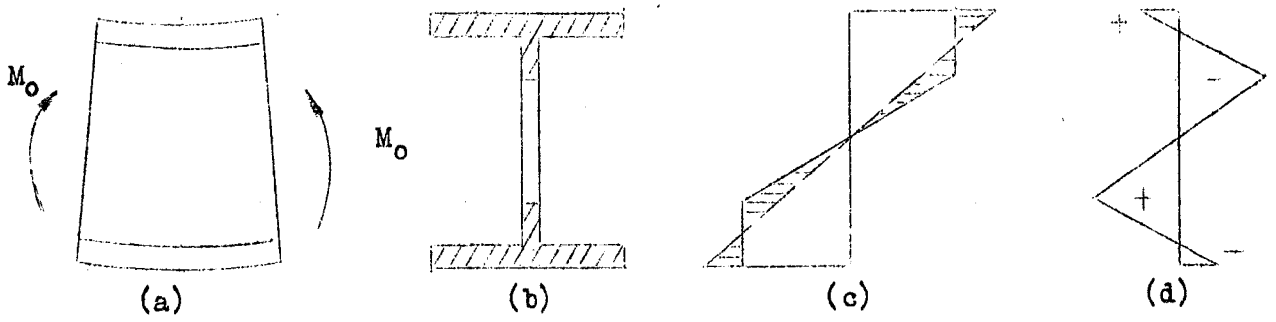

Fig. 1:- Development of residual stress due to cold bending.

When the moment on the section is removed a pattern of residual stress is left due to the plastic strain in the yielded zone. Assuming the section behaves in elastic fashion under an unloading moment equal to M_o, the stress distribution can be assumed as shown in dotted lines in Fig. 1c The residual stress pattern is actually the shaded area between these two stress distributions as replotted in Fig. 1d Vanden Broek has demonstrated the above in his book of Elastic energy theory (18). The section will behave elastically when it is subsequently loaded so long as the maximum moment is less than M_o.

The stress pattern of Fig. 1 as well as the deflection of the beam during unloading can be derived neglecting the shear strain in the beam.

With the beam initially under the moment, M_o, suppose the moment on the beam is reduced to a value M such that M is smaller than M_o. From Fig. m,

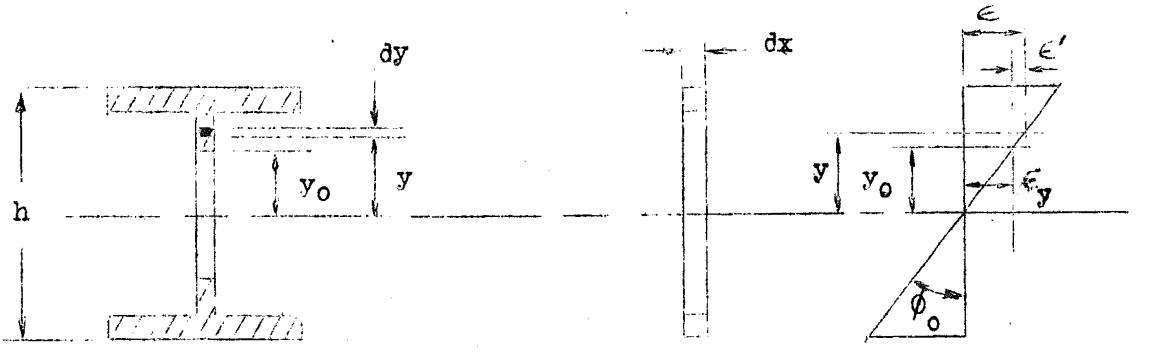

Fig. m:- Section yielded under moment M_o.

$$\frac{\epsilon_y}{y_o} = \frac{\epsilon}{y}$$

$$\epsilon = \frac{y}{y_o}\ \epsilon_y$$

Where ϵ_y = strain corresponding to the stress σ_y. In Fig. m ϕ_o is the unit angle change corresponding to moment M_o. Let

ϵ' = permanent strain at any point in the plastic zone (the total strain is made up of the elastic strain ϵ_y and the permanent strain ϵ' (Fig. n).

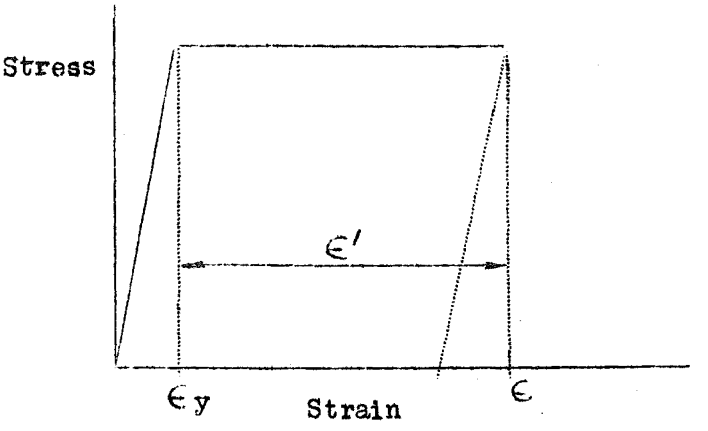

Fig. n

Then from Fig. m,

$$\epsilon' = \left(\frac{y}{y_o} - 1\right) \epsilon_y \qquad \text{----------(10)}$$

Now, under moment M, referring to Fig. p

$$\phi = \frac{d^2V}{dx^2} = -\frac{\epsilon}{y}$$

Where V = the vertical deflection of the bending member under moment M.

The value y_o is a constant for a constant M_o. For y less than y_o the region is elastic under the previous loads and the stress is dependent upon ϕ ($\sigma = E\, y\phi$). However, for y greater than y_o, the stress distribution is modifed by the prior plastic strain. For example the resultant stress distribution for a particular value of M is shown in Fig. p.

The relationship between M and ϕ will now be developed, M being the total applied moment subsequent to a moment M_o.

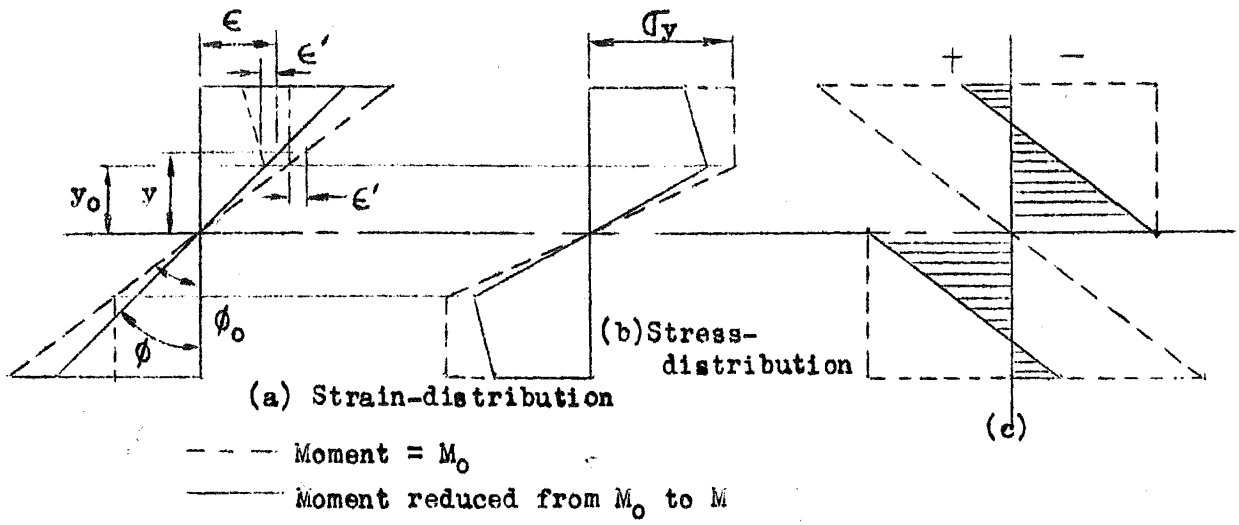

Fig. p

Let σ_1 = stress at area above y_o

σ_2 = stress at area below y_o

Then $\sigma_1 = E (\epsilon - \epsilon')$

$$\sigma_1 = -E \left[y \frac{d^2v}{dx^2} + \epsilon_y \left(\frac{y-y_o}{y_o} \right) \right] \text{----------(11)}$$

$$\sigma_2 = -Ey \frac{d^2v}{dx^2} \text{----------(12)}$$

In developing the following expressions for the magnitude of residual stress, only the positive side of the neutral axis is considered. This is the lower side according to the engineering convention. On the upper side, stresses will be reversed.

Then

$$M = \int_{-h/2}^{h/2} \sigma_y \, dA = -\left[2E \int_0^{y_o} y^2 \frac{d^2y}{dx^2} \, dA + 2E \int_y^{\frac{h}{2}} y^2 \frac{d^2y}{dx^2} \, dA + 2E \epsilon_y \int_{y_o}^{\frac{h}{2}} y \left(\frac{y - y_o}{y_o} \right) dA \right]$$

Since $\frac{d^2y}{dx^2}$ does not depend on y,

$$M = -EI \frac{d^2v}{dx^2} - \sigma_y \frac{I_p}{y_o} + \sigma_y Z_p \qquad \text{----------(13)}$$

where the moment of inertia of the plastic portion is

$$I_p = 2 \int_{y_o}^{\frac{h}{2}} y^2 dA,$$

the plastic modulus of the plastic portion is

$$Z_p = 2 \int_{y_o}^{\frac{h}{2}} y \, dA,$$

and $$\sigma_y = E \epsilon_y$$

From Eq. (2),

$$\frac{d^2v}{dx^2} = -\left[\frac{M}{EI} + \frac{\sigma_y}{EI} \left[\frac{I_p}{y_o} - Z_p \right] \right] \qquad \text{----------(14)}$$

$$v = \iint \left[\frac{M}{EI} + \frac{\sigma_y}{EI} \left[\frac{I_p}{y_o} - Z_p \right] \right] dx dx$$

When M = 0, i.e., the section is unloaded,

$$\left| \frac{d^2v}{dx^2} \right|_{M=0} = -\frac{\sigma_y}{EI} \left[\frac{I_p}{y_o} - Z_p \right] \qquad \text{----------(15)}$$

The magnitude of residual stress remaining in the beam after plastic bending followed by complete removal of moment may be computed using Eq. (11) and (12) for σ_1 and σ_2. Thus,

$$\sigma_{r1} = -E\left[y \left|\frac{d^2v}{dx^2}\right|_{M=0} + \epsilon_y \left(\frac{y-y_o}{y_o} \right) \right] \text{---------(16)}$$

$$\sigma_{r2} = - E\, y \left|\frac{d^2v}{dx^2}\right|_{M=0} \text{----------(17)}$$

Substituting the value from Eq. (15) into (16) and (17)

$$\sigma_{r1} = \sigma_y \left[\frac{y}{I} \left(\frac{Ip}{y_o} - Z_p \right) - \left(\frac{y-y_o}{y_o} \right) \right] \text{---------(18)}$$

and $$\sigma_{r2} = \frac{\sigma_y\, y}{I} \left[\frac{Ip}{y_o} - Z_p \right] \text{----------(19)}$$

When $y = y_o$, from Eq. (19)

$$\sigma_{r1} = \sigma_{r2} = \frac{y_o\, \sigma_y}{I} \left[\frac{Ip}{y_o} - Z_p \right] \text{---------(20)}$$

When $y = \frac{h}{2}$ from Eq. (18) and using $\epsilon_y = \frac{\sigma_y}{E}$

$$\sigma_{r1} = \sigma_y \left[\frac{h}{2I} \left(\frac{Ip}{y_o} - Z_p \right) - \left(\frac{h-2y_o}{2\, y_o} \right) \right] \text{----(21)}$$

When the moment M_o is equal to the plastic hinge moment, M_p, then y_o approaches zero (Fig. 6). From Eq. (6),

$$\sigma_{r2} = \sigma_y \text{----------(22)}$$

At the extreme fibre when $y_o \to o$ and $y = h/2$, from expression (21)

$$\left| \sigma_{r1} \right|_{\substack{y_o \to o \\ y = h/2}} = -\sigma_y \left(\frac{Z}{S} - 1 \right)$$

and since the shape factor is defined by

$$f = \frac{Z}{S}$$

Then $$\left| \sigma_{r1} \right|_{\substack{y_o \to o \\ y = h/2}} = - \sigma_y (f - 1) \text{ ----------(23)}$$

which gives a compressive stress on the lower and tension on the upper fibre. Such a distribution for the condition that $M_o = M_p$ has been shown in Fig. 37 of Ref. 39 and is also shown in Fig. p. It may be obtained by use of Eqs. (22) and (23) which give the maximum possible residual stresses at the two points.

The general expression (14) holds when a moment in the opposite sense is applied and until the yield condition is reached. Referring to Fig. q these expressions would apply until the reversed moment reached the value M_2, the magnitude of which depends, theoretically, upon the magnitude of M_1. (The Bauschinger effect is ignored, but this would lower M_2 still further.).

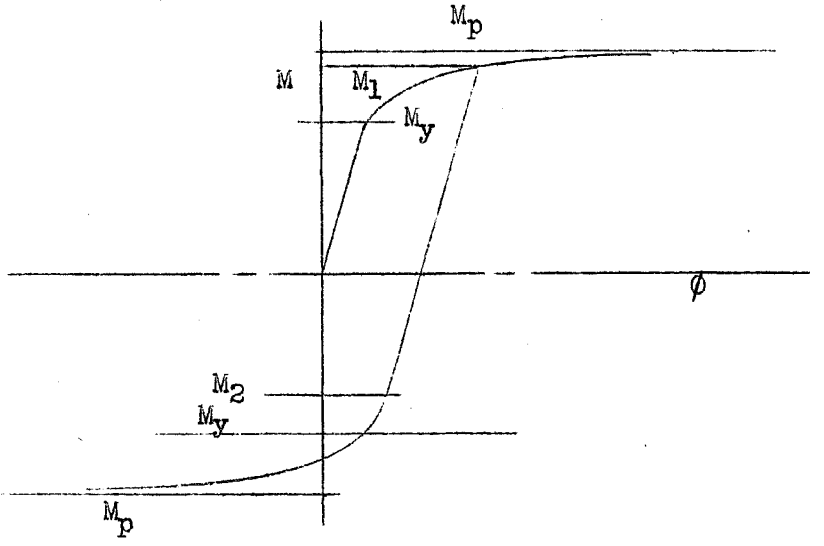

Fig. q

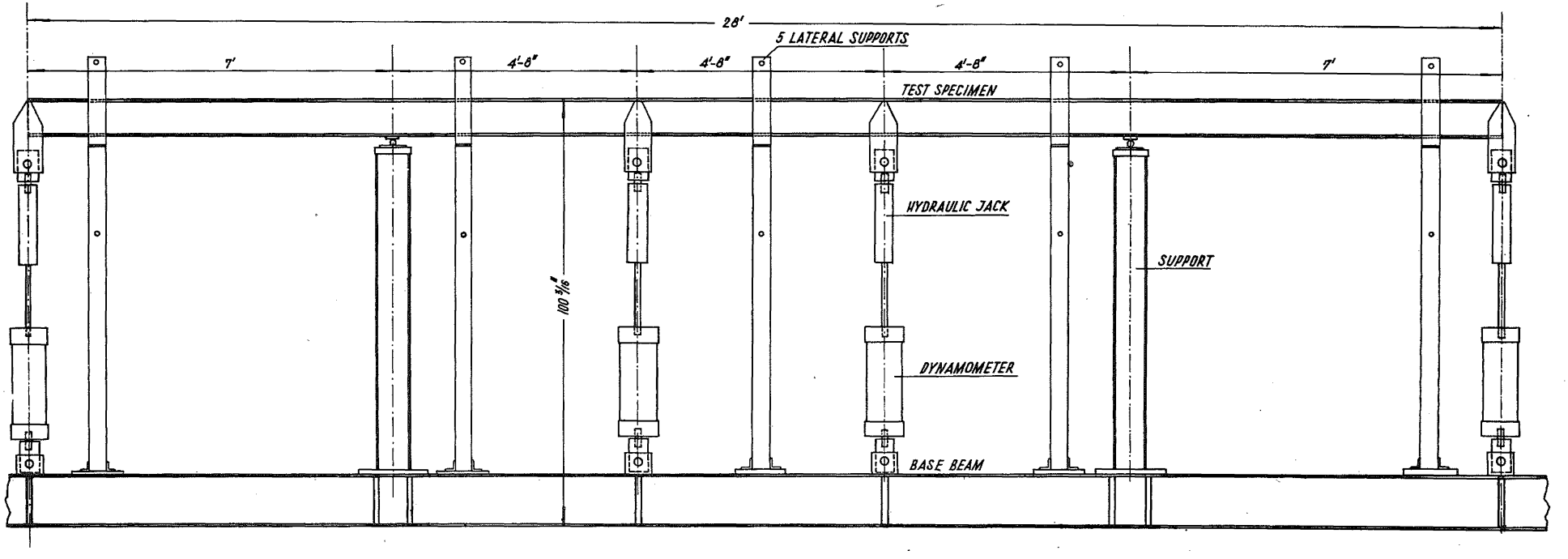

Fig. 1

CONTINUOUS BEAM TEST SET UP. CONCENTRATED LOADS ARE APPLIED AT THIRD POINTS OF CENTRAL SPAN AND END LOADS ARE USED TO BRING SPECIMEN TO PROPER LOAD CONDITION

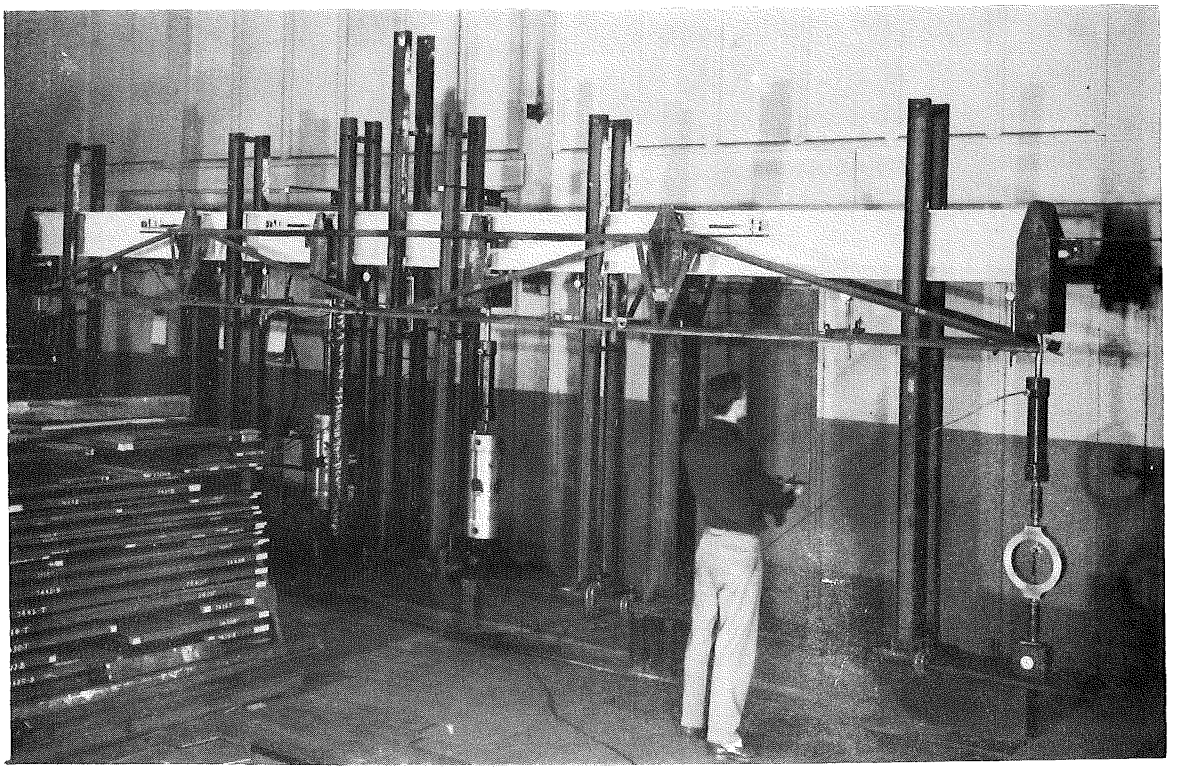

Fig. 2 - Continuous Beam B7 under test

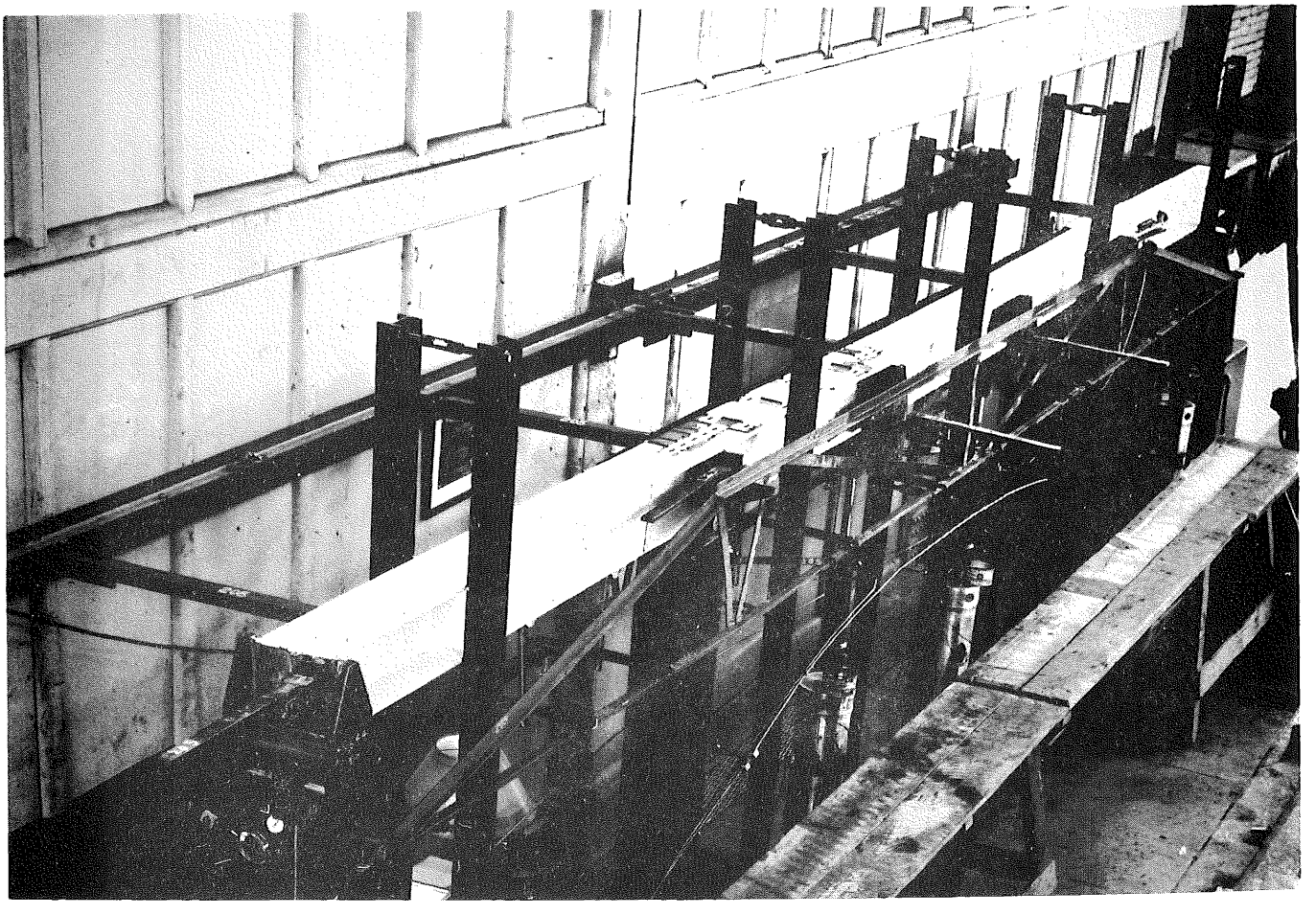

Fig. 3 - Vertical Guide Support System Designed to Prevent Lateral Displacement

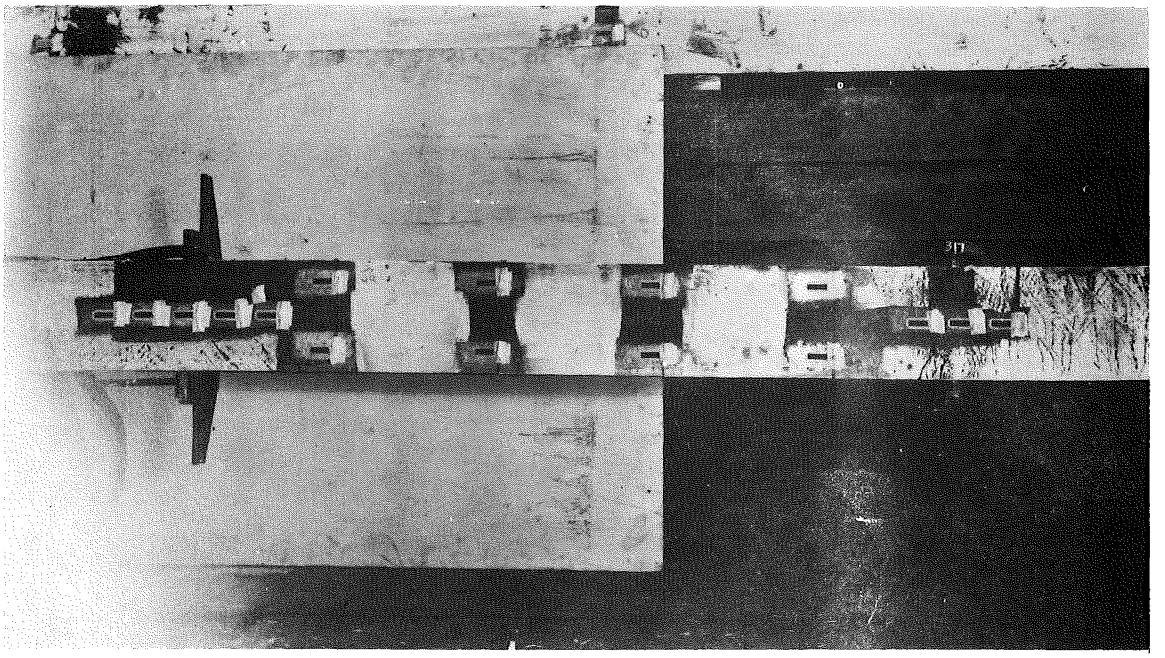

Fig. 4

View of Top Flange of B3 between support (left) and load point (right) showing typical arrangement of SR-4 gages.

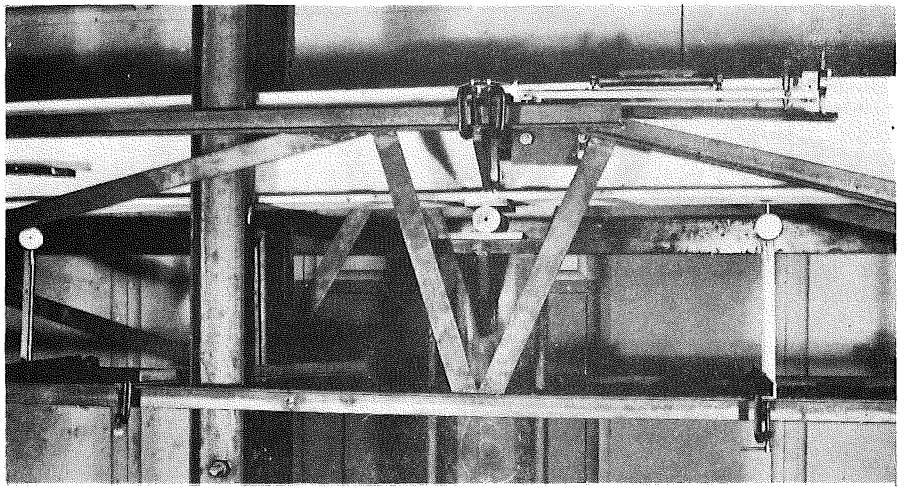

Fig. 5

Test B3 showing detail of deflection gage rig at support point. Level bar was used to measure rotations at supports.

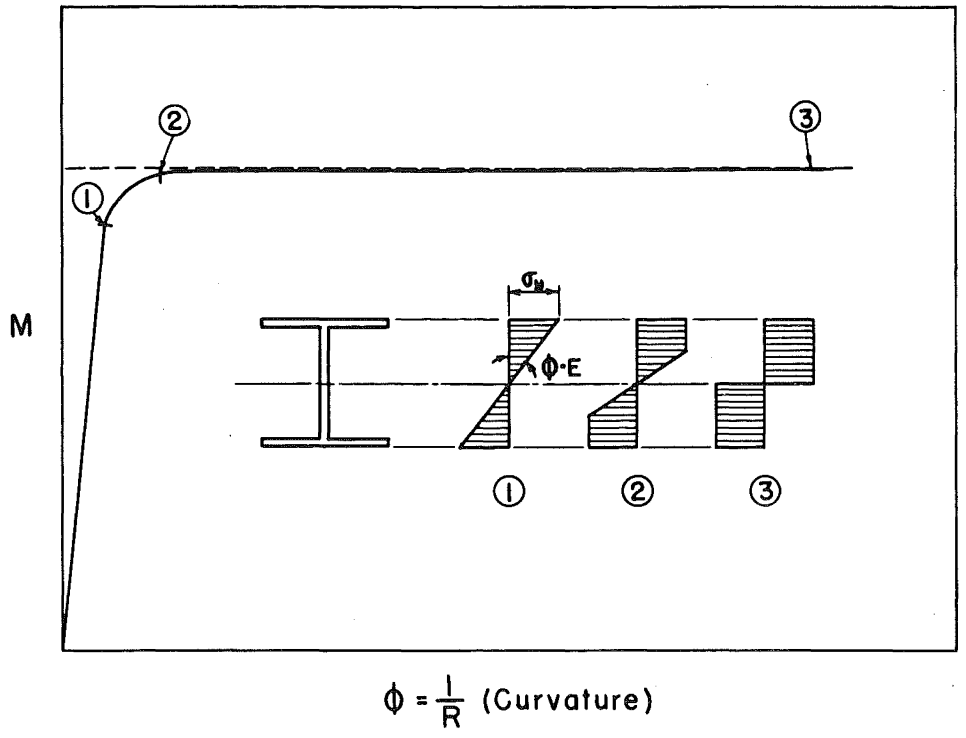

Fig. 6

Moment-Curvature (M-Ø) relationship for WF-shape according to the Simple Plastic Theory. Corresponding stress distributions are shown for various points on the curve.

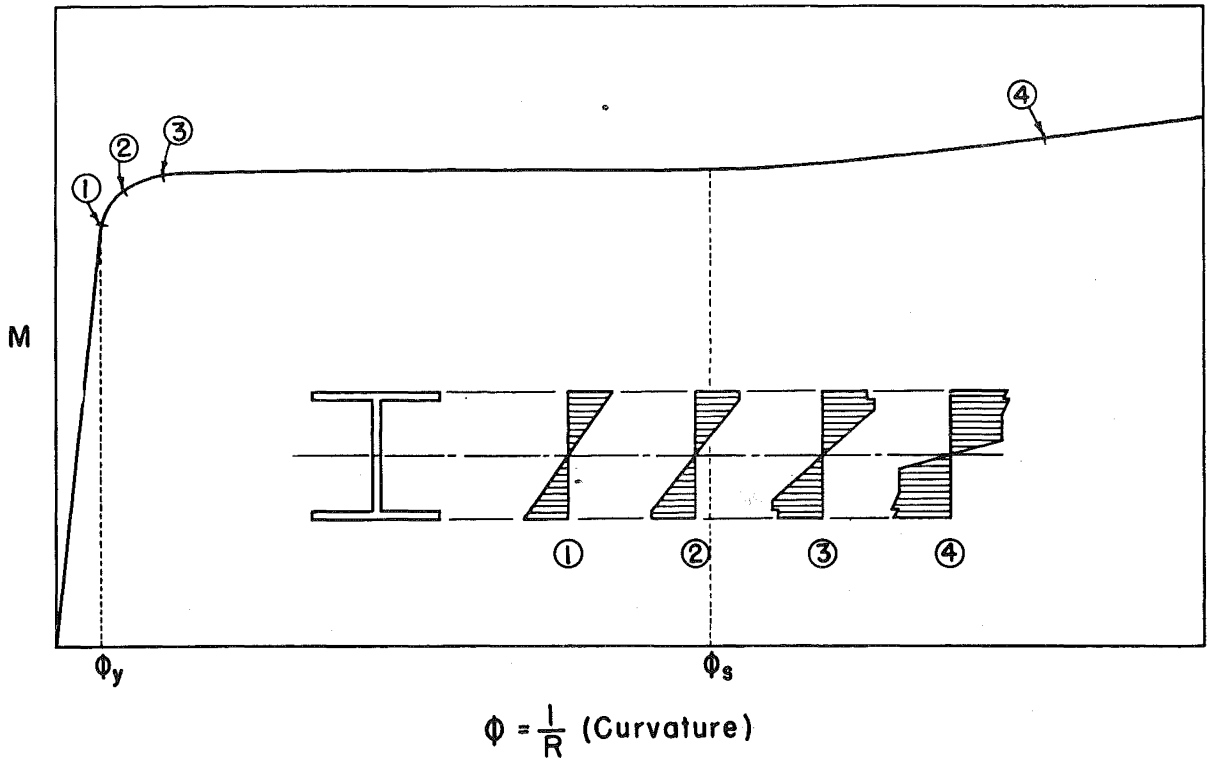

Fig. 7

M-Ø relationship for WF-shape, due account having been taken of strain-hardening

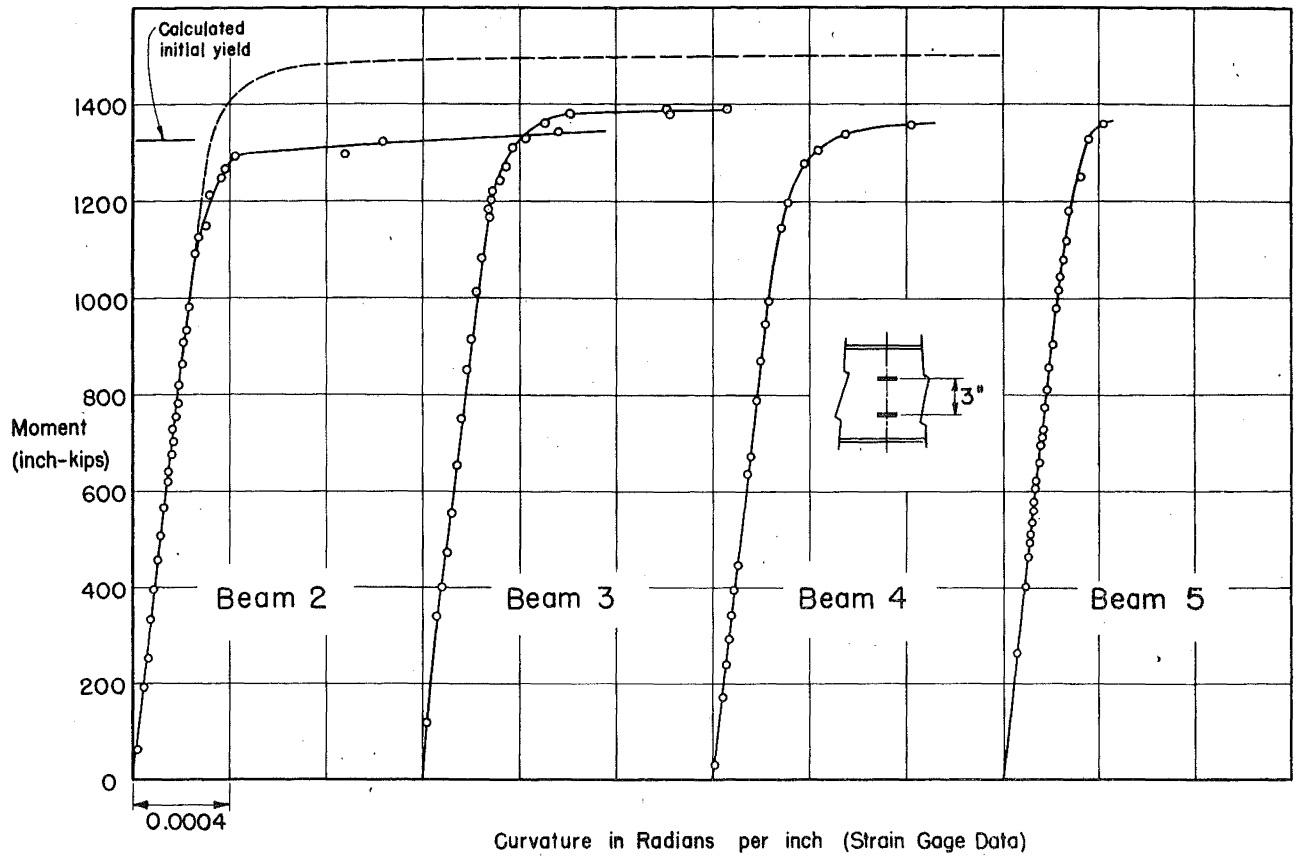

Fig. 8

EXPERIMENTAL M-Ø CURVES DETERMINED FROM SR-4 GAGE MEASUREMENTS IN THE CENTRAL SPAN OF FOUR CONTINUOUS BEAMS

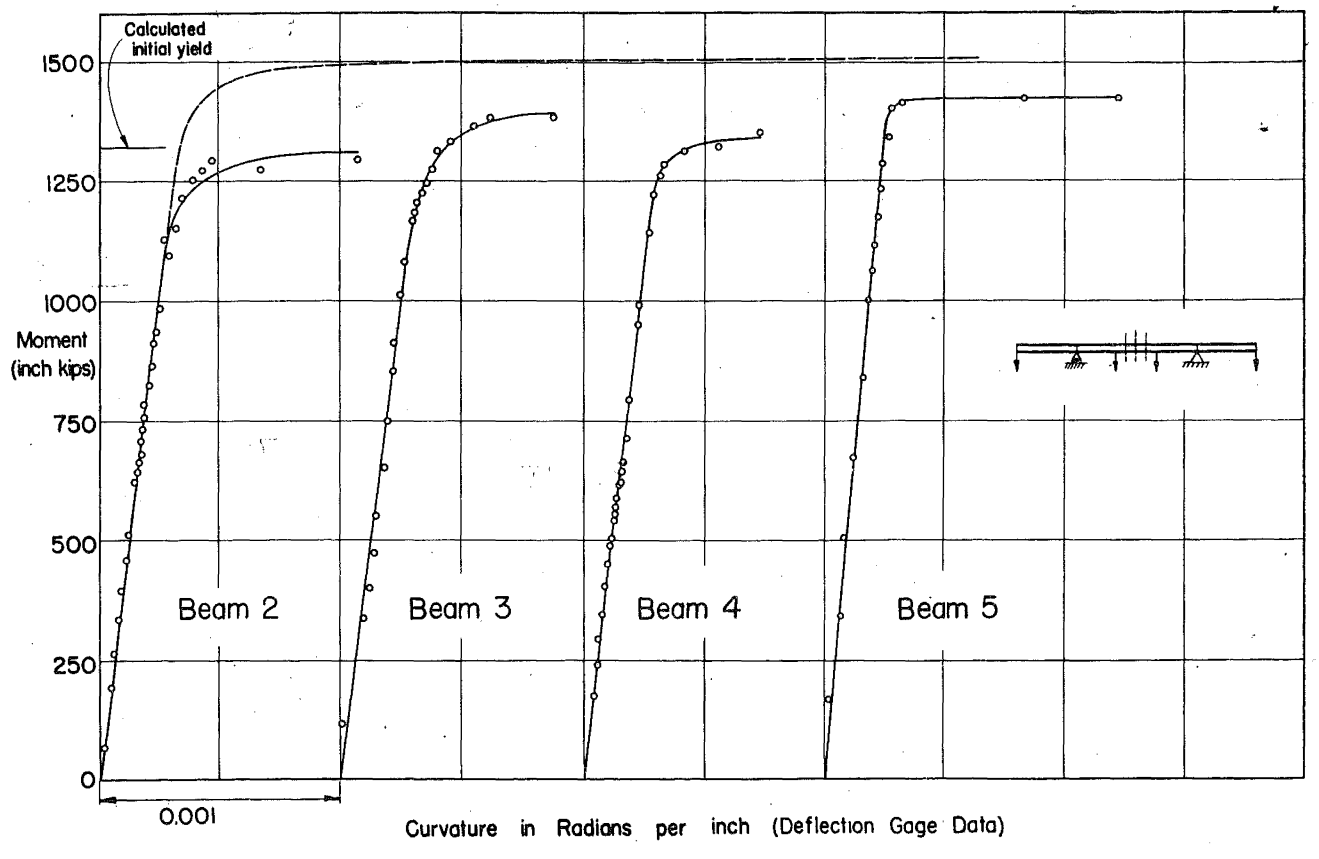

Fig. 9

M-Ø CURVES DETERMINED FROM DEFLECTION GAGE MEASUREMENTS

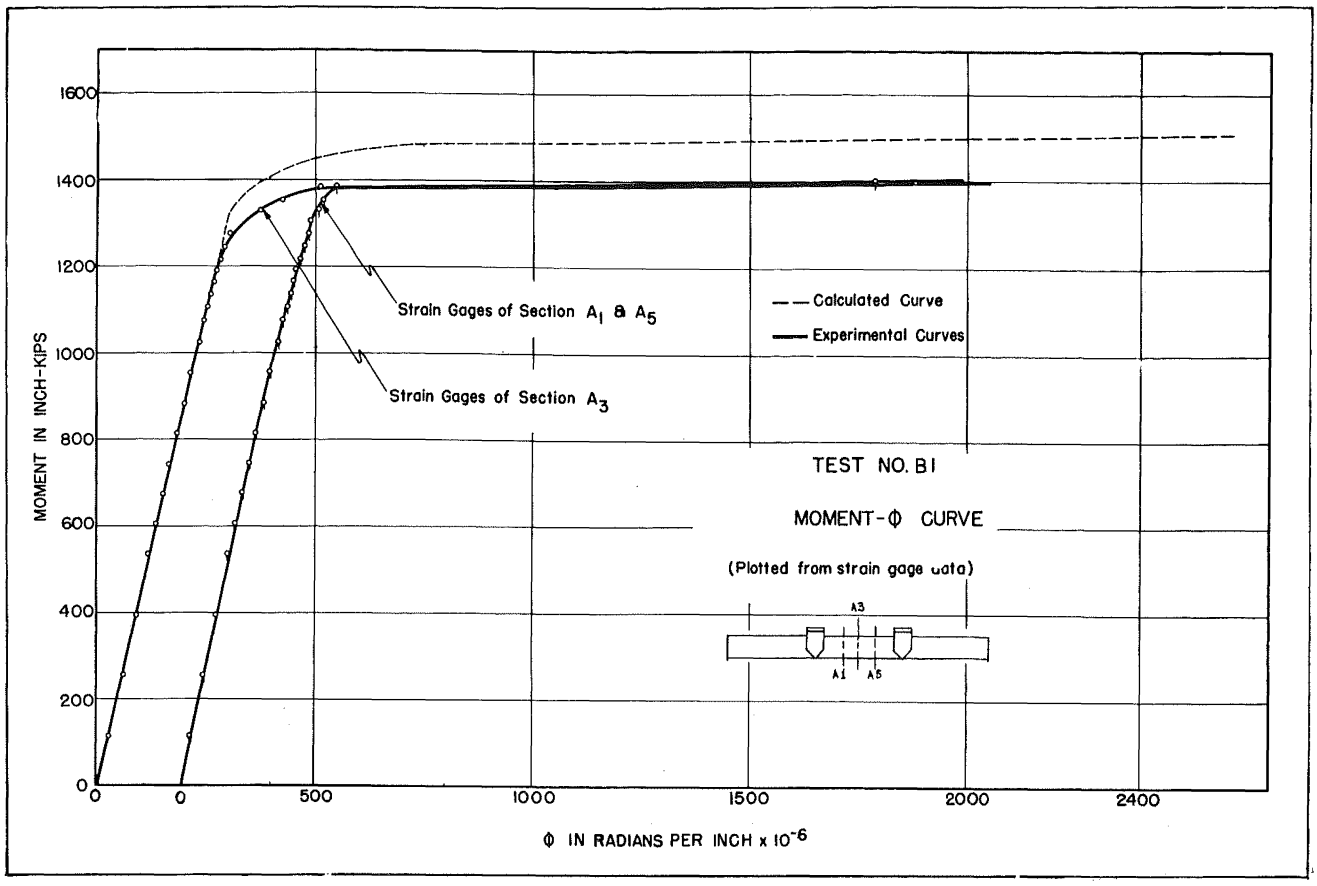

Fig. 10

M-ϕ CURVES FOR CONTROL BEAM B1 AS DETERMINED FROM STRAIN GAGE MEASUREMENTS

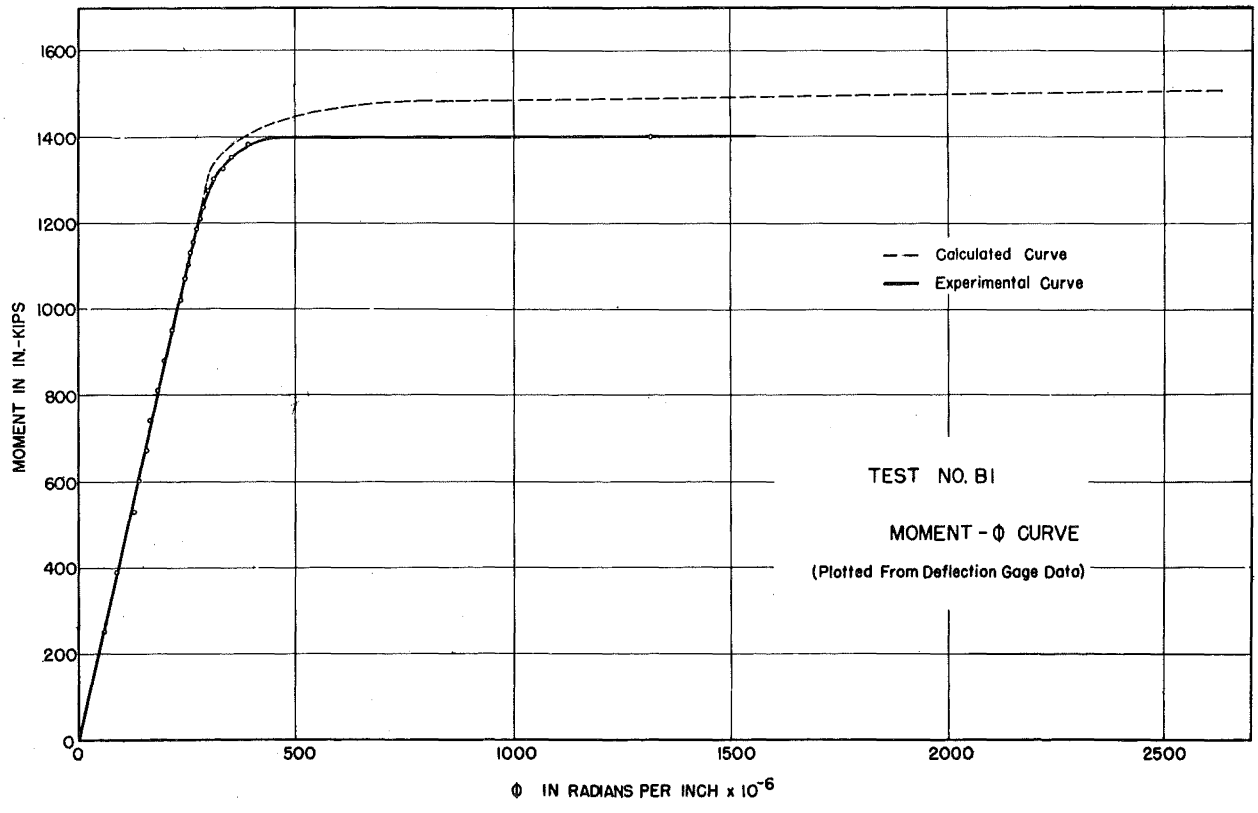

Fig. 11

M-ϕ CURVES FOR CONTROL BEAM B1 AS DETERMINED FROM DEFLECTION GAGE DATA

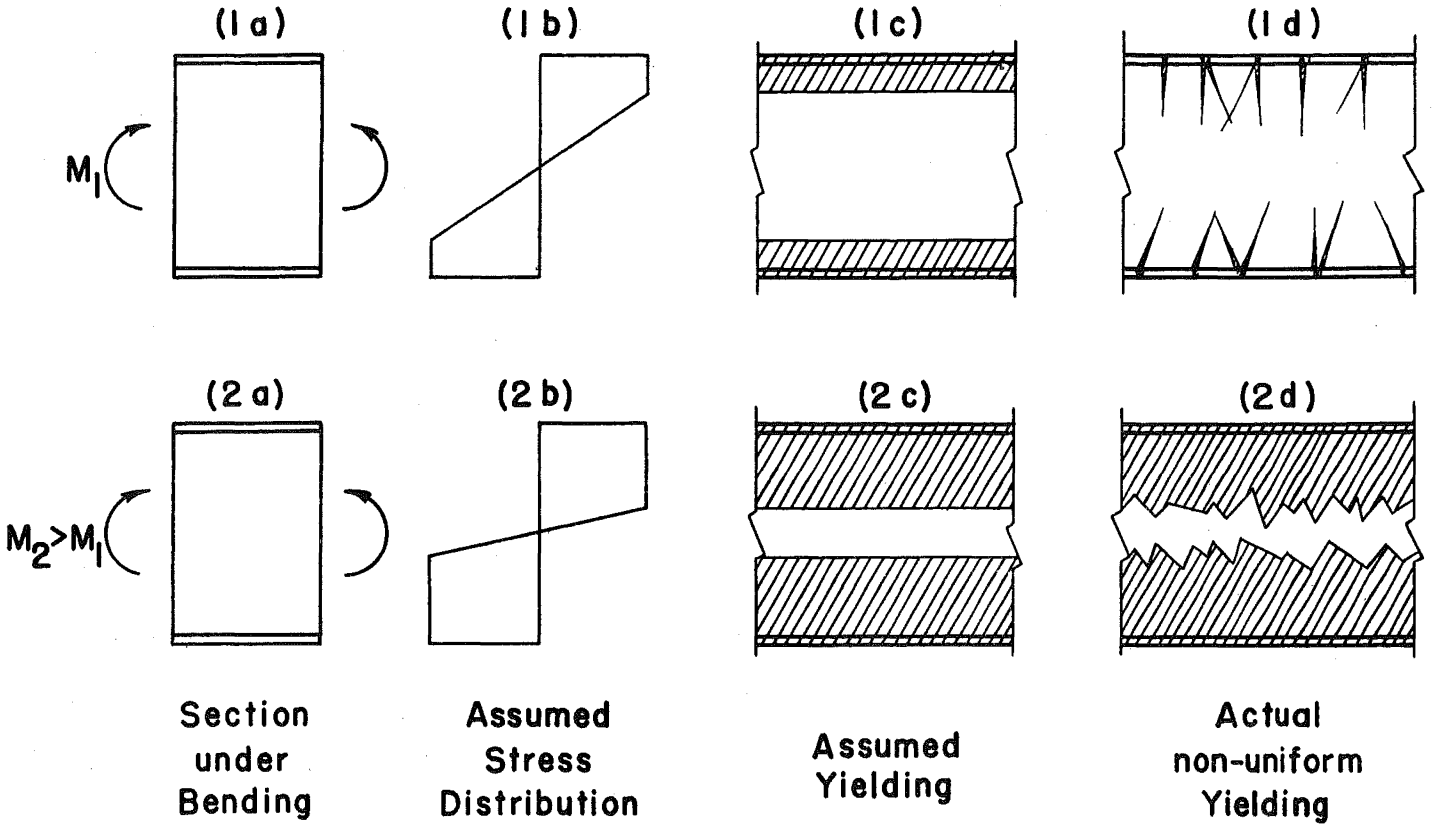

Fig. 12 - Assumed and actual yield zones in structural steel beams.

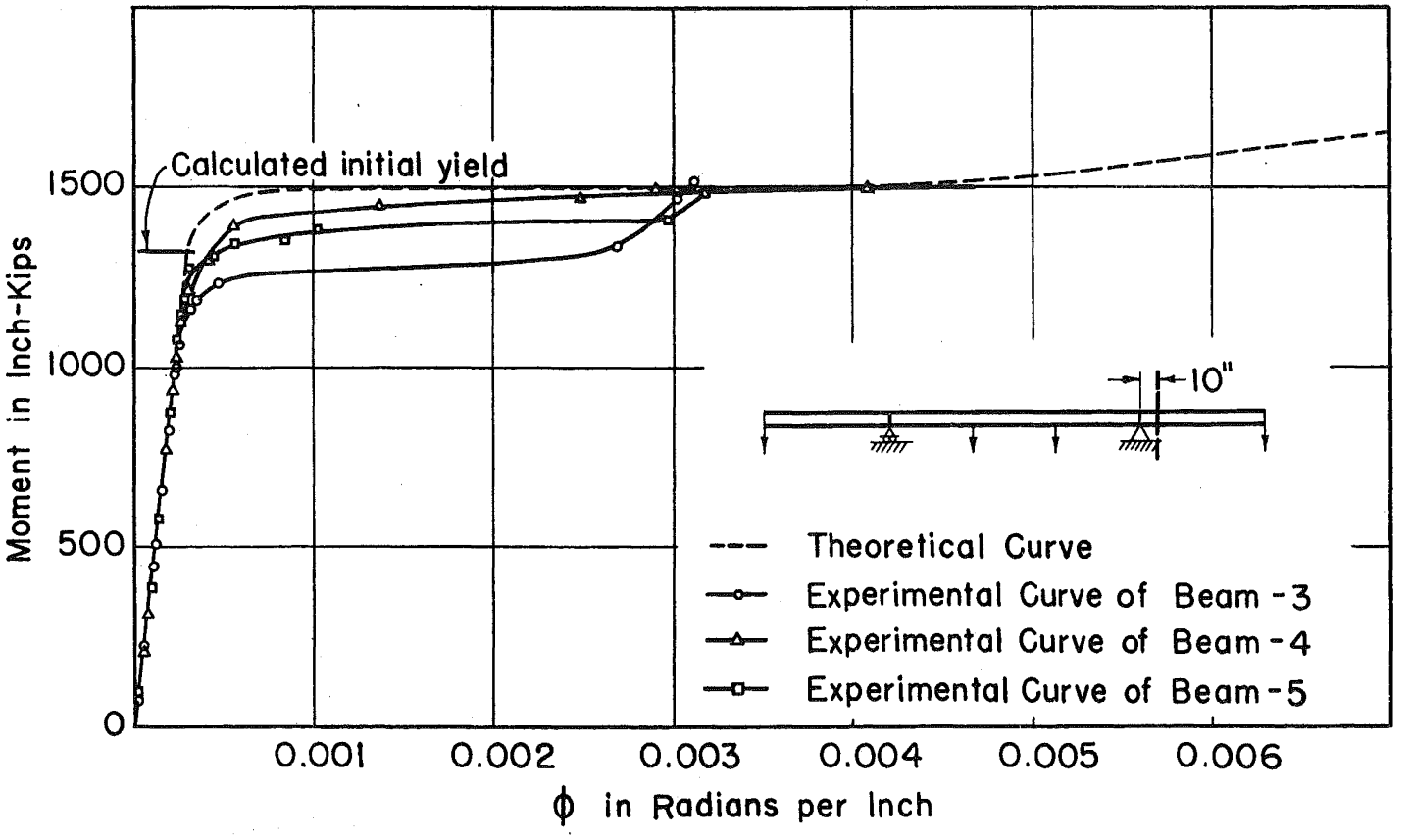

Fig. 13 - Moment-Curvature relationship of continuous beams of 8WF40 shape at a section near a support

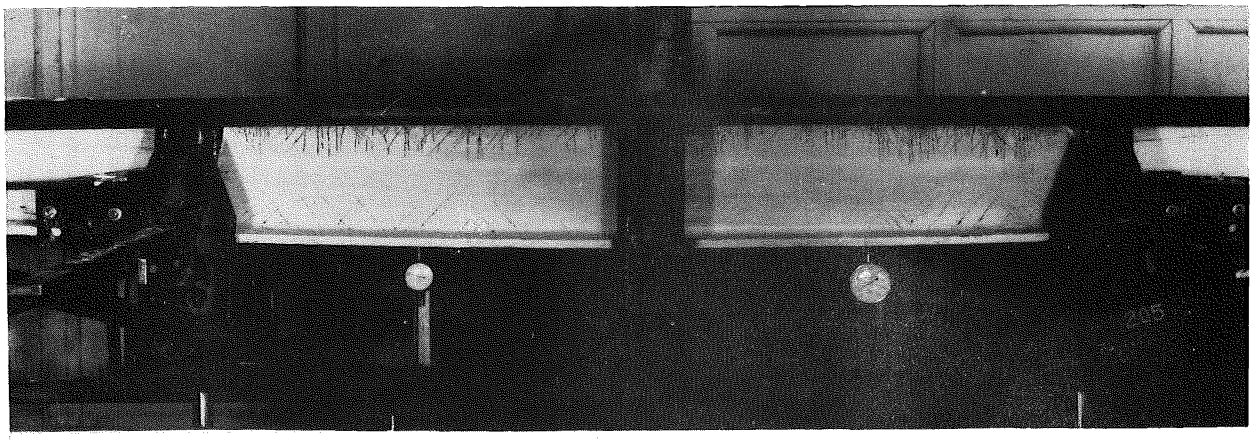

Fig. 14 - Yield zones in central span of 8WF40 beam (B3)

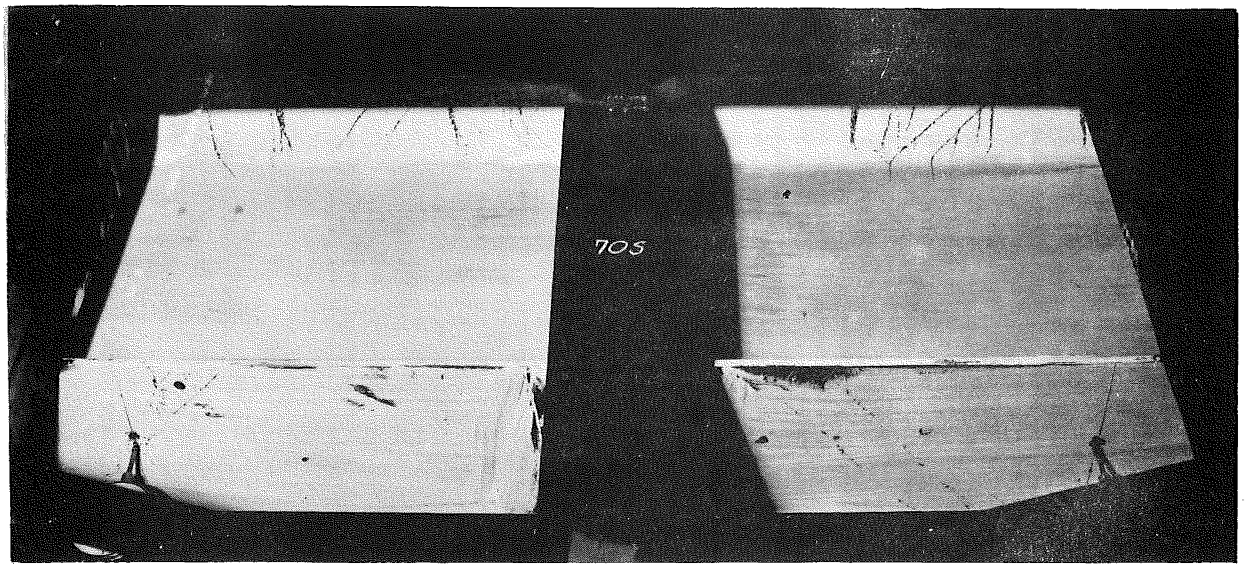

Fig. 15 - View looking up at B7 (14WF30) showing yield zones in compression commencing to penetrate into the web.

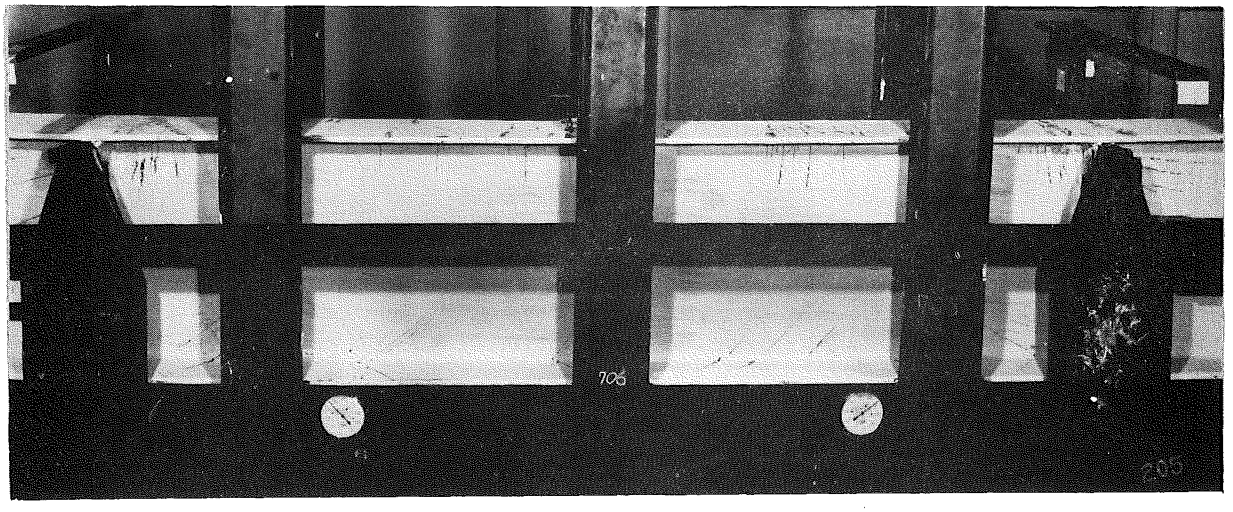

Fig. 16 - B7 showing further development of yield zones.

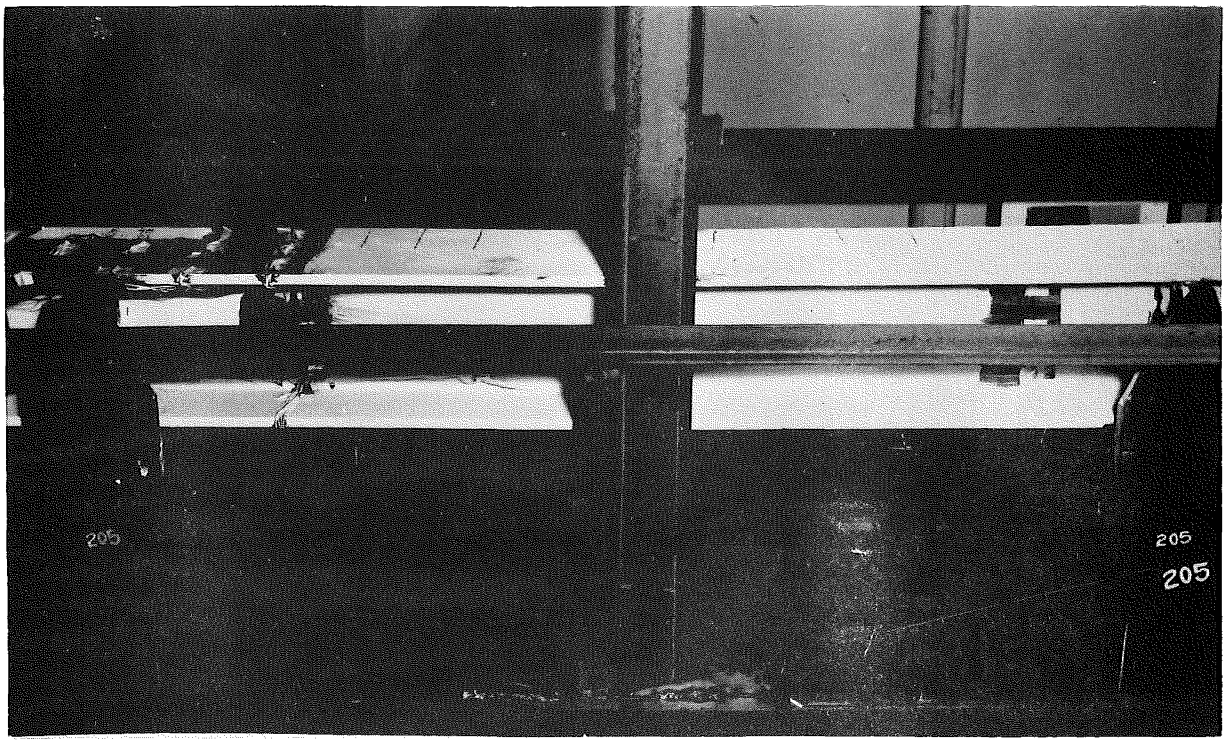

Fig. 17 - Yield lines formed in compression flange of B2 due to residual stress

Fig. 18 - Yield lines formed in compression flange of B3 due to residual stress

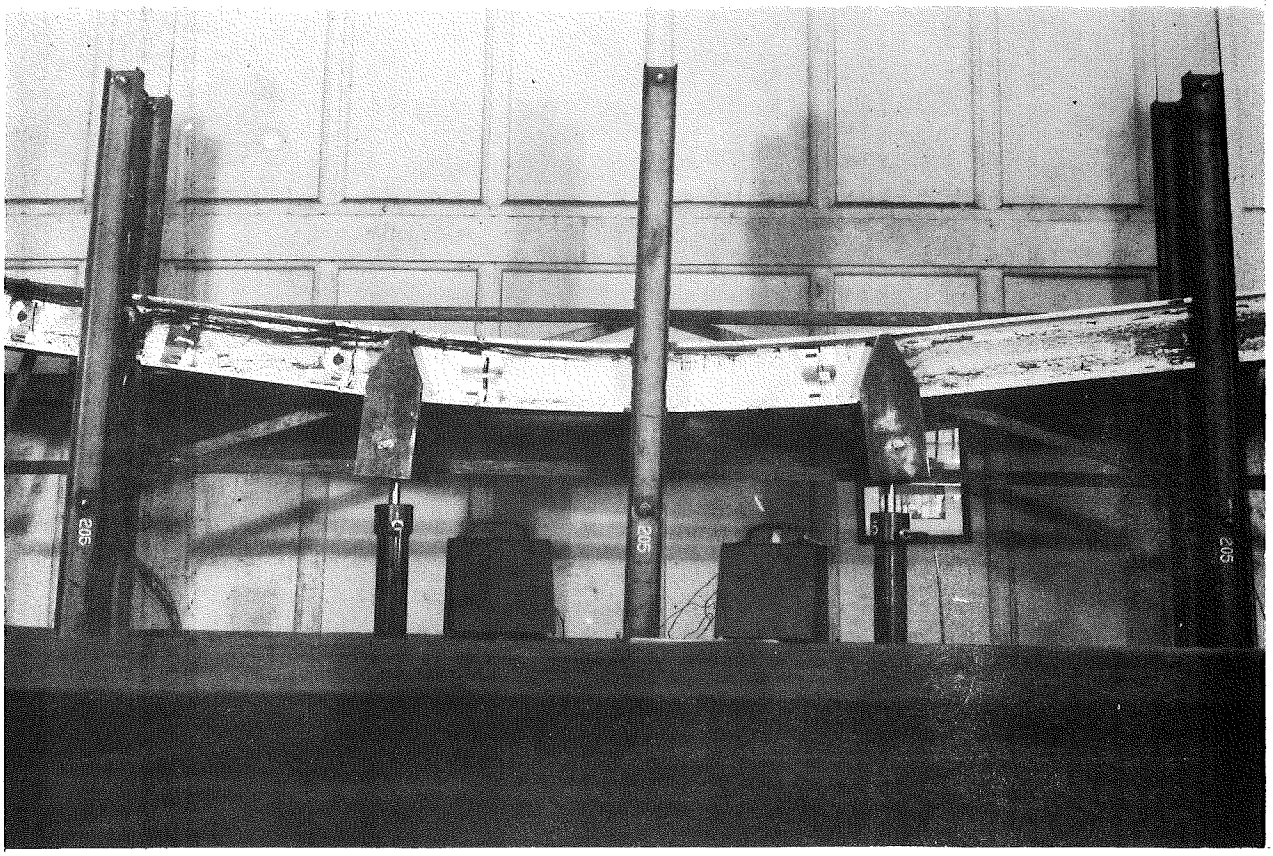

Fig. 19 - Beam 2 at end of test.

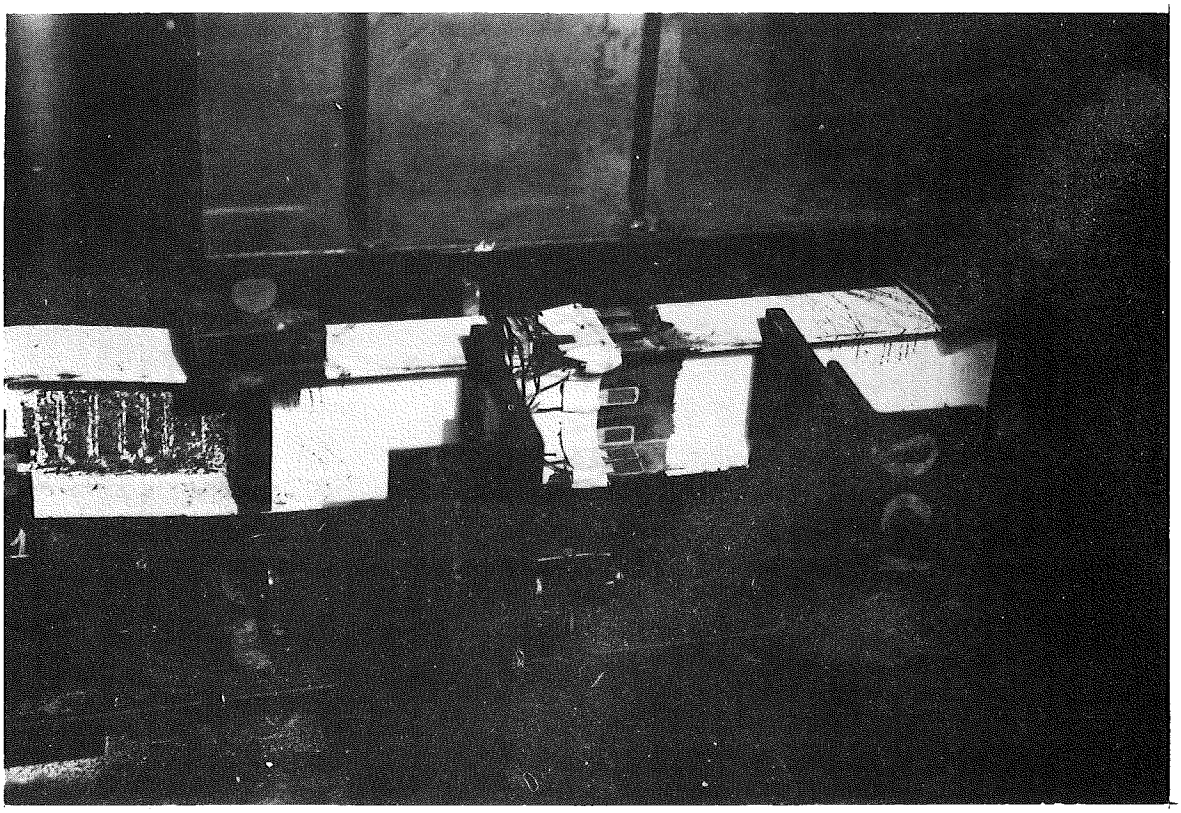

Fig. 20 - Annealed member of 4I7.7 shape showing yield zones progressing from load points toward beam center.

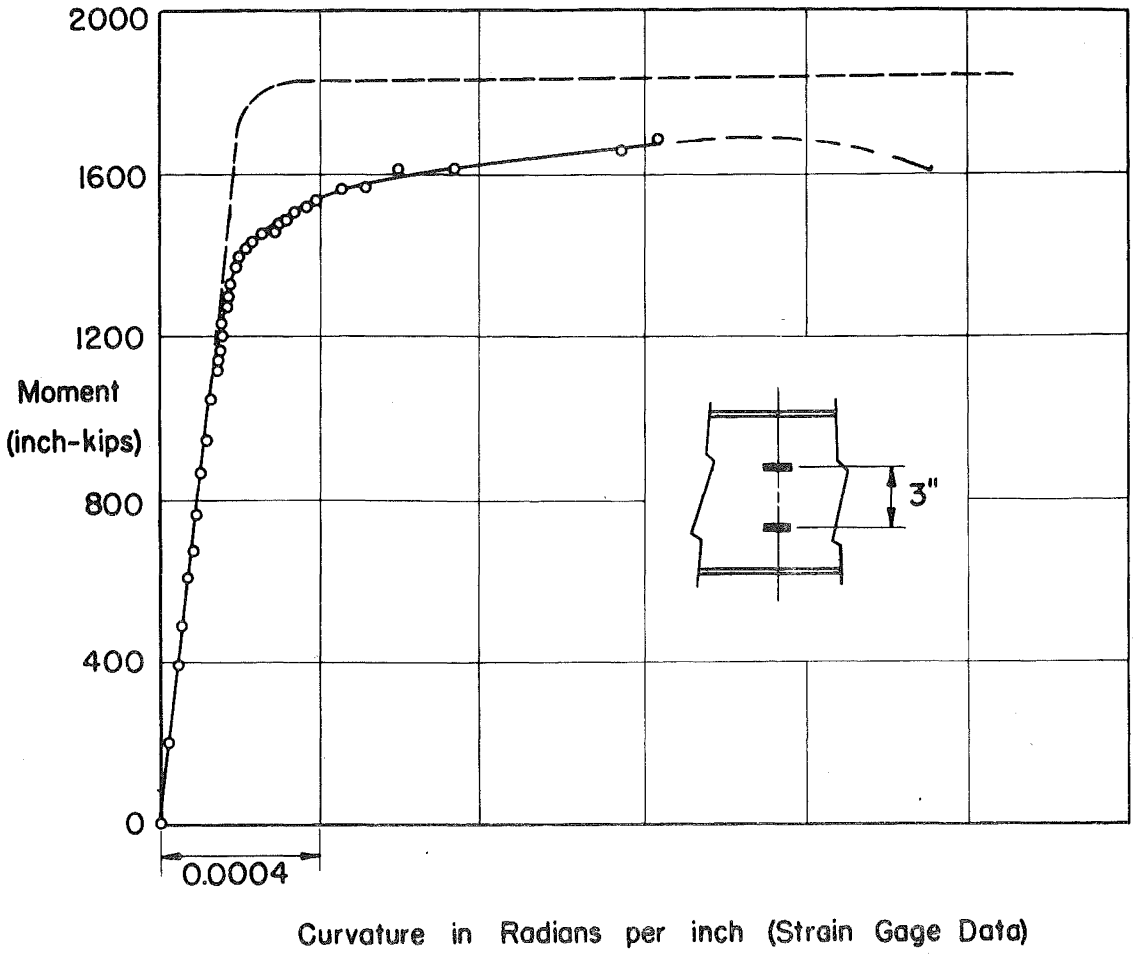

Fig. 21 - M-Ø curve for B7 (14WF30) near a support point.

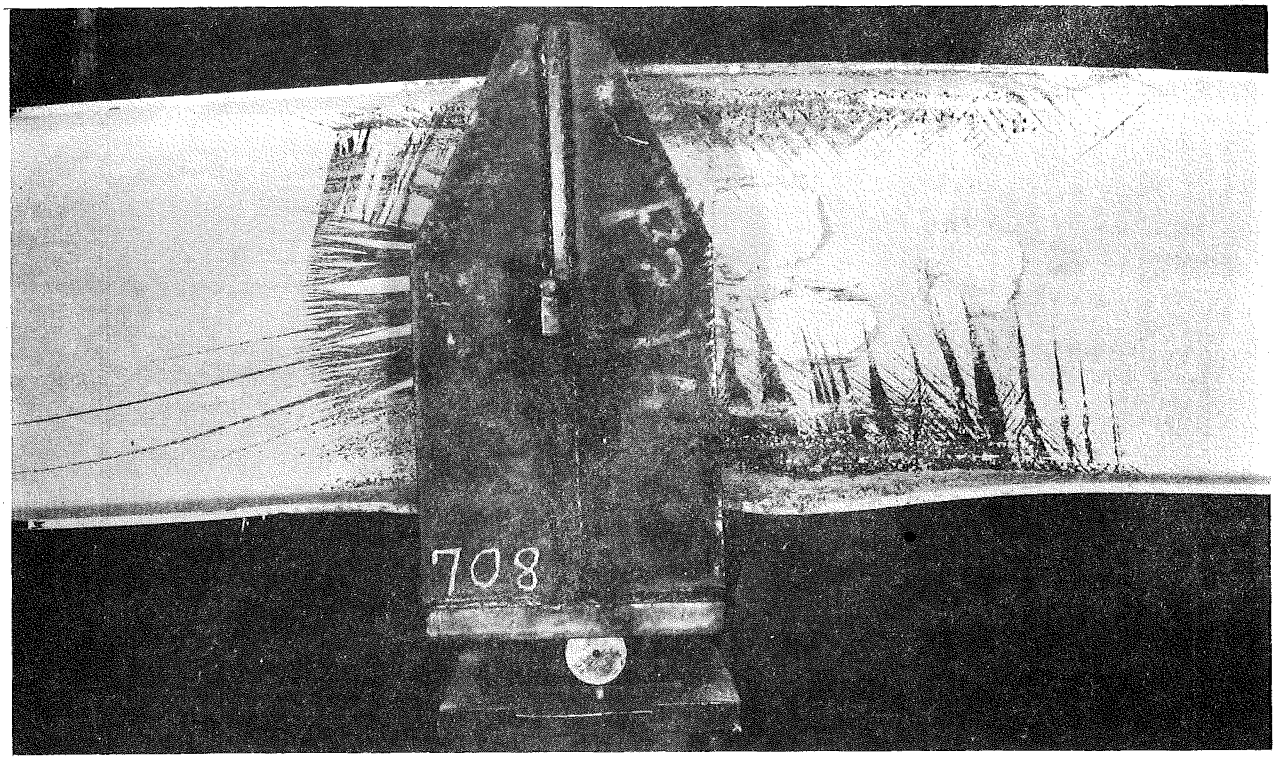

Fig. 22 - Local buckling of 14WF30 shape

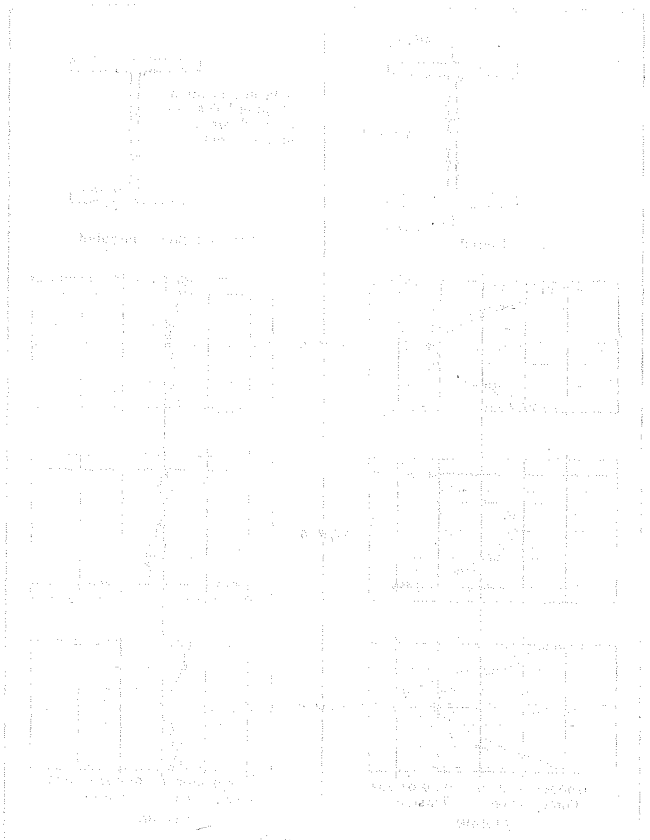

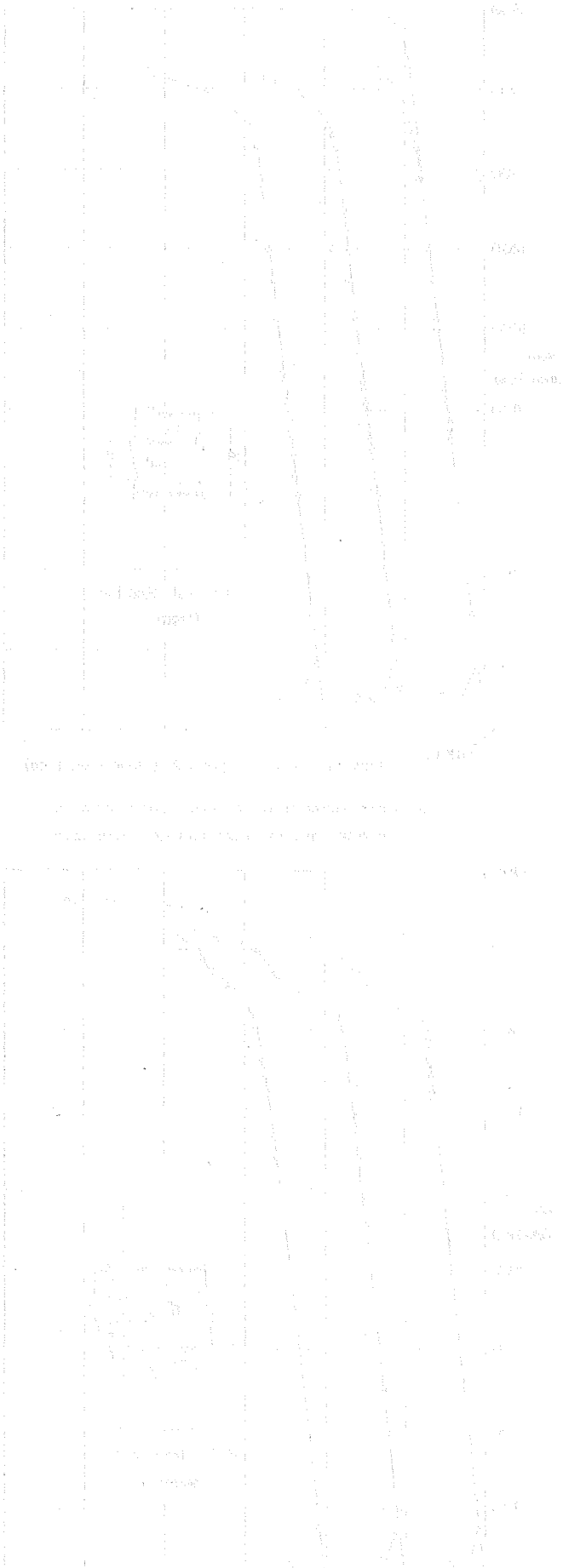

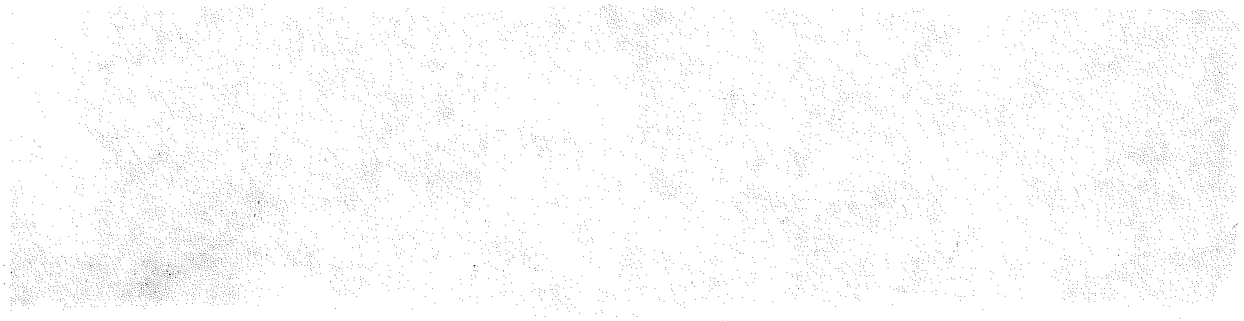

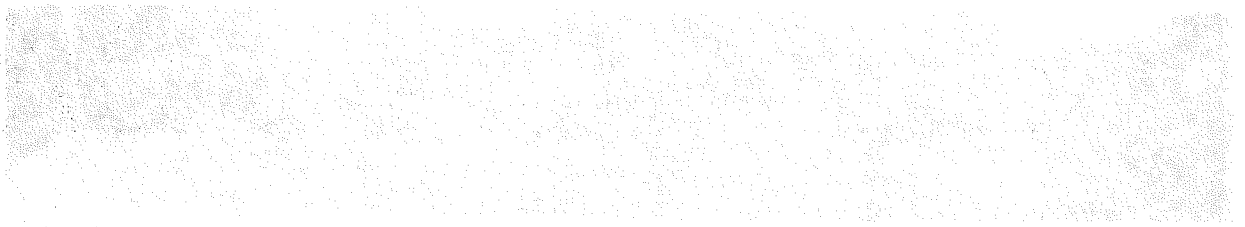

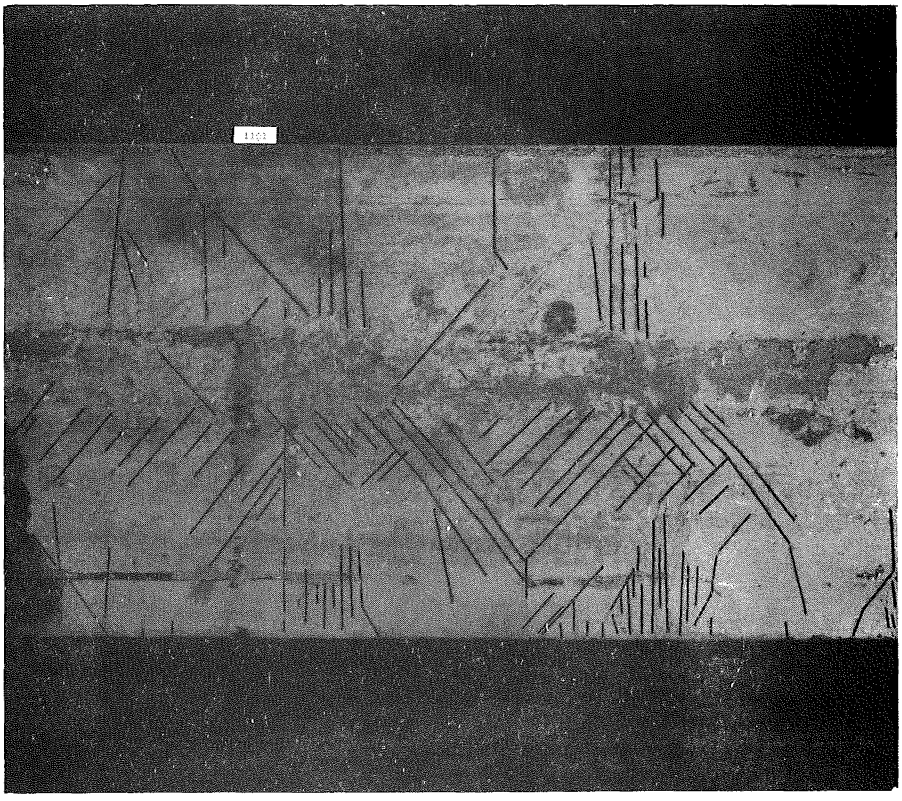

Fig. 30

Example of yield lines formed in flange of 8WF31 section due to cold bending after rolling. (The pattern has been accentuated by tracing the original lines in ink).

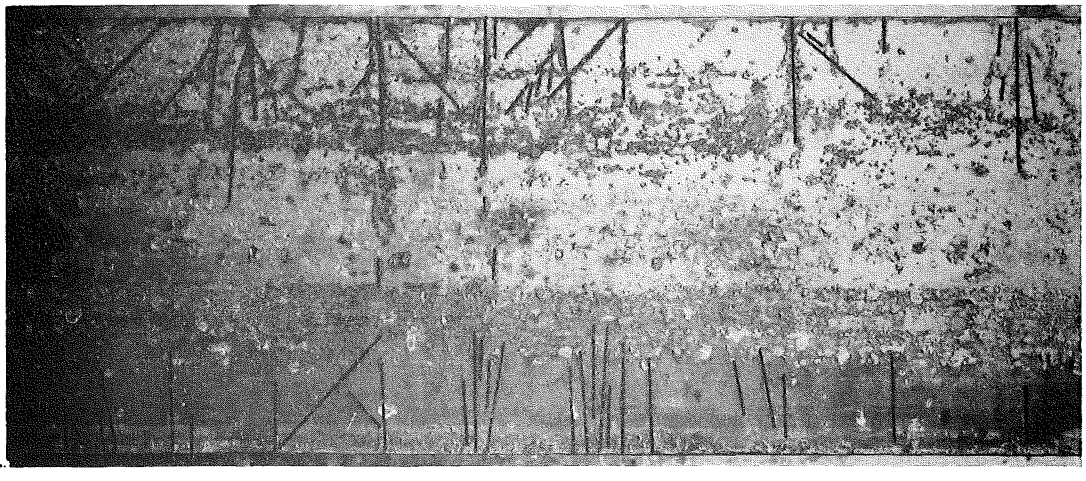

Fig. 31

An additional example of yield lines formed in the flange of a rolled shape due to cold bending. Flexure was probably about the minor axis of the section.

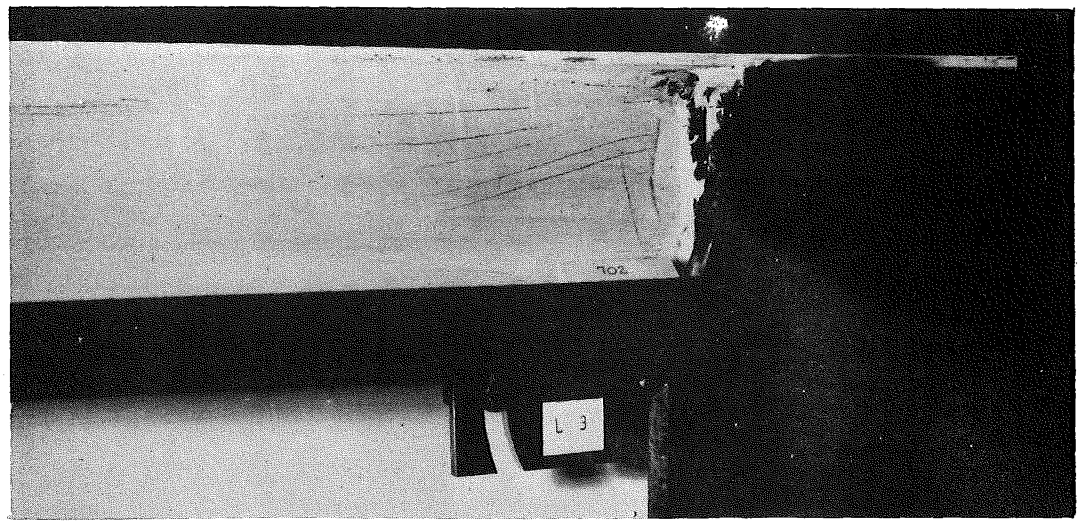

Fig. 32 - Yield lines formed in web of B7 near load point

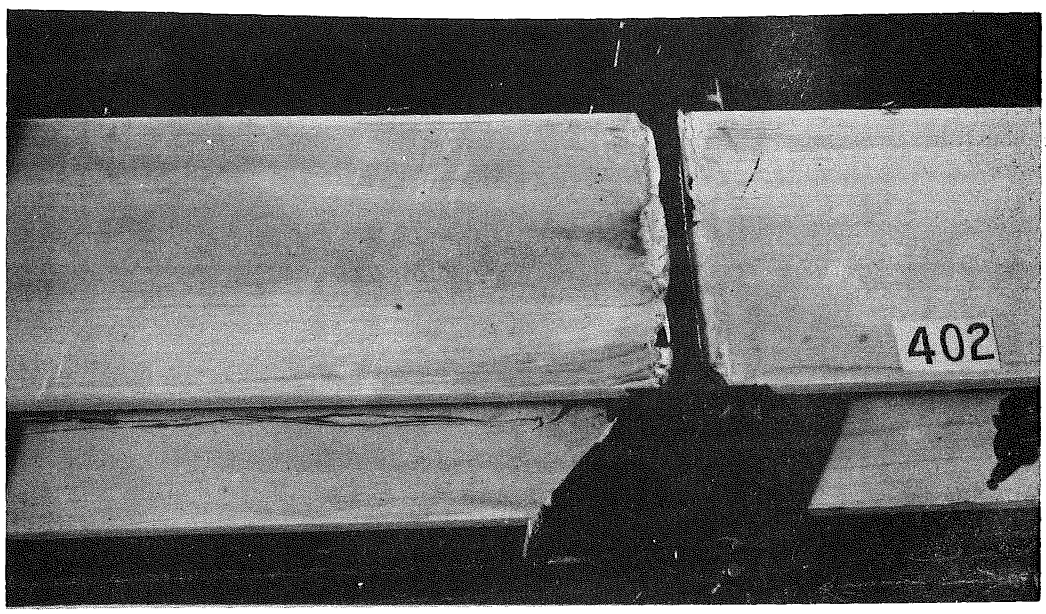

Fig. 33 - Yield lines in compression flange of B4 at support

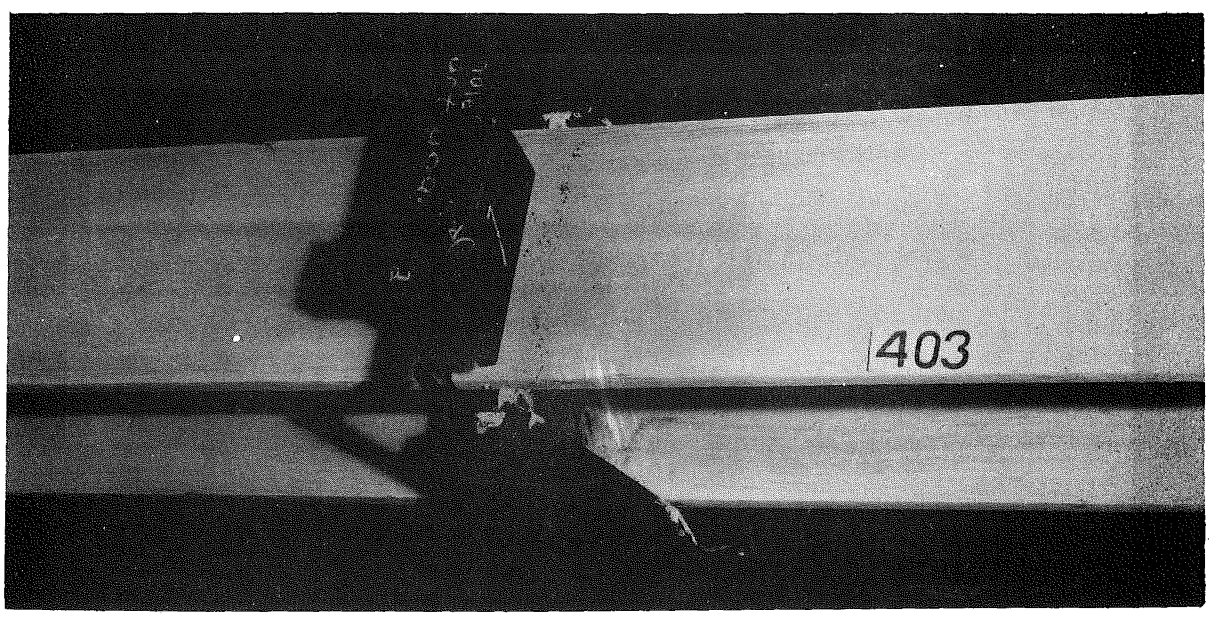

Fig. 34 - Local yielding in compression flange of B4 at load point

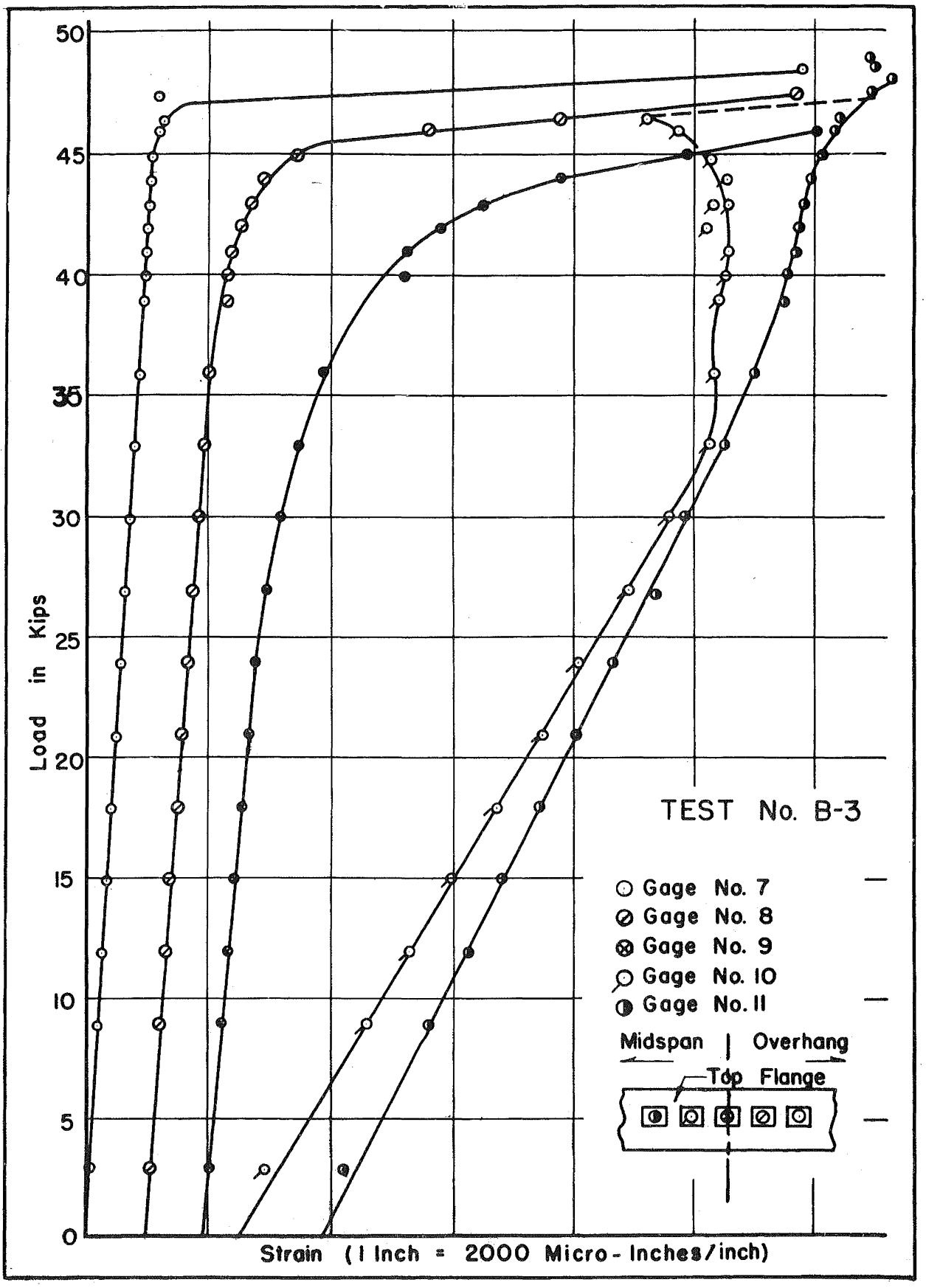

Fig. 35 - Load-strain curves for gages mounted on the flange of B3 in the vicinity of a support

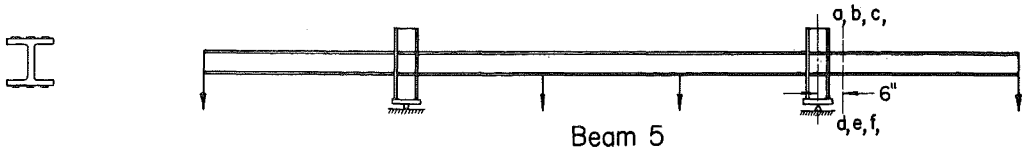

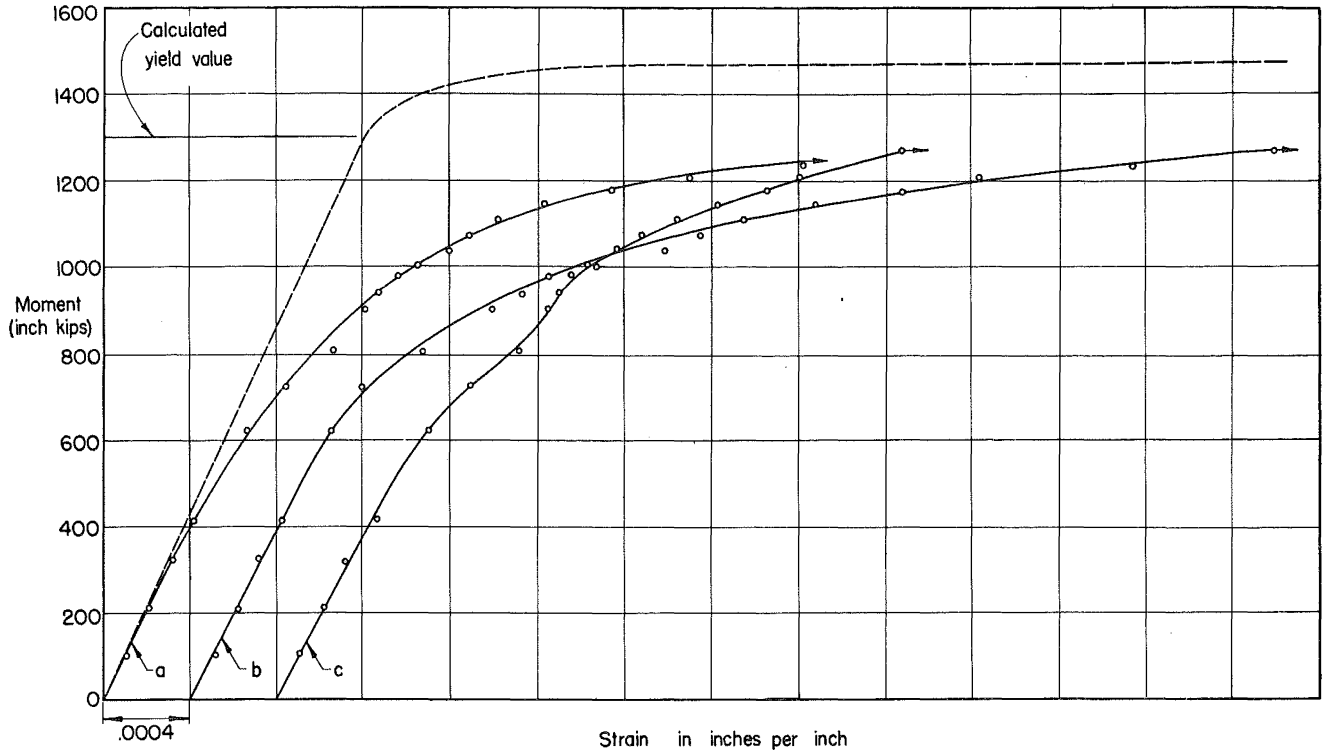

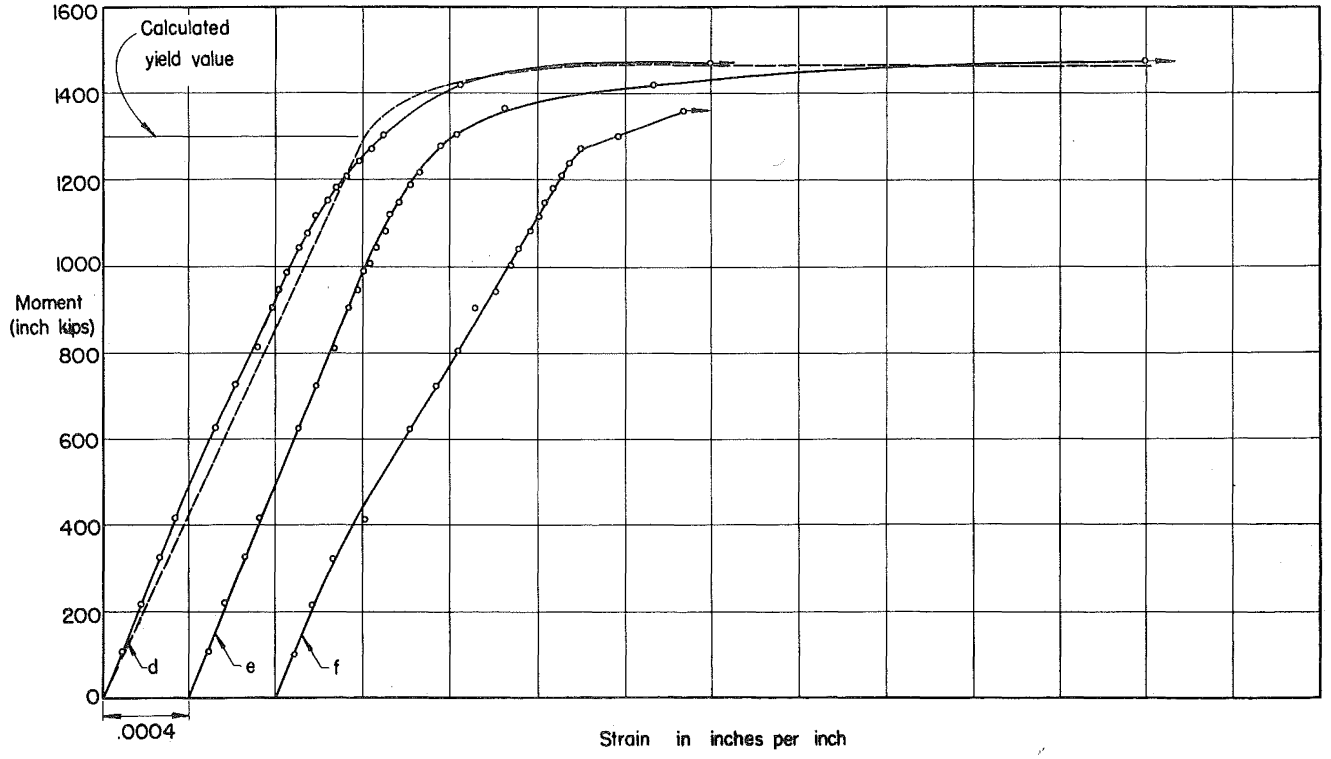

Fig. 36 - STRAIN MEASUREMENTS OF BEAM 5 AT A DISTANCE OF 6" FROM LINE OF SUPPORT

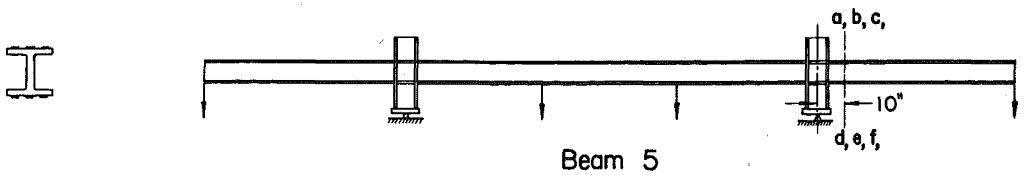

Beam 5

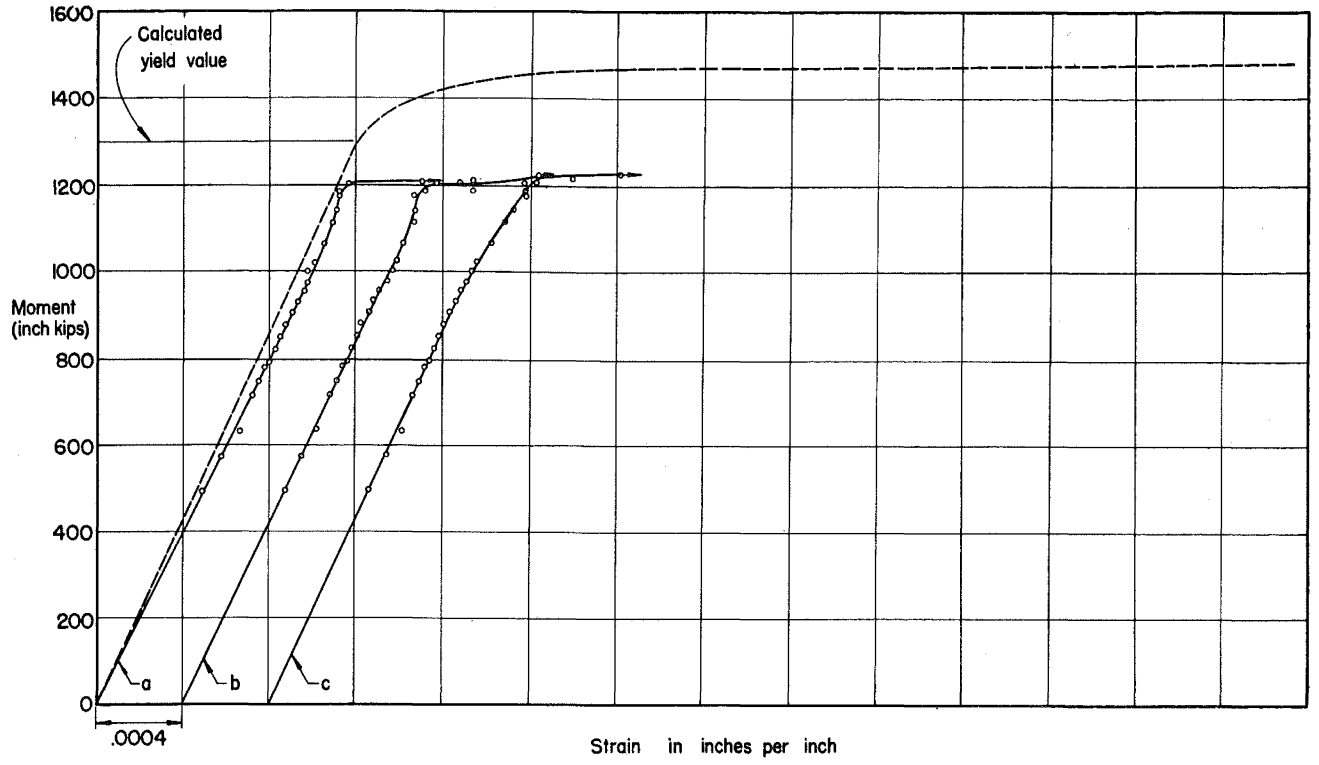

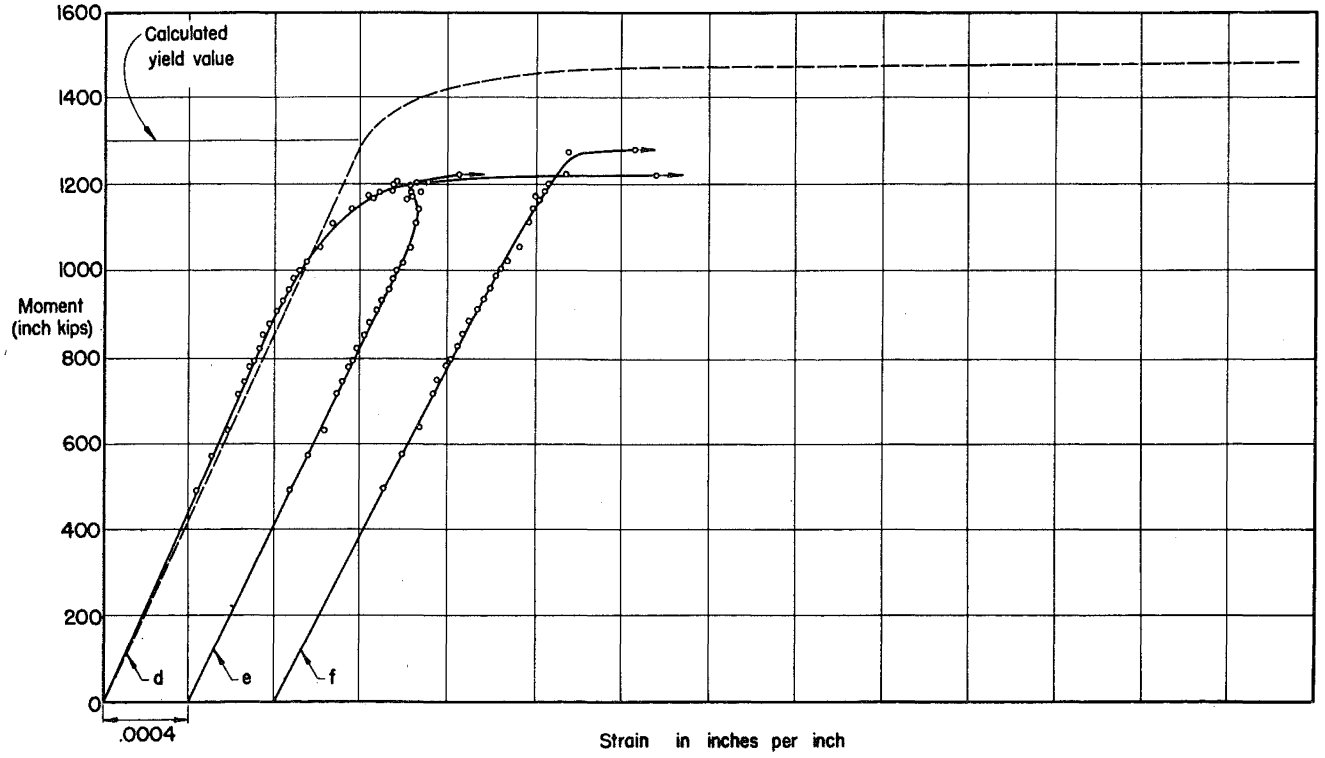

Fig. 37 - STRAIN MEASUREMENTS OF BEAM 5 AT A DISTANCE OF 10" FROM LINE OF SUPPORT

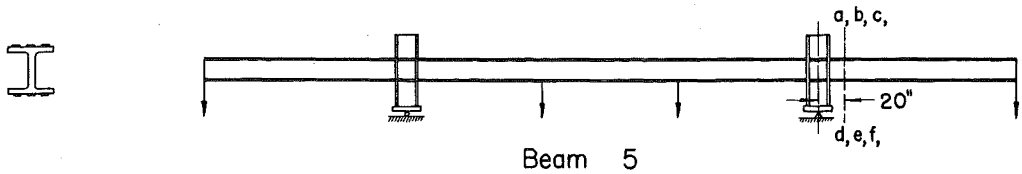

Beam 5

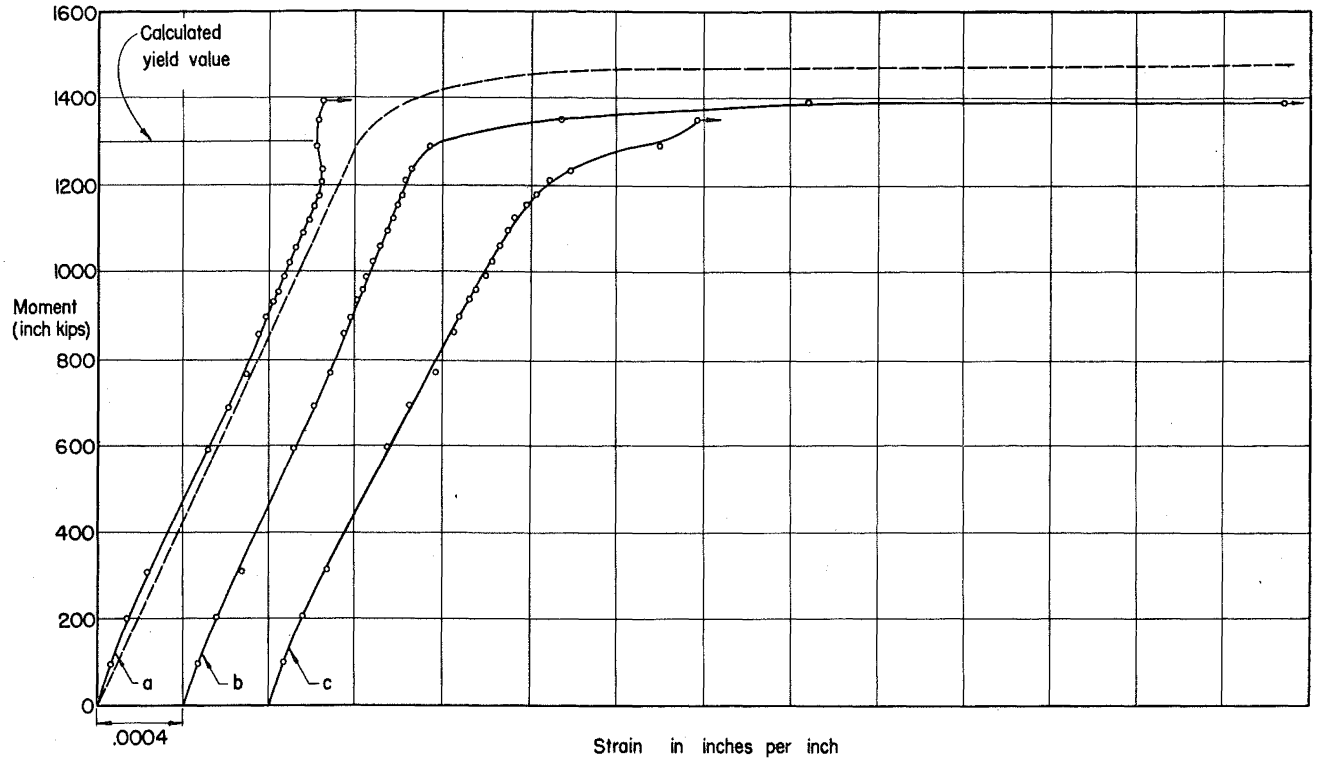

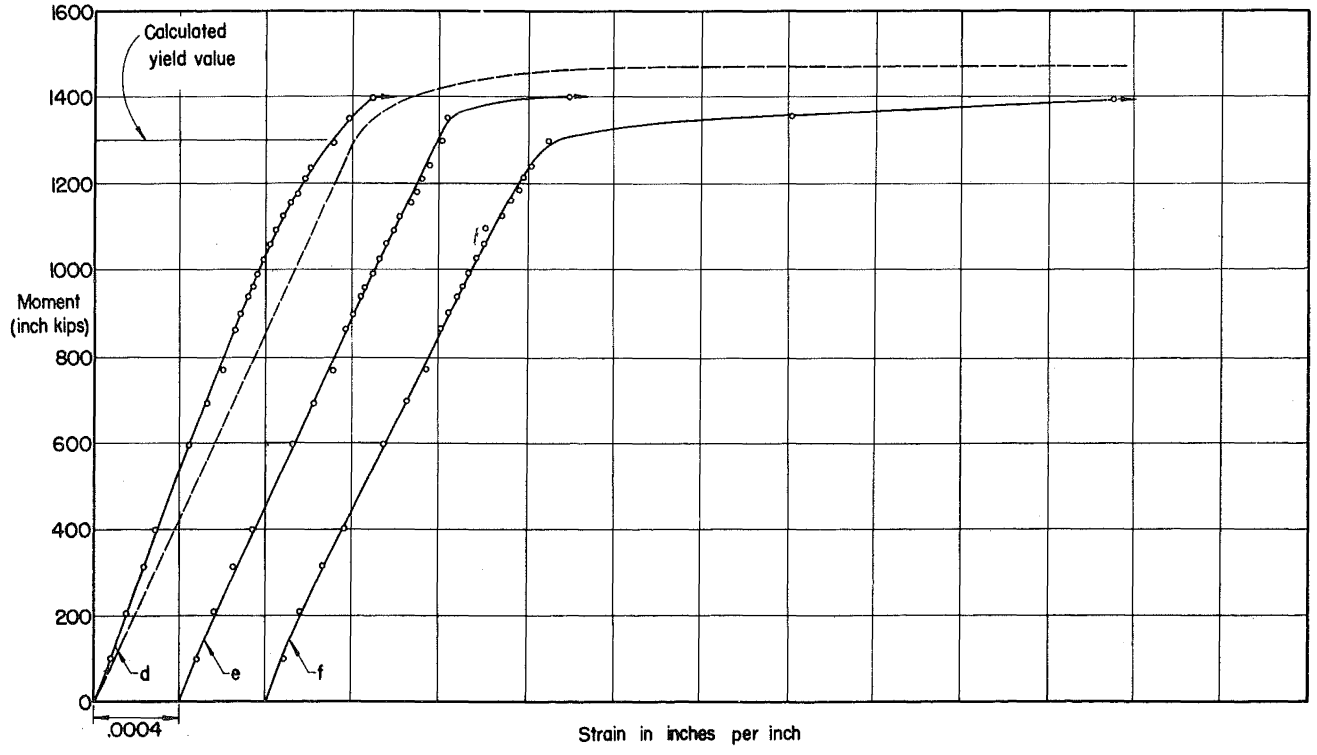

Fig. 38 - STRAIN MEASUREMENTS OF BEAM 5 AT A DISTANCE OF 20" FROM LINE OF SUPPORT

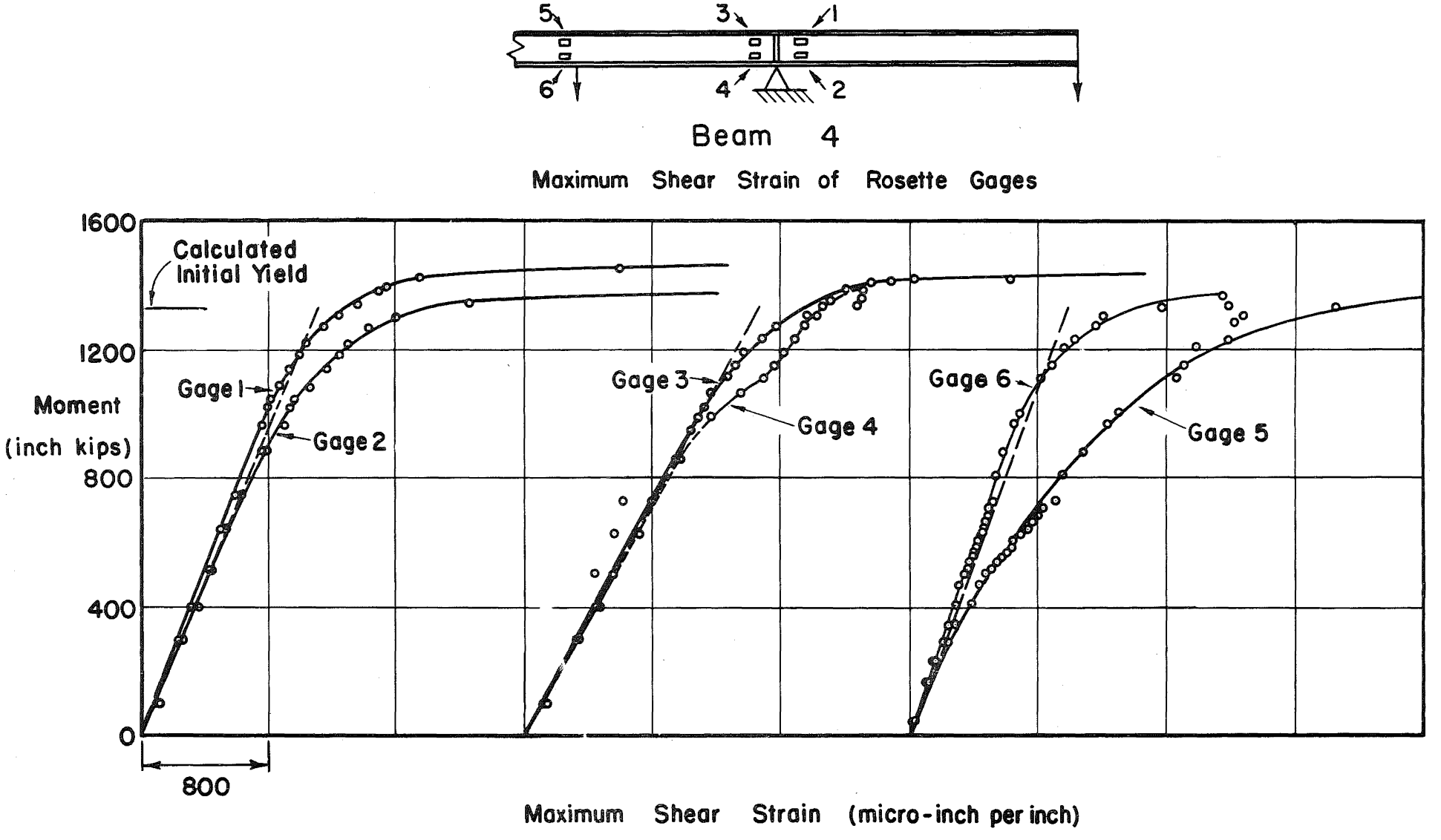

Fig. 39 - THEORETICAL AND EXPERIMENTAL MAXIMUM SHEAR STRAINS AT THREE CROSS-SECTIONS OF BEAM 4

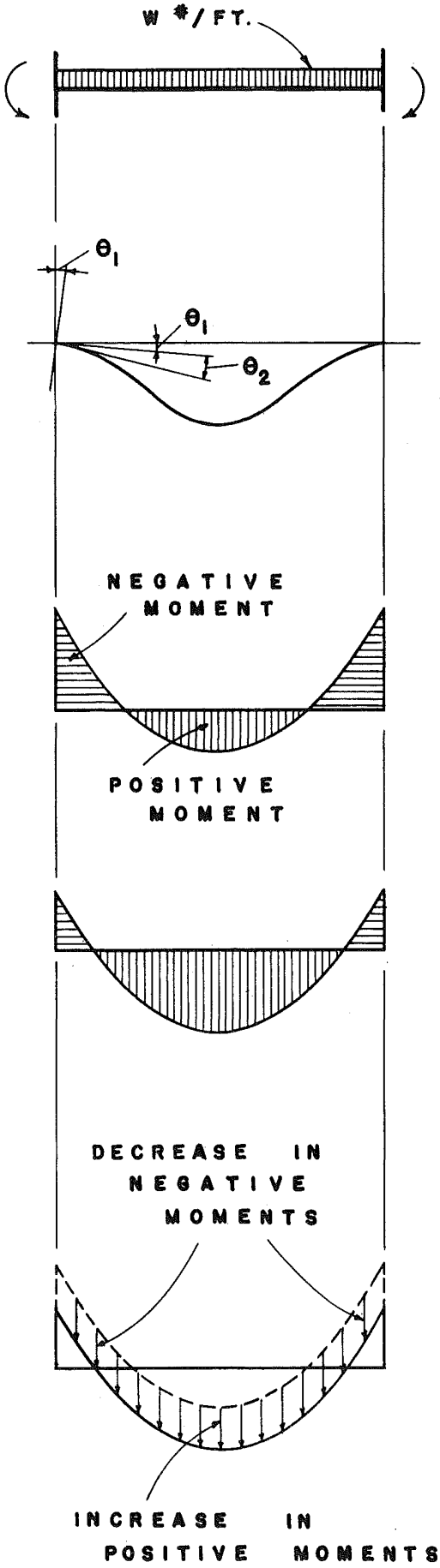

(a) RESTRAINED MEMBER AND LOADING

(b) ELASTIC CURVE
θ_1 = DEFLECTION ANGLE DUE TO ELASTIC BEHAVIOR
θ_2 = DEFLECTION ANGLE DUE TO PLASTIC DEFORMATIONS AT JOINTS

(c) MOMENT DIAGRAM FOR ELASTIC BEHAVIOR (DUE TO θ_1)

(d) MOMENT DIAGRAM FOR ELASTIC-PLASTIC BEHAVIOR (DUE TO $\theta_1 + \theta_2$)

(e) CHANGE IN STRESS PATTERN DUE TO PLASTIC DEFORMATIONS

Fig. 40

Redistribution of moment due to plastic deformation -- Amirikian [7]

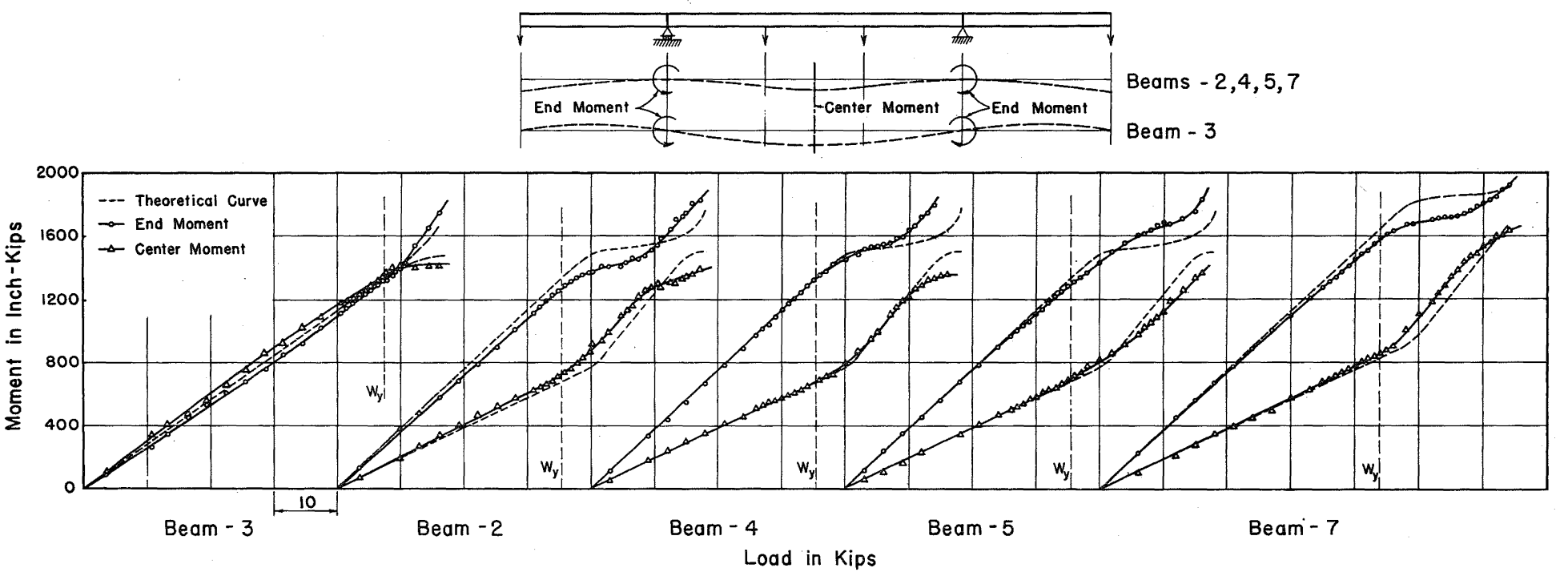

Fig. 41 - MOMENT - LOAD RELATIONSHIPS FOR CONTINUOUS BEAMS

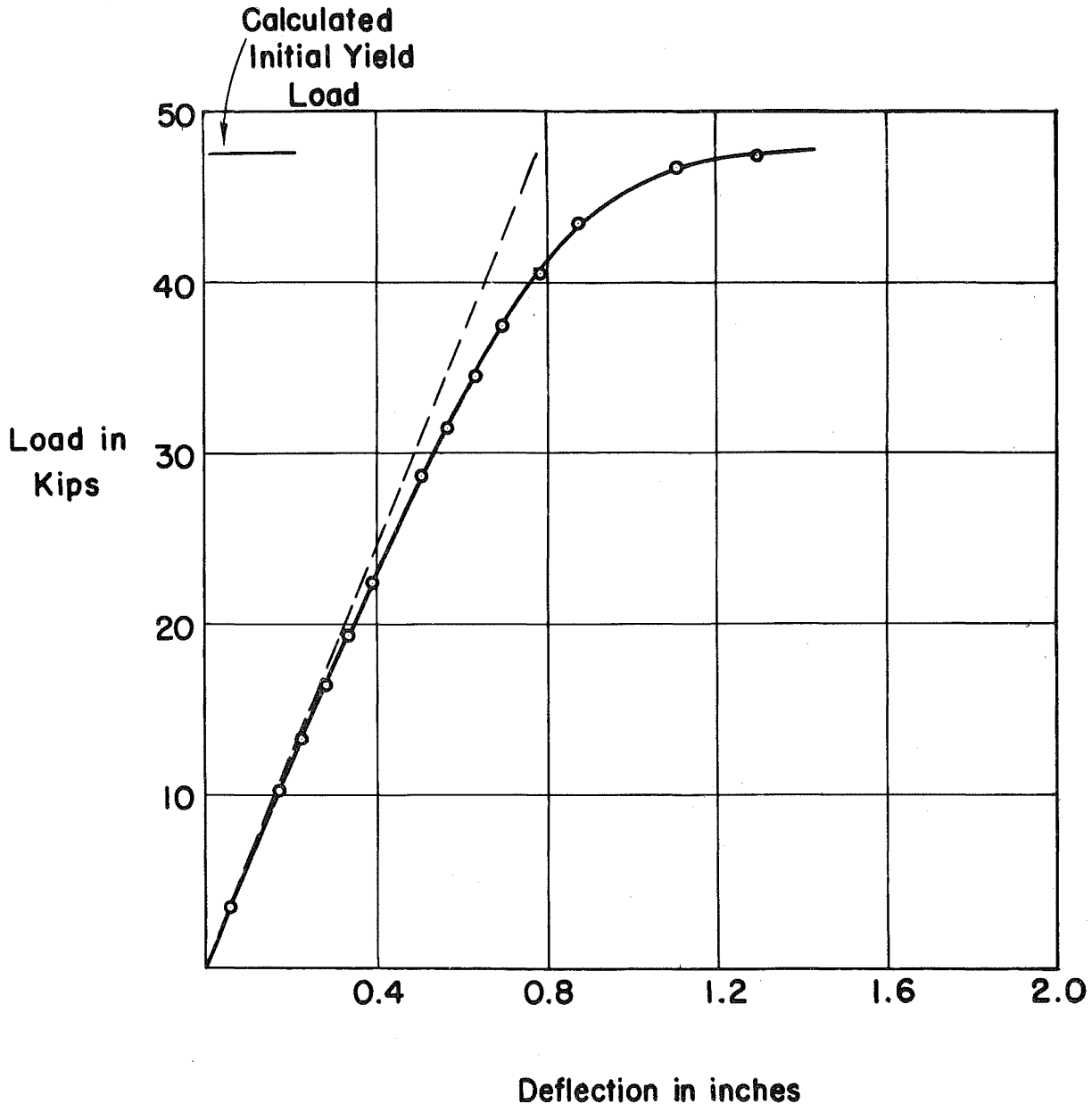

Fig. 42 - Load deflection relation of B3 in the region below the calculated initial yield load.

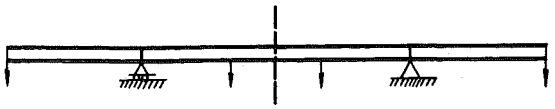

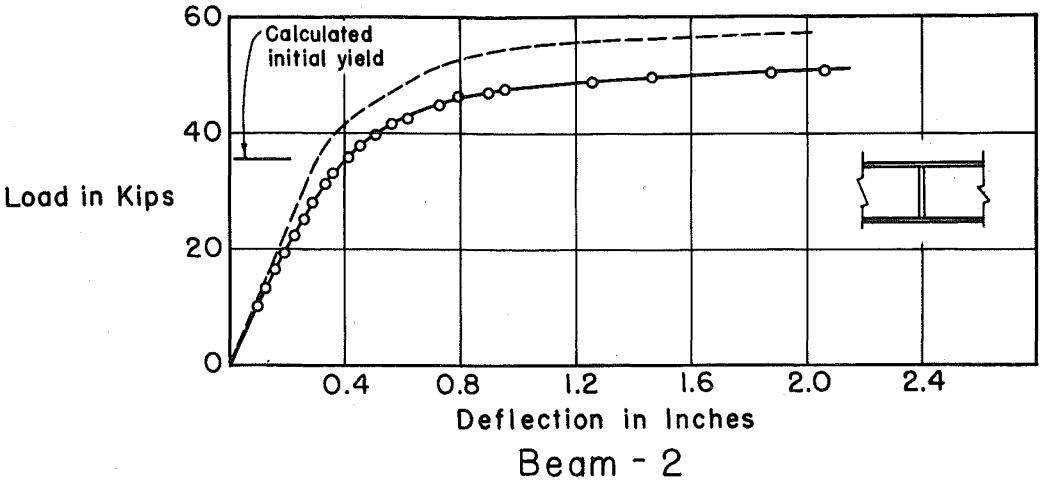

Beam - 2

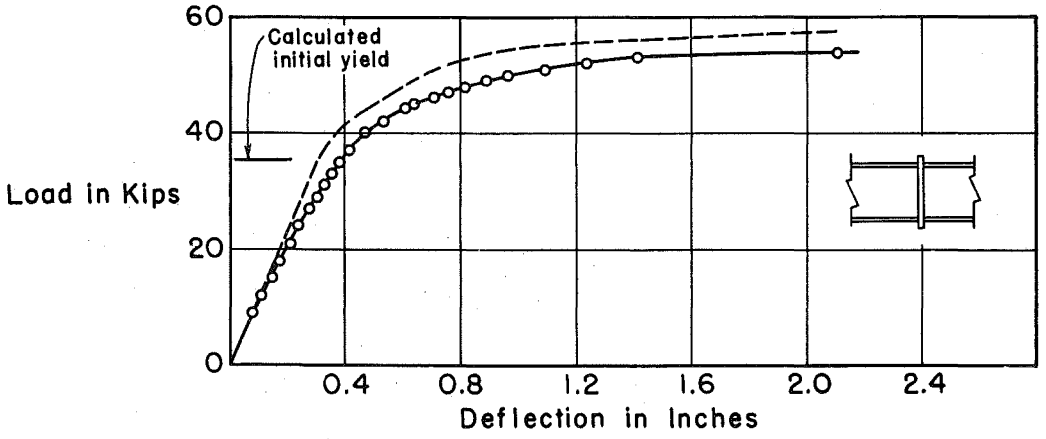

Beam - 4

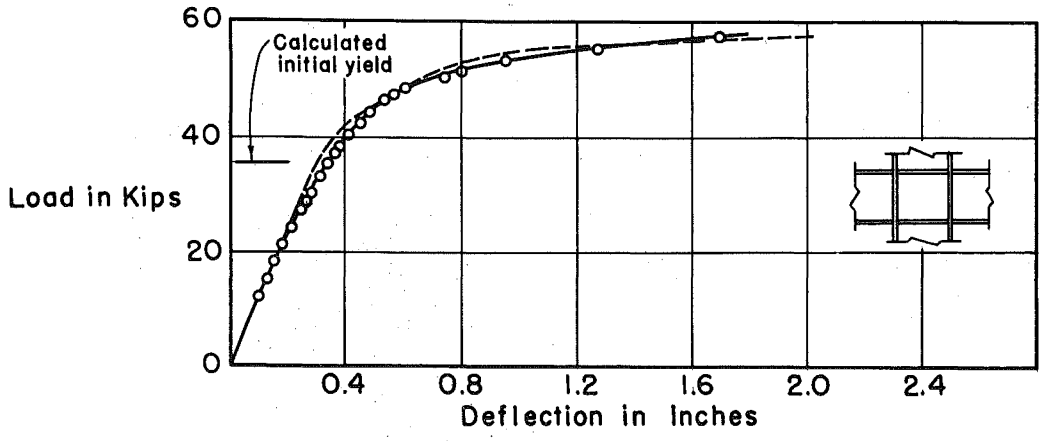

Beam - 5

Fig. 43

EXPERIMENTAL AND THEORETICAL LOAD-DEFLECTION CURVES FOR CONTINUOUS BEAMS 2, 4 and 5. DEFLECTION MEASURED AT CENTERLINE

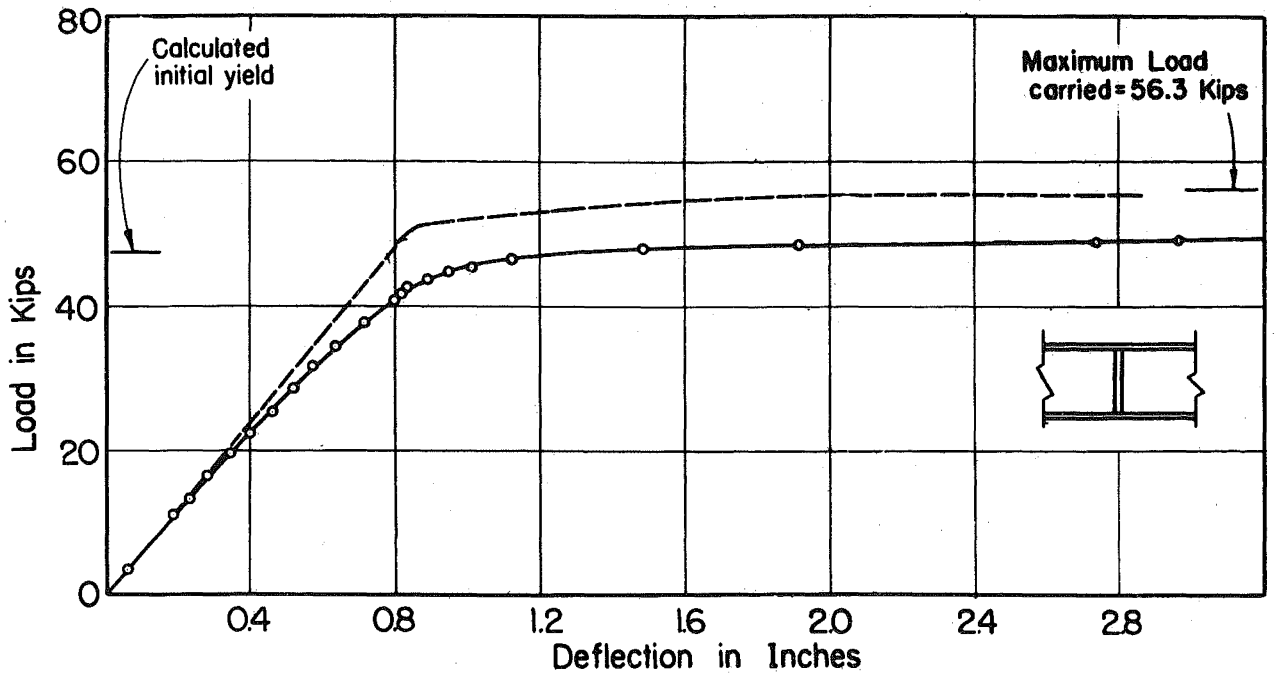

Fig. 44

EXPERIMENTAL AND THEORETICAL LOAD - CENTERLINE DEFLECTION CURVES FOR B3

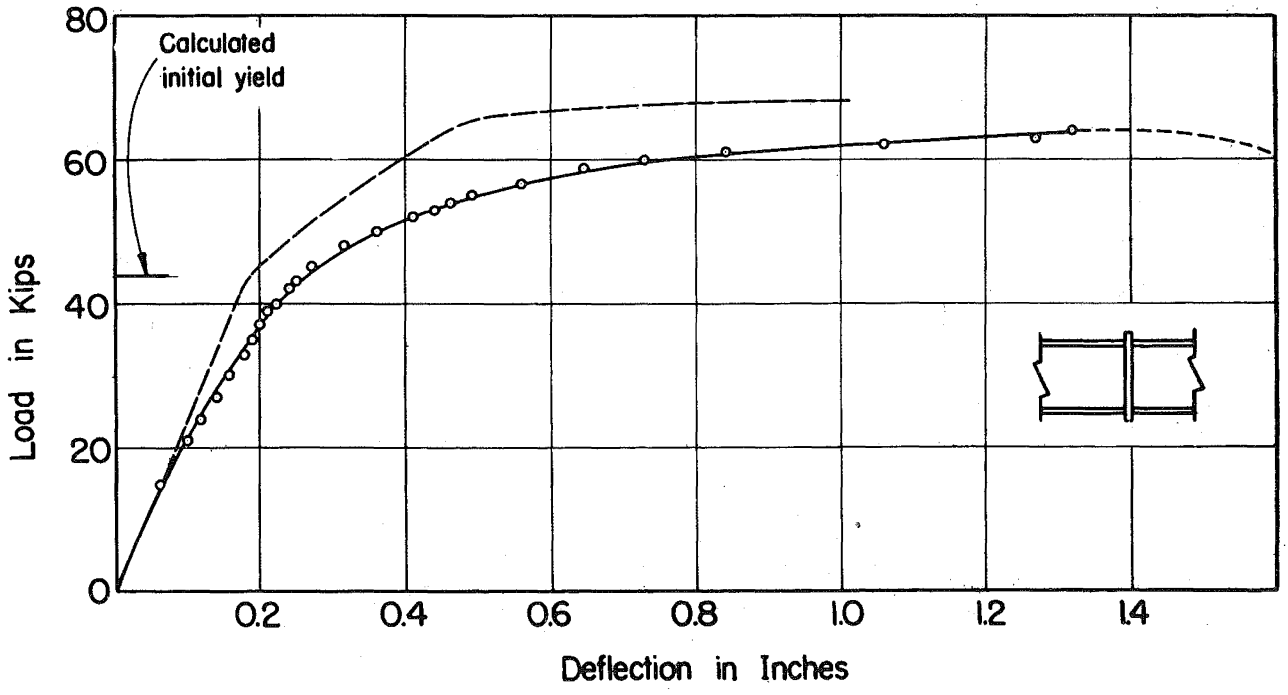

Fig. 45

EXPERIMENTAL AND THEORETICAL LOAD - CENTERLINE DEFLECTION CURVES FOR B7

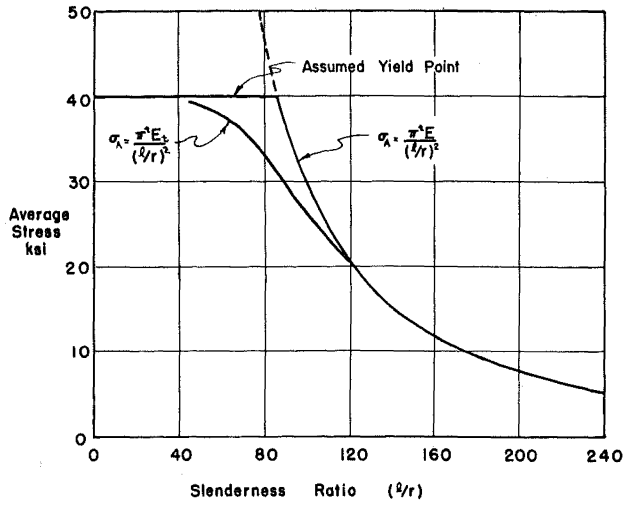

Fig. 46. - EFFECT OF RESIDUAL STRESS ON COLUMN CURVE

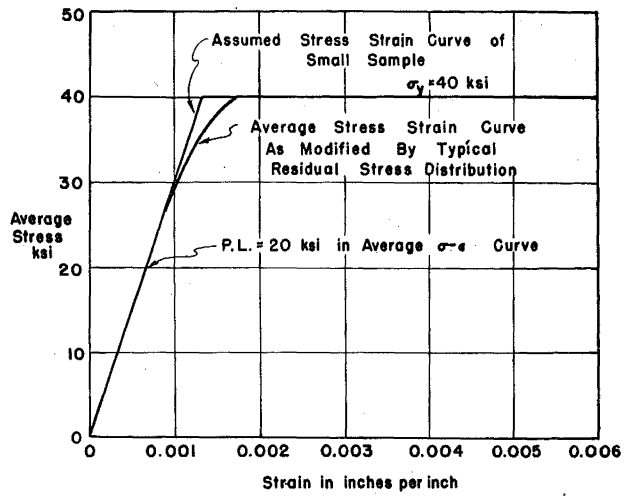

Fig. 47 - STRESS-STRAIN DIAGRAM FOR STEEL AS MODIFIED BY RESIDUAL STRESS

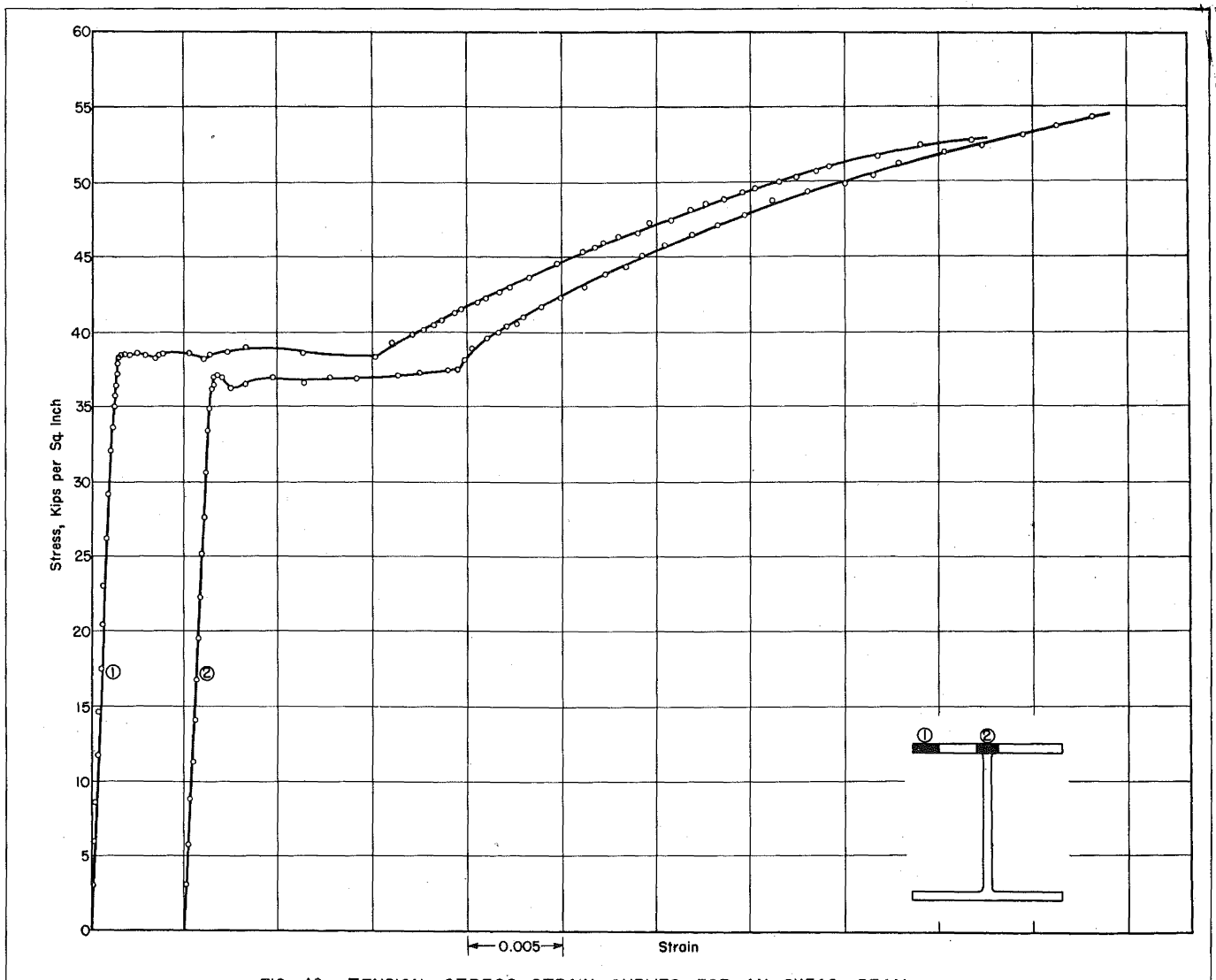

FIG. 48 - TENSION STRESS-STRAIN CURVES FOR AN 8WF40 BEAM
(Including strain-hardening range)